FACILITY SITING AND LAYOUT OPTIMIZATION BASED ON PROCESS SAFETY

A Dissertation

by

SEUNGHO JUNG

Submitted to the Office of Graduate Studies of
Texas A&M University
in partial fulfillment of the requirements for the degree of

DOCTOR OF PHILOSOPHY

December 2010

Major Subject: Chemical Engineering

Facility Siting and Layout Optimization Based on Process Safety

FACILITY SITING AND LAYOUT OPTIMIZATION BASED ON PROCESS SAFETY

A Dissertation

by

SEUNGHO JUNG

Submitted to the Office of Graduate Studies of
Texas A&M University
in partial fulfillment of the requirements for the degree of

DOCTOR OF PHILOSOPHY

Approved by:

Chair of Committee,	M. Sam Mannan
Committee Members,	Carl D. Laird
	Mahmoud El-Halwagi
	Guy L. Curry
Head of Department,	Michael Pishko

December 2010

Major Subject: Chemical Engineering

ABSTRACT

Facility Siting and Layout Optimization Based on Process Safety. (December 2010)

Seungho Jung, B.S.; M.S., Seoul National University, South Korea

Chair of Advisory Committee: Dr. M. Sam Mannan

In this work, a new approach to optimize facility layout for toxic release, fire & explosion scenarios is presented. By integrating a risk analysis in the optimization formulation, safer assignments for facility layout and siting have been obtained. Accompanying with the economical concepts used in a plant layout, the new model considers the cost of willing to avoid a fatality, *i.e*. the potential injury cost due to accidents associated with toxic release near residential areas. For fire and explosion scenarios, the building or equipment damage cost replaces the potential injury cost. Two different approaches have been proposed to optimize the total cost related with layout.

In the first phase using continuous-plane approach, the overall problem was initially modeled as a disjunctive program where the coordinates of each facility and cost-related variables are the main unknowns. Then, the convex hull approach was used to reformulate the problem as a Mixed Integer Non-Linear Program (MINLP) that identifies potential layouts by minimizing overall costs. This approach gives the coordinates of each facility in a continuous plane, and estimates for the total length of pipes, the land area, and the selection of safety devices. Finally, the 3D-computational fluid dynamics (CFD) was used to compare the difference between the initial layout and

the final layout in order to see how obstacles and separation distances affect the dispersion or overpressures of affected facilities. One of the CFD programs, ANSYS CFX was employed for the dispersion study and Flame Acceleration Simulator (FLACS) for the fires and explosions.

In the second phase for fire and explosion scenarios, the study is focused on finding an optimal placement for hazardous facilities and other process plant buildings using the optimization theory and mapping risks on the given land in order to calculate risk in financial terms. The given land is divided in a square grid of which the sides have a certain size and in which each square acquires a risk-score. These risk-scores such as the probability of structural damage are to be multiplied by prices of potential facilities which would be built on the grid. Finally this will give us the financial risk. Accompanying the suggested safety concepts, the new model takes into account construction and operational costs. The overall cost of locations is a function of piping cost, management cost, protection device cost, and financial risk. This approach gives the coordinates of the best location of each facility in a 2-D plane, and estimates the total piping length. Once the final layout is obtained, the CFD code, FLACS is used to simulate and consider obstacle effects in 3-D space. The outcome of this study will be useful in assisting the selection of location for process plant buildings and risk management.

ACKNOWLEDGEMENTS

First of all, I would like to thank Dr. M. Sam Mannan for his support and guidance throughout the course of my graduate studies. He has been a great teacher and mentor. I also thank my committee members, Carl D. Laird, Mahmoud El-Halwagi, Guy L. Curry. I am indebted to my colleagues in the Mary K O'Connor Process Safety Center for their help, advice, scrutiny and collaborations. I specifically thank Dr. Richart Vazquez and Jinhan Lee for their help and in initiating my research. Also I thank my research team leader Dr. Dedy Ng for his guidance and for motivating me when I was in a very sluggish mood. I thank God for providing me with the ability, will, and opportunity to complete this degree. Lastly, I thank my family and friends in South Korea for their love and encouragement.

TABLE OF CONTENTS

CHAPTER Page

LIST OF FIGURES

FIGURE Page

LIST OF TABLES

TABLE Page

CHAPTER I

INTRODUCTION

1.1 Motivation

The arrangement of process equipment and buildings can have a large impact on plant economics. In effort to maximize plant efficiency, the design of plant layout should facilitate the production process, minimize material handling and operating cost, and promote utilization of manpower. The overall layout development should incorporate safety considerations while providing support for operations and maintenance. Good layout should also consider space for future expansion as well as access for installation, and thereby prevent design rework later. In plant layout, process units that perform similar functions are usually grouped within a particular block on the site. Each group is often referred to as a facility. In this proposal, the concept of facility is referred to any building or occupied unit such as control room and trailer (portable building), where operators can be exposed to any unsafe situation. In general, more land, piping, and cabling will increase the construction and operating costs, and can affect the plant economics. However, additional space tends to enhance safety. Therefore there is a need to integrate costs and safety into the optimization of plant layout. The Texas City refinery explosion on March 2005 has highlighted concerns for facility siting. Inadequate space between trailers and the isomerization process unit was identified as the contributing causes of fatalities [1].

This dissertation follows the style of *American Chemistry Society*.

One of the major causes of the accident in Flixborough (1974), which resulted in 28 fatalities, and Pasadena Texas, which led to 24 fatalities, was due to inadequate separation distances between occupied buildings (control rooms) and the nearby process equipment [2]. The siting of a hazardous plant near a densely populated area has resulted in fatal disasters, most notably in Seveso (1976) and Bhopal (1984) [3]. In the toxic gas released in Bhopal incident, major victims were not only workers within the plant but also residents who lived in the surrounding area [4]. Therefore, civilians who didn't partake in the risk assessment during the layout development should be considered in the stages of process design. The five of aforementioned incidents have similarity in contributing cause that the management can learn from. A preliminary identification of various hazards during early stages of layout development may substantially minimize the severity of damage. The aftermath of industrial disasters has shown that facility layout is an important element of process safety. Incidents associated to facility layout in chemical plants have brought material losses, environmental damage, and endangered human life.

1.2 Brief Literature Review

Ideally the plant siting and layout development should balance between risks and costs [5]. Few methods have been developed based on the location theory (heuristics approach) [6, 7], while others have focused on the optimization of economics of the optimal design to support decision makers in siting decisions [8-10]. However, research integrating risk assessment into the layout configuration has not been sufficiently reported in the

process safety area. Previous research in integrating safety in the optimization of plant layout has been partially reported. Penteado et al. developed a layout model to account for financial risk and protection device and assumed that the land occupied by each unit is characterized by a circular footprint [11]. This model was further evaluated with a rectangular footprint [12] and it incorporates the Dow Fire and Explosion Index (F&EI) as a risk analysis tool for evaluating new and existing plants [13, 14]. Other researchers have focused on risk evaluation of layout designs of particular cases at the conceptual level [15-17]. Literature reviews depending on each chapter have been explained in the corresponding contents for each chapter.

1.3 Purpose of This Research

From the safety viewpoint, plant layout is largely constrained by the need to maintain minimum safe separation distances between facilities. Adequate separation is often done by grouping facilities of similar hazards together. However, space among facilities is limited and will increase the capital costs (more land, piping, etc.) and operating costs as units are separated. If future plant modifications are anticipated which might impact separation distances, consideration should be given to employing larger initial separation distance and applying protection devices. Therefore, it is essential to determine minimum distances at which costs can be integrated in the plant layout optimization.

The approaches suggested in this proposal can be used to aid decision makers for low-risk layout structures and determining whether the proposed plant could safely and

economically be installed in a nearby residential area. With the motivation that well-arranged facility layout is very important to make the loss less inherently, and scarce researches from the literature review, it is essential to do research in order to obtain safer facility layout. Thus, including safety cost into the economic optimization of facility layout is suggested in this proposal. The safety cost term will be carefully considered to include in the objective function. Also, making the model closer to realistic is another issue to produce a better model. Toxic gas release and Vapor Cloud Explosion are related to wind effect a lot. With these two concepts, including safety cost due to hazards and making a more realistic model, the well-arranged facility layout will be obtained based on safety and optimization.

Another purpose of this research is the development of optimization formulation in achieving optimal layout in having hazardous situations. In continuous plane approach, the global optimal is not guaranteed due to non-linear functions such as risk formulations and the Euclidian distances in the objective function. In grid-based approach, all terms in the objective function has been linearized to make sure to have global optimal solutions.

1.4 Consequence Modeling

1.4.1 Dispersion Modeling of Toxic Materials

Building occupants or people near plants can be affected by toxic materials which are released to the atmosphere by process plants. Toxic vapors may enter a building and cause damage to the occupants because its concentration, and the exposure

time depending on the material[18]. The dispersion of toxic materials depend on many site-related factors, such as release conditions and the physical properties of the material, the weather conditions, the quantity released, obstacles, and the direction of the release. Dispersion models depict the airborne transport of toxic materials away from the accident site. The wind in a characteristic plume or a puff can carry away the airborne toxic materials. As the wind speed increases, the plume becomes longer and narrower; the toxic material is carried downwind quicker but is diluted faster by a larger amount of air.

Atmospheric stability relates to vertical mixing of the air. It is classified in three stability classes: unstable, neutral, and stable. For unstable atmospheric conditions the sun heats the ground quicker than the heat can be discharged so the air temperature near the land is higher than the air temperature at higher elevations, as might be observed in the early morning. This makes unstable stability since lower density air is below greater density air. This influence of buoyancy enhances atmospheric mechanical turbulence. For neutral stability the air above the land warms and the wind speed increases, reducing the outcome of solar energy input, or insolation. For stable atmospheric conditions the sun cannot heat the land as rapid as the ground cools; as a result the temperature near the land is lower than the air temperature at higher elevations. This situation is stable because the higher density air is below lower density air. The influence of buoyancy suppresses mechanical turbulence.

Ground conditions have an effect on the mechanical mixing at the surface and on the wind profile with height. Buildings and trees increase mixing, whereas open areas, like lakes, reduce it.

The height of releasing affects ground-level concentrations. As the release height increases, ground-level concentrations drop because the plume should disperse in a larger distance vertically.

The momentum and buoyancy of the released material alter the effective height of the release. The drive of a high-velocity jet will carry the gas higher than the released point, resulting in a much higher effective release height. If the gas has a density less than air, the released gas will be positively buoyant initially. If the gas has a greater density than air, then the released gas will be negatively buoyant initially and will slump toward the land. For all gases, as the gas moves downwind and is mixed with fresh air, a point will eventually be reached where the gas has been diluted adequately to be considered neutrally buoyant. At this point the dispersion is dominated by ambient turbulence.

Neutrally buoyant dispersion models are employed to guess the concentrations downwind of a release where the gas is mixed with fresh air to the point that the mixture becomes neutrally buoyant. Accordingly, these models concern low concentration gases, typically in the ppm range. There are two types of neutrally buoyant dispersion models, the plume model and the puff model. The steady-state concentration from a source continuously releasing is described as the plume model. The temporal concentration of material from a single release of a fixed amount of material is explained as the puff

model. The puff model can be used to describe a plume; Continuous puffs can be assumed as a plume simply. However, the plume model is easy to use and recommended if the required information is only steady-state plume.

Dispersion modeling equations described in Equation (1-1 to 1-13) are from the book "Chemical Process Safety" 2nd edition[3].

Let us suppose Qm is the instantaneous release amount into an infinite expanse of air. Then the concentration, C, of the material resulting from this release is given by the advection equation

$$\frac{\partial C}{\partial t} + \frac{\partial}{\partial xj}\left(u_j C\right) = 0 \qquad (1\text{-}1)$$

where the subscript j represents the summation for all coordinate directions x, y, and z, and u_j is the air velocity. Equation (1-1) may predict the concentration accurately if the wind velocity could be specified with position and time exactly, including the effects caused from turbulence. There are no models to adequately describe turbulence currently. As a result, an approximation can be used. Suppose the velocity is represented by a stochastic quantity and average

$$u_j = < u_j > + u_j' \qquad (1\text{-}2)$$

where $< u_j >$ is the average velocity and u_j' is the stochastic fluctuation by turbulence. Then the concentration, C, will also fluctuate as a result of the velocity field;

$$C = < C > + C' \qquad (1\text{-}3)$$

where C' is the stochastic fluctuation and <C> is the average concentration.

Because the fluctuations in both u_j and C are the mean or average values,

$$<u_j'> = 0, <C'> = 0 \qquad (1\text{-}4)$$

Substituting Equations (1-2) and (1-3) into Equation (1-1) and averaging the result over time yields

$$\frac{\partial <C>}{\partial t} + \frac{\partial}{\partial x_j}\left(< u_j >< C >\right) + \frac{\partial}{\partial x_j}\left(< u_j{}'C' >\right) = 0 \quad (1\text{-}5)$$

The turbulent flux term $<u_j'C'>$ is not zero and remains in the equation, though other terms are zero when averaged.

Another equation is required to explain the turbulent flux. An eddy diffusivity Kj (with units of area/time) is introduced for usual approach;

$$< u'_j C' > = -K_j \frac{\partial <C>}{\partial x_j} \quad (1\text{-}6)$$

Substituting eqn. (1-6) into eqn. (1-5) yields

$$\frac{\partial <C>}{\partial t} + \frac{\partial}{\partial xj}\left(< u_j >< C >\right) = \frac{\partial}{\partial x}(K_j \frac{\partial <C>}{\partial x_j}) \quad (1\text{-}7)$$

If the atmospheric is incompressible, then

$$\frac{\partial <u_j>}{\partial x_j} = 0 \quad (1\text{-}8)$$

And eqn. (1-7) becomes

$$\frac{\partial <C>}{\partial t} + < u_j > \frac{\partial <C>}{\partial xj} = \frac{\partial}{\partial x}(K_j \frac{\partial <C>}{\partial x_j}) \quad (1\text{-}9)$$

Pasquill-Gifford Model (Gaussian Model)

Generally K_j changes with wind velocity, time, and weather conditions. It is not convenient experimentally and not suitable for a useful correlation framework, though it is useful to use the eddy diffusivity approach theoretically. This difficulty is solved by suggesting the definition for a dispersion coefficient:

$$\sigma_x^2 = \frac{1}{2}\langle C\rangle^2 (ut)^{2-n} \quad (1\text{-}10)$$

The dispersion coefficients represent the standard deviations of the concentration in the downwind, crosswind, and vertical (x, y, z) directions, each with similar expressions for σ_y and σ_z. It is much easier to get values for the dispersion coefficients experimentally than eddy diffusivities. They are a function of the distance downwind from the release and atmospheric conditions. For a continuous source, σ_y and σ_z are given in Table 1.1 and 1.2. Values for σ_x are not provided assuming $\sigma_x = \sigma_y$,.

Table 1.1. Recommended Equations for Pasquill-Gifford Dispersion coefficients for Plum dispersion (the downwind distance x has units of meters).

Stability class		σ_y (m)	σ_z(m)
Rural conditions	A	$0.22x(1+0.0001x)^{-1/2}$	0.20x
	B	$0.16x(1+0.0001x)^{-1/2}$	0.12x
	C	$0.11x(1+0.0001x)^{-1/2}$	$0.08x(1+0.0002x)^{-1/2}$
	D	$0.08x(1+0.0001x)^{-1/2}$	$0.06x(1+0.0015x)^{-1/2}$
	E	$0.06x(1+0.0001x)^{-1/2}$	$0.03x(1+0.0003x)^{-1}$
	F	$0.04x(1+0.0001x)^{-1/2}$	$0.016x(1+0.0003x)^{-1}$
Urban conditions	A-B	$0.32x(1+0.0004x)^{-1/2}$	$0.24x(1+0.0001x)^{+1/2}$
	C	$0.22x(1+0.0004x)^{-1/2}$	0.20x
	D	$0.16x(1+0.0004x)^{-1/2}$	$0.14x(1+0.0003x)^{-1/2}$
	E-F	$0.11x(1+0.0004x)^{-1/2}$	$0.08x(1+0.0015x)^{-1/2}$

Equation (1-1 to 1-9) and (1-10) are used to derive a equation for Plume with continuous steady-state source at height H_r above ground level and wind moving in x direction at constant velocity u as:

$$\langle C\rangle(x,y,z) = \frac{Q_m}{2\pi\sigma_y\sigma_z u} exp\left[-\frac{1}{2}\left(\frac{y}{\sigma_y}\right)^2\right]$$

$$\times\left\{exp\left[-\frac{1}{2}\left(\frac{z-H_r}{\sigma_z}\right)^2\right] + exp\left[-\frac{1}{2}\left(\frac{z+H_r}{\sigma_z}\right)^2\right]\right\} \qquad (1-11)$$

The ground level concentration is found by setting z=0:

$$\langle C\rangle(x,y,0) = \frac{Q_m}{\pi\sigma_y\sigma_z u} exp\left[-\frac{1}{2}\left(\frac{y}{\sigma_y}\right)^2 - \frac{1}{2}\left(\frac{H_r}{\sigma_z}\right)^2\right] \qquad (1\text{-}12)$$

The ground-level centerline concentrations are found by setting y = z = 0:

$$\langle C\rangle(x,0,0) = \frac{Q_m}{\pi\sigma_y\sigma_z u} exp\left[-\frac{1}{2}\left(\frac{H_r}{\sigma_z}\right)^2\right] \qquad (1\text{-}13)$$

Equation (1-12) was used in Chapter II to describe the toxic gas dispersion. The gas concentrations of receptors, which were spread out from the release point, were calculated using equation (1-12). But there are some limitations to Pasquill-Gifford dispersion modeling. It applies only to neutrally buoyant dispersion of gases in which the turbulent mixing is the dominant feature of the dispersion. The concentrations predicted by Gaussian models are time averages and the model presented in Chapter II is 10-minute averaged. So when we use this model, the receptors in the effect model must inhale 10-minutes of toxic gas as a probit function. Actual instantaneous concentrations

may vary by as much as a factor of 2 from the concentrations computed using Gaussian models.

Dense Gas Model Box modeling: Dense Gas DISpersion (DEGADIS)

Gaussian models are typically used for neutrally buoyant gases, or so called light gases, which are lighter than air. For some gases denser (heavier) than air, another dispersion model is required to predict more a accurate concentration as well as the effect. The release of a heavier-than-air gas in the atmosphere has three stages: negative buoyancy-dominated dispersion, stable stratified shear flow, and passive dispersion. All stages must be integrated into the model to simulate it successfully.

DEGADIS was developed by Jerry Havens, et. al. at the request of USCG (Spicer & Havens,1986). DEGADIS is a dense gas dispersion model that predicts the ground level dispersion. The Richardson number is used to determine what stage is dominant. By using the following equation:

$$R_i = \frac{g}{U^2}\left(\frac{\rho-\rho_a}{\rho_a}\right)\left(\frac{\dot{M}}{\rho UD}\right) \qquad (1\text{-}14)$$

$R_i \leq 1.0$ Release essentially passive from the source i.e., passive dispersion

$1.0 \leq R_i \leq 30$ No significant lateral spreading i.e., stably stratified shear flow

$R_i \geq 30$ Significant upstream spreading i.e., dense gas dominant

where g is the acceleration due to gravity, ρ is the cloud density, ρ_a is the ambient air density and *U* is the wind velocity, assumed to be constant in x-direction.

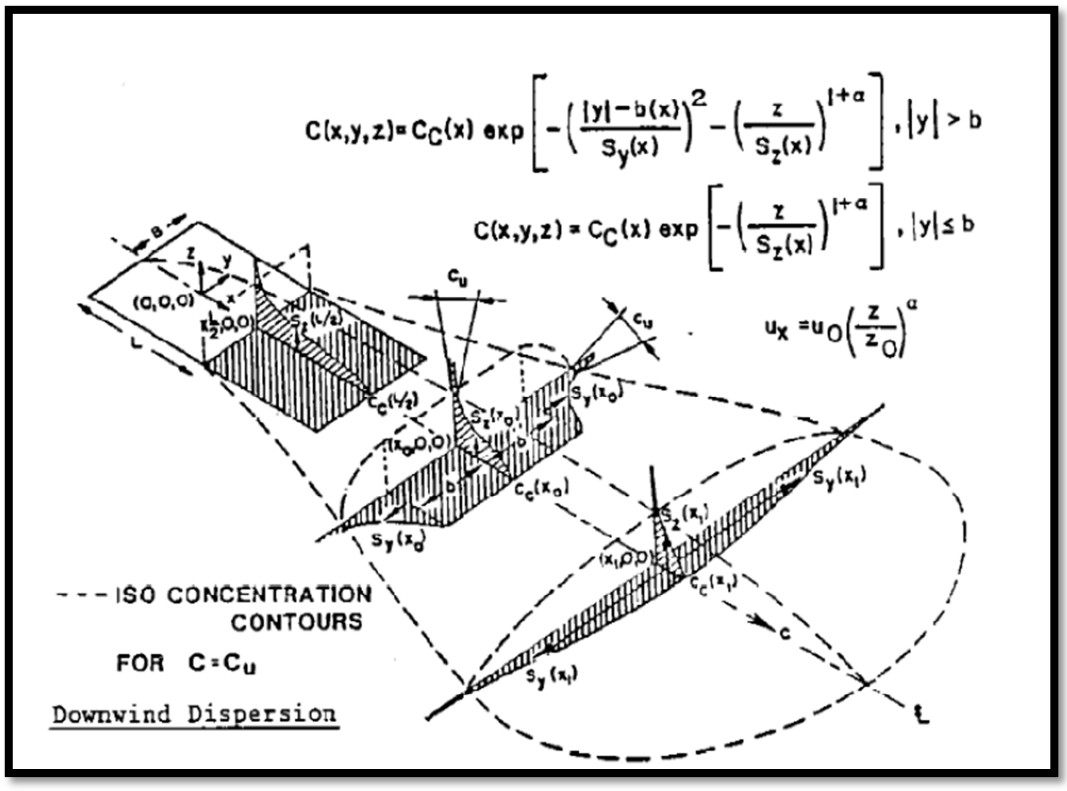

Fig. 1.1. Vapor modeling in DEGADIS (Spicer & Havens, 1987)
This figure was reproduced by permission from Spicer, T. O., & Havens, J. A. (1987). Field test validation of the DEGADIS model. *Journal of Hazardous Materials*, *16* (1987), 231-245.

DEGADIS is divided into three different codes for each regime with respect to the Richardson number. The negative buoyancy dispersion phase is based on experimental data from a laboratory release performed by Havens and Spicer(Spicer & Havens, 1986). For the stably stratified shear flow phase, it is also modeled from experimental laboratory data. Established passive atmospheric dispersion modeling principles are used for the passive dispersion phase (i.e., Gaussian modified). The concentration profile used the first two equations illustrated in Figure 1.1. The wind profile is developed with the following equations, where α is evaluated from the stability

conditions, also illustrated in Figure 1.1. The source model represents an averaged concentration of gas present over the primary source, while the downwind dispersion phase of the calculation is shown in Figure 1.2. A secondary source is created on top of the initial source for the vapor dispersion model shown in Figure 1.1. The near field buoyancy regime is modeled by using a lumped parameter model of a denser-than-air gas "secondary source" cloud which incorporates air entrainment at the gravity spreading front using a frontal entrainment velocity. The downwind dispersion phase assumes a power law concentration distribution in the vertical direction and a modified Gaussian profile in the horizontal direction with a power law specification for the wind profile.

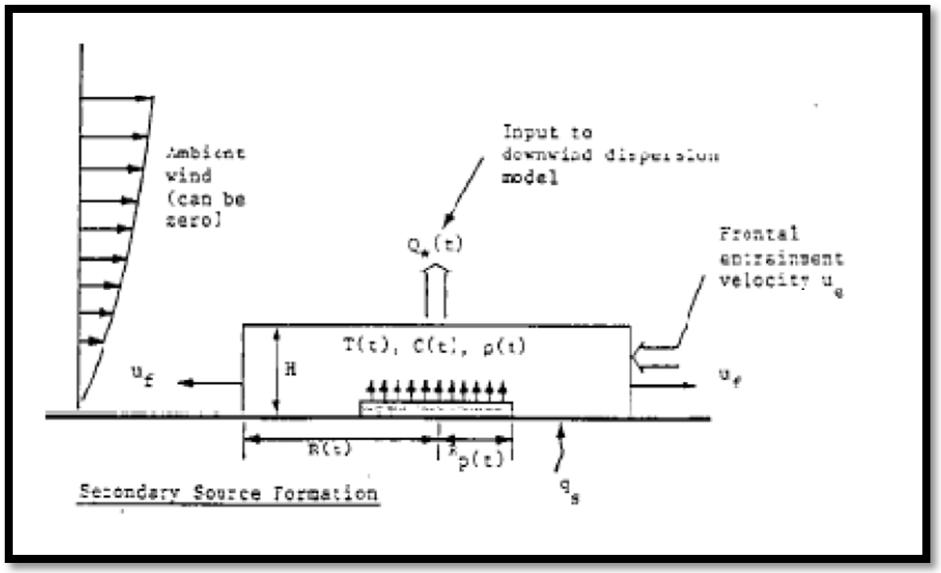

Fig. 1.2. Source modeling in DEGADIS (Spicer & Havens, 1987, Spicer & Havens, 1989). This figure was reproduced by permission from Spicer, T. O., & Havens, J. A. (1987). Field test validation of the DEGADIS model. *Journal of Hazardous Materials*, *16* (1987), 231-245.

DEGADIS has been used in Chapter II to calculate toxic effect in the area and in Chapter IV to calculate dispersed amount of flammable gas.

1.4.2 Fire and Explosion Modeling

When flammable gases are released, various consequences can occur depending on the process condition, ignition source, material property, and weather situation. Types of fires and explosions include Jet fire, Flash fire, Pool fire, Running liquid fire, Boiling liquid expanding vapor explosion (BLEVE) or fireball, and Vapor cloud explosions. Chapters III and IV address these consequences for the probability of structural damage. Thus in this section VCE and BLEVE mechanisms and models are described with a detailed background for those chapters.

1.4.2.1 Vapor Cloud Explosion (VCE) modeling (Baker-Strehlow-Tang Method) in (PHAST 6.53.1)

In this dissertation two methods to calculate VCE overpressures have been used, one in TNT-equivalency model described in Chapters IV and the other is BST method which is described as follows.

Baker and Tang have given graphs of scaled overpressure P_s against scaled distance R_s for eleven different values of flame speed, and graphs of scaled impulse I_s against scaled distance R_s for nine different values of flame speed, where the scaling is as follows:

$$K_{scale} = \left(\frac{E_{exp}}{P_{amb}}\right)^{\frac{1}{3}}$$

$$R_S = \frac{R}{K_{scale}}$$

$$P_S = \frac{P}{P_{amb}}$$

$$I_S = \frac{Iv_{sound}}{K_{scale}P_{amb}}$$

(1-15)

where P_{amb} is ambient pressure, E_{exp} is the explosion energy, P is the explosion overpressure, R is the distance of interest, I is the impulse, and v_{sound} is the speed of sound in air.

In order to get the impulse and overpressure at a given distance, the value of R_s needs to be calculated for that distance, then use lookup tables to obtain the value of I_s and P_s for a flame speed. I_s and P_s for the flame speed are obtained by interpolation, and I_s needs to be convert to an impulse and P_s to an overpressure.

The energy of the explosion is calculated as:

$$E_{exp} = m_{exp}R_{Ground}H_{Combustion}$$

$$m_{exp} = min\left[\rho_f(P_{amb}, T_{amb})V_cC_T, m_f\right]$$

$$m_f = min\left[f_{vapor}F_{mod}, 1\right]M_{flam}$$

(1-16)

where R_{Ground} is the ground reflection factor, taken from the input data, $H_{Combustion}$ is the heat of combustion of the material, taken from the Properties Library, ρ_f is the ideal gas

fuel density at P_{amb} and T_{amb}, V_c is the confined volume set, C_T is the stochiometric ratio for the fuel, f_{vapor} is the post-flash vapor fraction, F_{mod} is the Early Explosion Mass Modification Factor, and M_{flam} is the total flammable mass in the release. The mass of flammable material is calculated from the concentration profile for the cloud at the time of the explosion.

Assuming that air behaves ideally at ambient conditions, the speed of sound in air is calculated as:

$$v_{sound} = \sqrt{\frac{\gamma_{air} R_g T_{amb}}{M_{air}}} \tag{1-17}$$

where γ_{air} is the ratio of specific heats for air, T_{amb} is the ambient temperature, and M_{air} is the molecular weight of air.

If a value for the Mach Number is supplied, that value will need to be used directly. Otherwise the value needs to be calculated as described in the following.

The Lagrangian flame speed needs to first be obtained; this refers to the velocity of heat addition following ignition, measured relative to a fixed observer. The Lagrangian flame speed is a function of the geometry (i.e. whether the flame is able to expand in one, two or three dimensions) of the reactivity of the material, and of the density of obstacles. These are all taken from the input data, and the flame speed is obtained from the table below. Values in Table 1.2 have been used for the Lagrangian flame speed.

Table 1.2. Lagrangian Flame Speed value on fuel reactivity and obstacle density.

Flame expansion	Fuel reactivity	Obstacle density		
		High	Medium	Low
1D	High	5.2	5.2	5.2
	Medium	2.265	1.765	1.029
	Low	2.265	1.029	0.294
2D	High	DDT	DDT	0.588
	Medium	1.6	0.662	0.47
	Low	0.662	0.471	0.079
3D	High	DDT	DDT	0.36
	Medium	0.5	0.44	0.11
	Low	0.34	0.23	0.026

DDT stands for Deflagration to Detonation Transition. The flame-speed tables do not suggest a numeric value for flame speed to simulate DDT. The flame expansion value can be selected between 1 and 3, depending on the situation.

The Baker-Strehlow-Tang curves describe the behavior of explosions as a function of the explosion's prevailing Eulerian flame speed, v_{flame}, which refers to the velocity of heat addition following ignition, measured relative to a fixed observer.

The BST model uses a simple, direct relationship between the Lagrangian and Eulerian flame speeds, and the program obtains the value of the Eulerian flame speed from Table 1.3. using linear interpolation where necessary to obtain the Eulerian flame speed for an intermediate value of the Lagrangian flame speed:

Table 1.3. Eulerian Flame Speed value for an intermediate value of the Lagrangian.

Mach Number	
Lagrangian	Eulerian
0.037	0.070
0.074	0.120
0.125	0.190
0.250	0.350
0.500	0.700
0.750	1.000
1.000	1.400
2.000	2.000

Data extracted from published plots for each flame-speed curve have been categories into three regions (PHAST 6.53.1).

1.4.2.2 BLEVE Modeling (PHAST 6.53.1)

The blast effects of BLEVEs are caused by the expansion of vapor and the rapid flashing of liquid in the vessel when the pressure drops drastically to atmospheric pressure by releases or cracks. A BLEVE can occur when the vessel contains a liquid above its atmospheric pressure. BLEVE process is started from an expansion of the initial volume which causes a shock wave thattravels faster than sonic speed. The steps are as followings. A fire occurs and develops near a vessel which contains liquid and the fire heats up the vessel → The wall of vessel below liquid level are cooled by liquid and the liquid's T and P are increased → If the flames touch some part of the vessel, the

temperature rises until the vessel loses its strength → The vessel ruptures, vaporizing its content explosively.

The most important parameters for predicting structural damage at a certain position are the peak overpressure and the impulse for the duration of positive pressure of the main shock. In order to determine the effects by blast, it is important to have the explosion energy as a main variable.

A thermodynamic approach is to use the model used in the BLEVE simulation of the PHAST program to calculate the explosion energy, where the energy is given by the difference between the internal energy of the material before and after the explosion. There are two main approaches to calculate the energy, by treating the material as an ideal or a non-ideal gas. The model assumes isentropic expansion for the non-ideal gas. The model employs a set of curves for the scaled impulse I_s and the scaled overpressure P_s as a function of scaled distance R_s:

$$K_{scale} = \left(\frac{E_{exp}}{P_{amb}}\right)^{\frac{1}{3}}$$

$$R_S = \frac{R}{K_{scale}}$$

$$P_S = \frac{P}{P_{amb}}$$

$$I_S = \frac{Iv_{sound}}{K_{scale}P_{amb}}$$

(1-18)

where P_{amb} is ambient pressure, E_{exp} is the explosion energy, P is the explosion overpressure, R is the distance of interest, I is the impulse, and v_{sound} is the speed of sound in air, which is exactly the same as Equation (1-15) so far.

This set of curves includes curves obtained by using a finite-difference method to predict the effects from a free-air burst of a spherical vessel containing an ideal gas, and also a curve obtained from experimental data for a high-explosives (Pentolite). The model uses different curves as Table 1.4. depending on whether ideal or non-ideal modeling is selected for the Model and depending on the value for the scaled distance:

Table 1.4. Curve for the model.

Model	**Distance**	**Over-Pressure**	**Impulse**
Ideal Gas	Near-Field	Gas-vessel curves	Gas-vessel curves
Ideal Gas	Far-Field	Pentolite curve	Gas-vessel curves
Non-Ideal Gas or Liquid	All	Pentolite curve	Gas-vessel curves

1.5 Research Summary and Objectives

Given optimization theories, we believe facility layout optimization can be developed with the incorporation of a Quantitative Risk Analysis approach. The principal goal of the following work is to understand how to develop the methodology for facility siting and layout. To this end, several objectives were developed:

1) Methodology using MINLP and Gaussian dispersion model with Monte-Carlo simulation against toxic gas release scenario (Chapter II)
2) Methodology using MINLP and DEGADIS with Monte-Carlo simulation against toxic gas release scenario near a residential area (Chapter III)
3) Methodology using MINLP (continuous plane approach) and PHAST 6.53.1 for consequence modeling against fire and explosion scenarios (Chapter IV)
4) Methodology using MINP (grid-based approach) and PHAST 6.53.1 for consequence modeling against fire and explosion scenarios (Chapter V)

Codes for Chapters II, III, and IV have been made using GAMS. The code in Chapter III is upgraded from the code in Chapter II only for a protection device approach. Thus Appendix A includes the code corresponding to Chapter III, and Appendix B includes the one for Chapter IV. The code used for Chapter V has been made using AMPL and it is in Appendix C.

CHAPTER II

OPTIMAL FACILITY LAYOUT FOR TOXIC GAS RELEASE SCENARIOS *

2.1 Introduction

Process layout is a multidisciplinary area by nature that demands help from different specialists such as civil, mechanical, electrical, and instrument engineers. The layout problem can be defined as allocating a given number of facilities in a given land to optimize an objective function that depends on the distance measure between facilities, subject to a variety of constraints on distances. Thus, process layout concerns the most economical spatial allocation of process units and their piping to satisfy their required interconnections. Starting with the full plant flow diagrams, this activity has been associated to the process design stage: the process design should not be declared as done if the plant layout has not been covered. Furthermore, facility layout problems also occur if there are changes in requirements of space, people or equipment.

The importance of the optimization approach is easy to understand by considering that piping costs can run as high as 80% of the purchased equipment cost [19], whereas 15-70% of total operational costs depends on the layout [20]. Experienced engineers also consider that the effect of several accidents could have been minimized with a better process layout. Hence, an appropriate layout must balance several factors such as sustainability by simply keeping space for future expansions, environmental

---

*Reprinted with permission from "Optimal Facility Layout under Toxic Release in process facilities: A stochastic approach" by R. Vázquez, J. Lee, S. Jung, and M. S. Mannan, Computers and Chemical Eng. 34 (2010) 122-133. © 2010 by Elsevier B.V.

concerns, efficiency, reliability and safety in plant operations, construction, land area and operating costs [21]. A good review on solving the facility layout problem can be found in [22]. In the past, the distribution of process units followed simple common sense rules such as following the order in the process and separating adjacent units by sufficient distances to allow all operations without waste of space [6, 7, 23]. The inherent difficulty is provided by the large number of possible combinations that exist when the problem contains even a rather small number of facilities to accommodate [24]. The complete problem is frequently divided into modules that are easier to solve and can be solved in a sequence [25]. In general, the approach based on heuristics does not yield optimal solutions but the approach can be improved by using this result as an initial assignment, *i.e.* a starting distribution. Thus, the initial layout can be evolved to eventually obtain a lower objective value. This strategy has been combined with Graphs Theory to generate a two-stage heuristic where the first stage consists of generating a hexagonal and maximum weight planar adjacency sub-graph while a tight upper bound is derived based on integer programming; then, the graph is converted into a rectangular block layout during the second stage [26]. Graph Theory has also been used to formulate algorithms for multi-floor facility layouts [27]. Several research papers using the Graph-Theoretic approach have been published where different algorithms and models have been explored [9, 10, 28-30]. Fuzzy set techniques have been added to this approach to analyze manufacturing firms [31].

The use of stochastic techniques has also been proved to be effective in obtaining practical solutions for the plant layout. A review of the use of early genetic algorithms in

layouts can be found in [32]. These methods do not guarantee the global optimum but they are able to solve optimization problems containing non-differentiable objective functions [33]. The sample average approximation method was used in a Monte Carlo simulation to solve the routing problem by considering it as a stochastic problem [34]. Genetic algorithms have been developed to solve layout problems in the fashion industry [35] and in manufacturing systems [36] in an acceptable amount of time. The packing problem, similar to the layout case, have been also solved using this approach [37]. A heuristic method within which another local heuristic search procedure is used at each step, regarded as a meta-heuristic approach, has been applied in the layout of manufacturing systems via simulated annealing [32, 38-40]. A comparison of both approaches genetic algorithms and simulated annealing has been done while solving the multi-period planning for the dynamic layout problem [41].

Programming techniques have been also applied in solving the layout problem. While analyzing the arrangement of departments with certain traffic intensity, it was shown that the linear ordering problem is strongly NP-hard [42]. It clearly reflects the degree of difficulty that the layout problem represents. The facility layout problem has been originally formulated as a quadratic assignment problem (QAP) in [43]. Several algorithms have been proposed based on the QAP to specifically solve the challenging layout problem [44, 45]. The equivalence of the QAP to a linear assignment with certain additional constraints have been demonstrated [46]. The contour line procedure developed for the optimal placement of a finite sized new facility in the presence of other facilities

[47] has been extended to the presence of arbitrarily shaped barriers under rectilinear travel to layout rectangular facilities [48, 49].

Mixed integer programming has received great attention to model the layout problem. Several models were produced by linear extension of the QAP that generate an MIP [50-52]. A new formulation for fixed orientation and rectangular shape of facilities was proposed where the big-M was first applied to improve the numerical calculation [53]. A two-step approach was proposed to solve the dynamic facility layout with unequal areas [54, 55]. The plot plan problem, *i.e.* allocation of process units, has been formulated as an MINLP; however, it was converted to a mixed integer linear program (MILP) to ensure a numerical solution [10]. Several MILP models have appeared where different particularities of the layout are solved by an ad hoc method or commercial package where the common part is the use of the big-M method to model disjunctions [56-61]. Improvements to the big-M formulation for the layout problem have been obtained via the convex-hull approach [62].

All above cited research work did not consider safety beyond the typical minimum separation distance constraints. Numerically, the non-overlapping constraint is a difficult problem because it results in a very non-convex feasible region and it ends up in having several local optimum points. In these cases, MILP formulation gives a reasonable representation of the overall layout problem to satisfy some given distance standards. However, extending the optimal layout determination with more safety issues will unavoidably lead to an MINLP. An extremely reduced number of papers have been published in this area: a model was developed to include the associated financial risk

with protection barriers cost where footprints of process units are assumed circular [11]. This model was extended [12] to include rectangular shape in the footprint and to include the Dow Fire and Explosion Index [13, 14]. The risk analysis of layout designs, without using a programming formulation, for particular cases have been also published [15-17, 63].

There is a need for better integration of safety and risk assessment in the optimal plant layout. In this chapter, a disjunctive program associated to the facility layout problem is modeled with the convex-hull approach. The system includes both existing and siting facilities. Then, the effect on the layout of having toxic release from any existing facility is included in the model. The following section contains a description of the problem to continue with the model formulation. Next, the reformulation of the problem as an MINLP is presented to continue with the results for a case study. Finally, the conclusions of this research are established.

2.2 Problem Statement

Solving the process layout problem has represented a creative task that traditionally demands experienced engineers in particular during the design stage. The rational behind is that it would be quite expensive to modify the layout once the site is constructed. The task can be divided in three main parts as follows. The first part corresponds to the "plot layout" and it concerns the finding of the best distribution of the process units in a given land. To essentially facilitate the access for firefighting, some units such as containers are separated from the rest of the units to form a facility. In addition, there already exist more facilities to provide services to the process under

siting or even facilities corresponding to other processes. In fact, it could be that several processes are to be sited in the whole land. The second part of the task refers to the facility layout problem where several facilities are to be accommodated in a given land. The third part corresponds to the pipe routing problem which is partially absorbed in the two previous parts and it is based on the interconnectivity between process units or facilities. This work concerns with the second part of the layout process, *i.e.* facility siting. Indeed the concept of facility has been extended to include the control room.

Placement one or more new facilities in the presence of existing facilities can be considered as a restricted layout problem where the existing facilities will act as barriers in the layout where a new facility placement is not permitted. It is considered here that the footprint of a facility can always be represented in a rectangular shape by its *(x,y)*-coordinates of the center point and corresponding length and depth values.

The minimum separation distance between facilities must include the width of the street to bring access for firefighting. The separation distance can increase to reduce toxic or escalating effects. Several examples of serious accidents emphasize the importance of improving the facility layout [6, 64]. This work aims at solving the layout when toxic release might occur in an already installed facility. A toxic release model is then required to estimate the effect of a release not only on the plant but on the community environment. Rather than providing direct risk assessment, this work is focus on showing the possibility of optimizing the facility layout using a particular scenario. There is no model comprehensive enough as to directly incorporate the effects of toxic release into a single optimization formulation. However, it is considered that the

strategy developed here can easily be adapted to different scenarios. The model should include the environmental factors affecting the atmospheric dispersion of toxic materials such as wind speed, wind direction and atmospheric stability [3]. This information should be provided for the geographic site where the facilities will be sited. The wind rose is thus divided in n_{slice} slices of equal size and the probability of death resulted from the toxic gas released is assumed to decay exponentially with distance in each slice direction. Thus, the overall problem is established as follows:

Given

- a set of already installed facilities $i \in I$;
- a set of facilities for siting $s \in S$;
- a set of release types $r \in R$;
- a subset of installed facilities $i \in I$ having a particular release $r \in R$, i.e. $ri(i,r)$, and displacement values, dx_{ri} and dy_{ri} to identify the exact releasing point with respect to the center of the releasing *i*-facility;
- the facilities interconnectivity for both types installed and siting facilities;
- length and depth of each facility for siting, Lx_s and Ly_s;
- length and depth of each installed facility, Lx_i and Ly_i, as well as their center point, (x_i, y_i);
- maximum length, Lx, and depth, Ly, of land;
- size of the street, *st*;

- parameters to calculate the probability of death in each facility that include expected population in the facility, number of slices with parameters to calculate the probability of death in each slice direction and the release frequency factor ;
- cost of pipe per meter, Cp ; cost per m^2 of land, L_C; fatal injury cost per each person in an accident, c_{pp} ; and life time of the layout, t_l .

Determine

- each siting facility center position (x_i, y_i);
- the occupied area out of the total land;
- the final piping, land and risk cost associated to the optimal layout;

To minimize the total plant layout cost.

2.3 Mathematical Formulation

The formulation in this section minimizes an objective function that contains land, piping and risk costs subject to the land, non-overlapping, and toxic-release-related constraints. The model is described in detail next.

2.3.1 Land Constraints

The siting facility must be placed inside the available land having a street around it to facilitate the firefighting job. Thus, the center point for any siting facility satisfies:

$$\frac{Lx_s}{2} + st \le x_s \le Lx - \left(\frac{Lx_s}{2} + st \right) \tag{2.1}$$

$$\frac{Ly_s}{2} + st \le y_s \le Ly - \left(\frac{Ly_s}{2} + st \right) \tag{2.2}$$

For the sake of simplicity, the East is represented by the direction *(0,0)* to (∞,0) and the North by the direction *(0,0)* to *(0,∞)*.

2.3.2 Non-overlapping Constraints

Two facilities cannot occupy the same physical space. To avoid this situation in the numerical solution, a disjunction is proposed by considering two facilities s and k. To accommodate facility *s* with respect to facility *k*, we start by expanding the footprint of facility *k* by the street size. Then, facility s could be layout anywhere on region "*L*", anywhere on region "*R*" or at the center in which case it would lay either in region "*A*" or "*D*", as indicated in Figure 2.1. The resulting disjunction used here is:

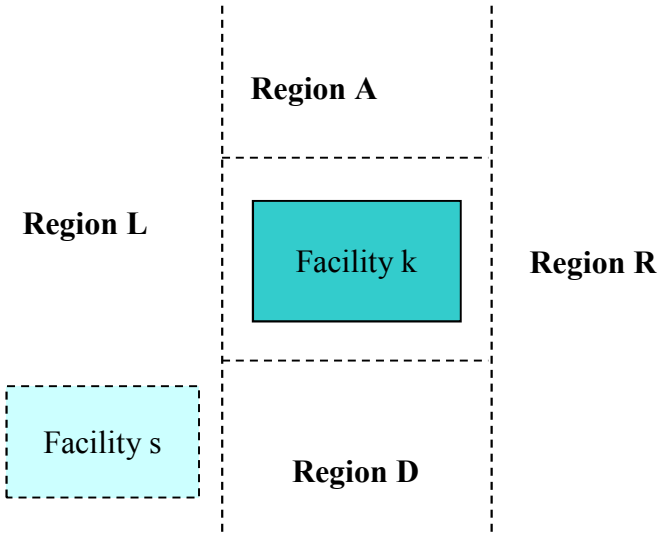

Fig. 2.1. Non-overlapping constraint.

$$\begin{bmatrix} "L" \\ x_s \le x_k - D_{s,k}^{\min,x} \end{bmatrix} \vee \begin{bmatrix} "R" \\ x_s \ge x_k + D_{s,k}^{\min,x} \end{bmatrix} \vee \begin{bmatrix} "A","D" \\ x_s \ge x_k - D_{s,k}^{\min,x} \\ x_s \le x_k + D_{s,k}^{\min,x} \\ \begin{bmatrix} "A" \\ y_s \ge y_k + D_{s,k}^{\min,y} \end{bmatrix} \vee \begin{bmatrix} "D" \\ y_s \le y_k - D_{s,k}^{\min,y} \end{bmatrix} \end{bmatrix} \tag{2.3}$$

being,

$$D_{s,k}^{\min,x} = \frac{Lx_s + Lx_k}{2} + st \tag{2.4}$$

$$D_{s,k}^{\min,y} = \frac{Ly_s + Ly_k}{2} + st \tag{2.5}$$

where the facility *s* is a siting facility but facility k can be either a siting facility or an already installed facility.

2.3.3 Toxic Release Constraints

It has been indicated above that meteorological conditions produce a direct influence in the layout under potential toxic release. Even the simplest model requires an estimate of the wind speed, wind direction and atmospheric stability while more complicated models require additional details on the geometry and other information on the release [65]. The problem to solve here can be established as follows: for a given source facility in which a continuous release is assumed, estimate the concentration profile over any target facility for siting in all possible positions that the receptor can

take. There are two ways to estimate the uncertainty propagation of the stochastic meteorological variables into the concentration estimation: applying the method of moments and Monte Carlo type methods [66]. The second way is used here to perform the required estimation since the advantage of Monte Carlo simulation in toxic release has been recently demonstrated [67]. A similar approach where directional or geographical effect can be quantified has been developed recently [68].

The variability nature of the weather represents a stochastic event where data is required to provide information about its probability distribution. Hence, a distribution function based on historical data must be developed and, then, Monte Carlo simulation can take thousands of random samples to calculate the expected values required as input values in the model. The approach used here to estimate the stochastic meteorological variables is given below.

The National Climatic Data Center in USA provides an hourly report of meteorological data at earth's surface, between ground level and 10 m height, which contains measured values of temperature, dew point, wind direction, wind speed, cloud cover, cloud layers, ceiling height, visibility, current weather and precipitation amount. A compilation of this information and solar data for the period 1961-1990 can be obtained from the Solar and Meteorological Surface Observation Network (SAMSON). Weather service locations as well as solar data provided by the National Renewable Energy Laboratory (NREL) are available on CDs and more information on meteorological data can be obtained in the Environmental Protection Agency [69]. These data is used here to estimate the following three important factors for the model:

- Wind direction

The probability of wind direction can be obtained from meteorological databases. Day and night data are treated in a separated way since there are meaningful differences in the historical behavior. For this purpose, it is considered nighttime here as the time from one hour before sunset to one hour after sunrise. These times can be calculated with the algorithm provided by the National Oceanic and Atmospheric Administration of the Department of Commerce [70]. To illustrate the procedure, the wind rose for Corpus Christi using 86096 records from SAMSON during the period 1981-1990 was calculated. The angular direction was divided in discrete intervals representing slices of 10º. Then the cumulative distribution function was determined. Figure 2.2 shows the wind direction distribution and the associated cumulative probability function.

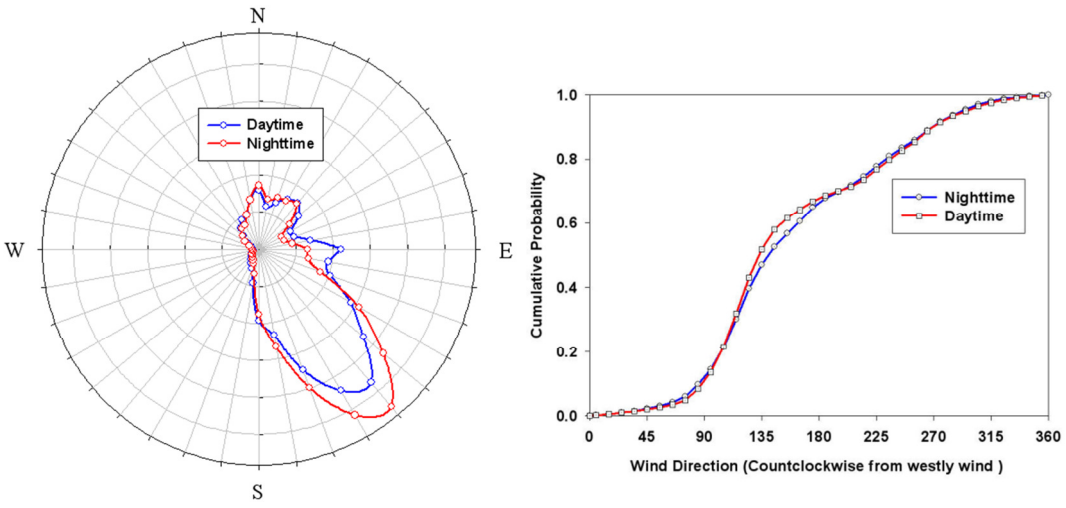

Fig. 2.2. Wind direction distribution in Corpus Christi.

- Wind speed

It has been observed that low wind velocity tends to cause severe effect on receptors because it remains undiluted in air. [71, 72] found that the actual wind velocity never exceeded a value of 6 m/s while analyzing 165 vapor cloud explosion accidents. However, low wind speed will not influence the layout since the concentration will not achieve high risk levels in long distances. A review of wind speed distributions indicates that the Weibull distribution is the preferred probability function applied in investigations [73]. Data of wind speed for Corpus Christi from the same above indicated source was used to fit the Weibull parameters with the classic least square method. Figure 2.3 shows the resulting frequency percent vs. wind speed curve.

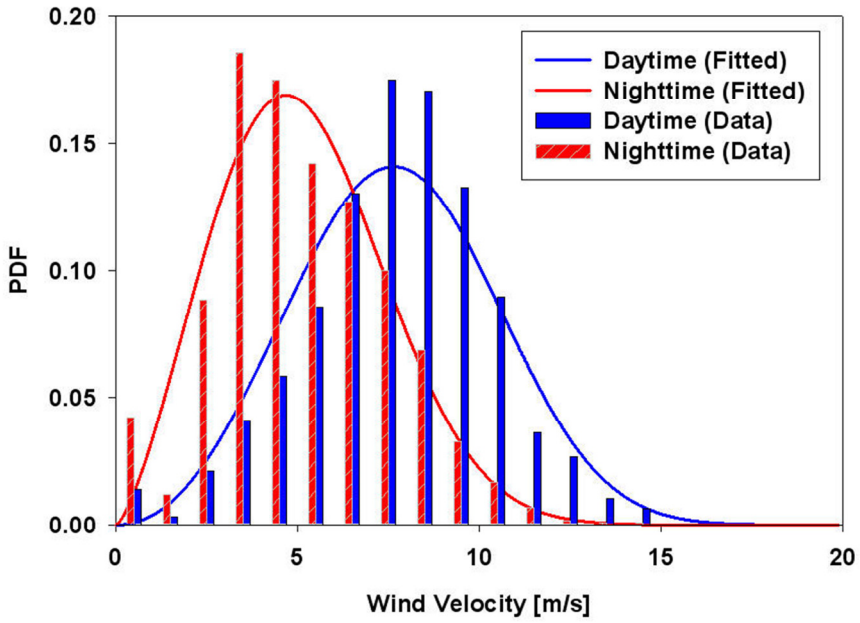

Fig. 2.3. Wind speed distribution in Corpus Christi.

- Air stability

Lateral and vertical dispersion of air for release models depends on the environmental air stability. The recommended stability scheme in regulatory air quality modeling applications is the scheme proposed by Pasquill, often referred as the Pasquill-Gifford model, see for instance [3, 74]. Then, a method to determine the stability according to this model based on typical data collected at National Weather Service stations can be used [75]. This method considers solar radiation and wind speed effects. Figure 2.4 gives the calculated probability of air class distribution in Corpus Christi.

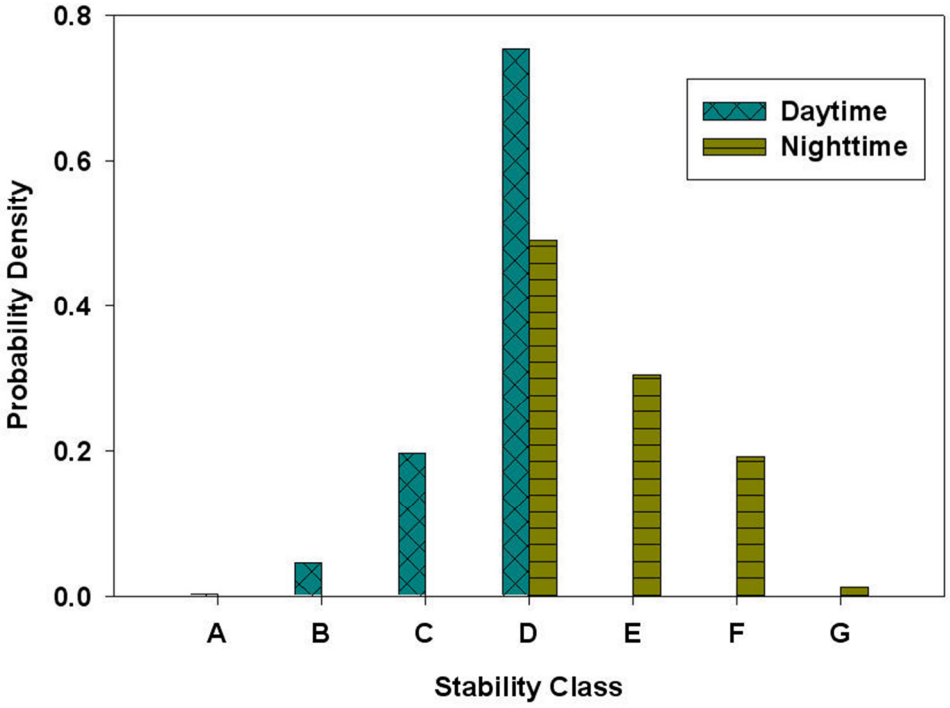

Fig. 2.4. Probability distribution of air stability in Corpus Christi.

Monte Carlo simulation is applied where values for the three above stochastic variables are randomly generated. These values are used in the appropriate equations, according to a release scenario, to calculate the concentration in every receptor point. This value could then be compared to some references according to the releasing substance. The definition and derivation of what is called a dangerous doses typically used in Quantitative Risk Assessments (QRA) has been described in detail by others [76]. In fact, the experimental response to several doses results in an asymmetrical S-shaped curve that is usually represented with the probit function [77, 78].

The probit function, originally proposed in [79, 80], transforms the dose-response curve to a linear relationship according to the following equation:

$$\mathrm{Pr} = \beta_0 + \beta_1 \ln(C^2 t) \tag{2.6}$$

where Pr is the probit variable, C is the concentration, t is the exposure time, and β_0 and β_1 are fitted parameters.

Thus a probit function is used at each point to convert the concentration of a toxic substance into probability values. The probit variable is normally distributed with mean value *5* and a standard deviation of one. The mean value of *5* is kept because there are several probit functions in the literature developed for several substances; however, those who are familiar with statistical methods may prefer using the typical mean value *0*. The probit value is related to the probability of death, *P*, by the following expression [81]:

$$P(\Pr) = \frac{1}{\sqrt{2\pi}} \int_{-\infty}^{\Pr-5} \exp\left(-\frac{u^2}{2}\right) du \tag{2.7}$$

This probability of death is calculated for a given direction at several distances. Assuming exponential decay, least squares are then used to fit these data for each slice to the following expression:

$$P_\alpha(d_{r,\alpha}) = a_\alpha e^{-b_\alpha d_{r,\alpha}} \tag{2.8}$$

where $d_{r,\alpha}$ is the distance from the release point r in the direction slice α, $P_\alpha(d_{r,\alpha})$ is the probability of death at distance $d_{r,\alpha}$, a_α and b_α are the corresponding parameters that fit the data to an exponential decay in slice direction α. Equation (2.8) provides the death probability of the receptor under the uncertainty of wind behavior.

To apply the described model to the facility layout problem, the first part consists of detecting the direction of each siting facility, *s*, with respect to the releasing facility. For the sake of simplicity, it was considered that only installed facilities, *i*, can release toxic materials, *r*. Thus, the following disjunction is proposed to determine the slice direction:

$$\bigvee_{i \in ri} \begin{bmatrix} \text{"}\alpha - \text{interval"} \\ s_\alpha^{\Delta y}(y_s - y_i) \geq 0 \\ s_\alpha^{\Delta x}(x_s - x_i) \geq 0 \\ s_\alpha^{\Delta x}(y_s - y_i) \leq s_\alpha^{\Delta x} m_\alpha (x_s - x_i) \\ s_\alpha^{\Delta x}(y_s - y_i) \geq s_\alpha^{\Delta x} m_{\alpha-1}(x_s - x_i) \end{bmatrix} \tag{2.9}$$

where m_α is an n_{int}-vector where each element represents the slope evaluated in each α slice angle:

$$m_\alpha = \left(\tan\left(\frac{2\alpha\pi}{n_{\text{int}}} \right) \right) \tag{2.10}$$

and $S_\alpha^{\Delta x}$ and $S_\alpha^{\Delta y}$ are convenient n_{slice}-vectors having elements with either positive or negative ones. These vectors are used to determine in which quadrant the facility *s* is positioned with respect to the releasing facility *i*: slices referring to the first quadrant will have positive ones in the elements of both $S_\alpha^{\Delta x}$ and $S_\alpha^{\Delta y}$ vectors, slices referring to the second quadrant will have positive ones in $S_\alpha^{\Delta y}$ and negative ones in $S_\alpha^{\Delta x}$, slices referring to the third quadrant will have negative ones in both $S_\alpha^{\Delta x}$ and $S_\alpha^{\Delta y}$, and slices referring to the fourth quadrant will have positive ones in $S_\alpha^{\Delta x}$ and negative ones in $S_\alpha^{\Delta y}$.

Therefore, the above disjunction leads to conveniently constraint n_{slice} to be strictly divisible by four. Disjunction (2.9) indicates that facility s is situated in the slice α if the four equations in the disjunction are satisfied. Let us take for example the case of having 16 slices with facility *s* in slice *3*. Then $S_3^{\Delta x} = S_1^{\Delta y} = 1$, $m_3 = \tan(3\pi/8)$, $m_2 = \tan(2\pi/8)$ and the four constraints are satisfied whereas all other slices contains at least one equation that cannot be satisfied.

The probability of death in facility s because of release type k in facility I is obtained from,

$$P_{death_{i,r,s}} = a_{i,r,\alpha*} \cdot e^{-b_{i,r,\alpha*} d_{i,s}} \tag{2.11}$$

where $\alpha*$ refers to the valid slice for the facility *s* respect to facility *i* with release *r* and $d_{i,s}$ is the Euclidian separation distance between both facilities. For the sake of simplicity, the release effect will be evaluated at the center point of the receptor facility.

2.3.4 The Objective Function

There are three costs considered here for the optimization of the facility layout: piping cost, land cost and financial risk. The Euclidian distance is used to evaluate the separation between two facilities from center to center, i.e.

$$d_{ij}^2 = (x_i - x_j)^2 + (y_i - y_j)^2 \tag{2.12}$$

where d_{ij} is the separation distance between facilities *i* and *j*, the point $(x_i - y_i)$ corresponds to the source or release point and the point (x_j, y_j) to the receptor point.

The piping cost, C_{piping}, is then estimated by

$$C_{piping} = \sum_{(i,j) \in M_{ij}} C_p d_{i,j} \tag{2.13}$$

where C_p is the cost of pipe, \$/m, and M_{ij} is a set whose elements indicate which pair of (i, j) facilities are interconnected.

In principle, the land has been already paid; however, the area occupied by the final layout should be minimized not to jeopardize future expansions. Assuming that the

layout starts from coordinates *(0,0)*, then the other extreme point should be calculated, Figure 2.5. Thus the land cost is,

$$C_{land} = c_l A_x A_y \tag{2.14}$$

where C_{land} is the cost of the total occupied land, c_l is the cost per square meter, and A_x and A_y are the lengths in the *x* and *y* directions calculated from:

$$A_x = \max(x_s + Lx_s / 2) \tag{2.15}$$

$$A_y = \max(y_s + Ly_s / 2) \tag{2.16}$$

It is worth mentioning that the above function is not implemented in some optimization packages because it represents a non-convex function. A more convenient formulation results by using constraint inequalities:

$$A_x \geq x_s + Lx_s / 2, \quad \forall s \in S \tag{2.17}$$

$$A_y \geq y_s + Ly_s / 2, \quad \forall s \in S \tag{2.18}$$

Finally, the cost of risk, C_{risk}, is calculated by

$$C_{risk} = c_{pp} t_l \sum_s \sum_{ri(i,r)} f_{i,r} p_s P_{death_{i,r,s}} \tag{2.19}$$

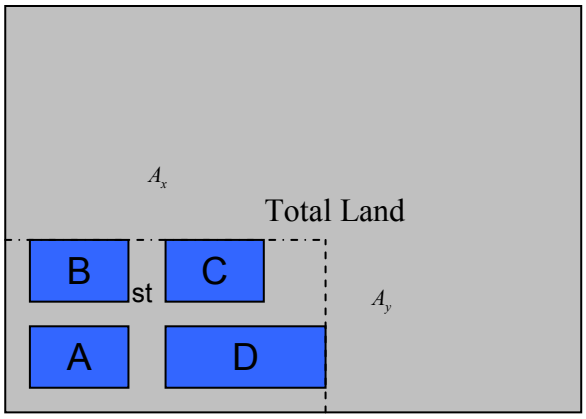

Fig. 2.5. Calculating occupied area.

where $f_{i,r}$ is the frequency of the type of release r in facility i, p_s is the expected population in facility s, c_{pp} is the compensation cost to pay per death, and t_l is the expected life time of the plant. The objective function consists on minimizing the sum of the three costs: piping, land and risk.

2.4 Modeling the Disjunctions

Formulating models in terms of disjunctions represents a normal way to represent discrete/continuous optimization problems containing logic relations [82-85]. The resulting model can be referred as a disjunctive program. However, commercial computer codes do not directly accept disjunctive formulations. Hence, the model has to be reformulated as an MINLP. There are three methods to make this transformation. The most straightforward method consists on defining a binary variable to indicate if the disjunction is active or not and multiply both sides of each constraint in the disjunction by this binary. The main disadvantage of this method is that it generates new bilinear

terms which are source of numerical difficulties [86]. A second method consists on using binary variables to replace the Boolean variables and modify the constraints with a "big-*M*", where *M* is a large valid upper bound [87, 88]. The main drawback of this method is that any bad selection for *M* yields poor relaxation [85]. Lately, the convex hull relaxation has been given best numerical behavior in the reformulated disjunction [83]. The convex hull formulation in [89] is used here to convert the above disjunctive model in an MINLP. It indicates there that the disjunction

$$\bigvee_{d \in D} \begin{bmatrix} Y^d \\ h_{i,d}(\mathbf{x}) = a_{i,d} \\ g_{j,d}(\mathbf{x}) \le b_{j,d} \end{bmatrix} \tag{2.20}$$

where $a_{i,d}$ and $b_{j,d}$ are constants, can be formulated as

$$\begin{aligned} & x_k = \sum_{d \in D} x_k^d \\ & h_{i,d}(\mathbf{x}^d) = a_{i,d} y^d \\ & g_{j,d}(\mathbf{x}^d) \le b_{j,d} y^d \\ & \sum_{d \in D} y^d = 1 \\ & 0 \le x_k^d \le U y^d \end{aligned} \tag{2.21}$$

where x_k^d are bounded disaggregated variables assigned to each term of the disjunction and y^d are binary variables associated to the Booleans to enforce that terms belonging to another disjunction be ignored.

Thus, applying the convex hull reformulation to disjunction (3) when the k-facility is an installed facility yields the following equations:

$$m_\alpha = \left(\tan\left(\frac{2\alpha\pi}{n_{\text{int}}} \right) \right) \tag{2.22}$$

$$x_s = x_{s,i}^L + x_{s,i}^R + x_{s,i}^{AD} \tag{2.23}$$

$$y_s = y_{s,i}^A + y_{s,i}^D + y_{s,i}^{LR} \tag{2.24}$$

$$x_{s,i}^L \le (x_i - D_{s,i}^{\min,x}) \cdot B_{s,i}^L \tag{2.25}$$

$$x_{s,i}^R \ge (x_i + D_{s,i}^{\min,x}) \cdot B_{s,i}^R \tag{2.26}$$

$$x_{s,i}^{AD} \ge (x_i - D_{s,i}^{\min,x}) \cdot B_{s,i}^{AD} \tag{2.27}$$

$$x_{s,i}^{AD} \le (x_i + D_{s,i}^{\min,x}) \cdot B_{s,i}^{AD} \tag{2.28}$$

$$y_{s,i}^A \ge (y_i + D_{s,i}^{\min,y}) \cdot B_{s,i}^A \tag{2.29}$$

$$y_{s,i}^D \le (y_i - D_{s,i}^{\min,y}) \cdot B_{s,i}^D \tag{2.30}$$

$$B_{s,i}^L + B_{s,i}^R + B_{s,i}^{AD} = 1 \tag{2.31}$$

$$x_{s,i}^{L} \geq 0,\ x_{s,i}^{R} \geq 0,\ x_{s,i}^{AD} \geq 0 \tag{2.32}$$

$$y_{s,i}^{A} \geq 0,\ y_{s,i}^{D} \geq 0,\ y_{s,i}^{LR} \geq 0 \tag{2.33}$$

$$x_{s,i}^{L} \leq (L_x - st - L_{xs}/2) \cdot B_{s,i}^{L} \tag{2.34}$$

$$x_{s,i}^{R} \leq (L_x - st - L_{xs}/2) \cdot B_{s,i}^{R} \tag{2.35}$$

$$x_{s,i}^{AD} \leq (L_x - st - L_{xs}/2) \cdot B_{s,i}^{AD} \tag{2.36}$$

$$y_{s,i}^{A} \leq (L_y - st - L_{ys}/2) \cdot B_{s,i}^{A} \tag{2.37}$$

$$y_{s,i}^{D} \leq (L_y - st - L_{ys}/2) \cdot B_{s,i}^{D} \tag{2.38}$$

$$y_{s,i}^{LR} \leq (L_y - st - L_{ys}/2) \cdot (1 - B_{s,i}^{AD}) \tag{2.39}$$

where $x_{s,i}^{L}$, $x_{s,i}^{R}$, $x_{s,i}^{AD}$, $y_{s,i}^{A}$, $y_{s,i}^{D}$, and $y_{s,i}^{LR}$ are disaggregated variables and $B_{s,i}^{L}$, $B_{s,i}^{R}$, $B_{s,i}^{AD}$, $B_{s,i}^{A}$ and $B_{s,i}^{D}$ are the binary variables.

If the *k*-facility in disjunction (2.3) refers to a siting facility, then the equations becomes different to the above case since the variables (x_k, y_k) corresponding to the center of the *k*-facility are not constant. Hence they have to be disaggregated as the (x_s, y_s) variables do. Thus, the resulting equations are as follows:

$$x_k = x_{s,k}^{L} + x_{s,k}^{R} + x_{s,k}^{AD} \tag{2.40}$$

$$y_k = y_{k,s}^{A} + y_{k,s}^{D} + y_{k,s}^{LR} \tag{2.41}$$

$$x_s = x^L_{s,k} + x^R_{s,k} + x^{AD}_{s,k} \tag{2.42}$$

$$y_s = y^A_{s,k} + y^D_{s,k} + y^{LR}_{s,k} \tag{2.43}$$

$$x^L_{s,k} \le x^L_{k,s} - D^{\min,x}_{s,k} \cdot B^L_{s,k} \tag{2.44}$$

$$x^R_{s,k} \ge x^R_{k,s} + D^{\min,x}_{s,k} \cdot B^R_{s,k} \tag{2.45}$$

$$x^{AD}_{s,k} \ge x^{AD}_{k,s} - D^{\min,x}_{s,k} \cdot B^{AD}_{s,k} \tag{2.46}$$

$$x^{AD}_{s,k} \le x^{AD}_{k,s} + D^{\min,x}_{s,k} \cdot B^{AD}_{s,k} \tag{2.47}$$

$$y^A_{s,k} \ge y^A_{k,s} + D^{\min,y}_{s,k} \cdot B^A_{s,k} \tag{2.48}$$

$$y^D_{s,k} \le y^D_{k,s} - D^{\min,y}_{s,k} \cdot B^D_{s,k} \tag{2.49}$$

$$B^L_{s,k} + B^R_{s,k} + B^{AD}_{s,k} = 1 \tag{2.50}$$

$$x^L_{s,k} \ge 0\,,\ x^R_{s,k} \ge 0\,,\ x^{AD}_{s,k} \ge 0 \tag{2.51}$$

$$y^A_{s,k} \ge 0\,,\ y^D_{s,k} \ge 0\,,\ y^{LR}_{s,k} \ge 0 \tag{2.52}$$

$$x^L_{s,k} \le (L_x - st - L_{xs}/2) \cdot B^L_{s,k} \tag{2.53}$$

$$x^R_{s,k} \le (L_x - st - L_{xs}/2) \cdot B^R_{s,k} \tag{2.54}$$

$$x^{AD}_{s,k} \le (L_x - st - L_{xs}/2) \cdot B^{AD}_{s,k} \tag{2.55}$$

$$y^{A}_{s,k} \le (L_y - st - L_{ys}/2) \cdot B^{A}_{s,k} \tag{2.56}$$

$$y^{D}_{s,k} \le (L_y - st - L_{ys}/2) \cdot B^{D}_{s,k} \tag{2.57}$$

$$y^{LR}_{s,k} \le (L_y - st - L_{ys}/2) \cdot (1 - B^{AD}_{s,k}) \tag{2.58}$$

where $x^{L}_{s,k}$, $x^{R}_{s,k}$, $x^{AD}_{s,k}$, $y^{A}_{s,k}$, $y^{D}_{s,k}$, $y^{LR}_{s,k}$, $x^{L}_{k,s}$, $x^{R}_{k,s}$, $x^{AD}_{k,s}$, $y^{A}_{k,s}$, $y^{D}_{k,s}$, $y^{LR}_{k,s}$ are the disaggregated variables and $B^{L}_{s,k}$, $B^{R}_{s,k}$, $B^{AD}_{s,k}$, $B^{A}_{s,k}$, $B^{D}_{s,k}$, $B^{L}_{k,s}$, $B^{R}_{k,s}$, $B^{AD}_{k,s}$, $B^{A}_{k,s}$, and $B^{D}_{k,s}$ are the binary variables. Equations (40-50; 53-58) are formulated for $ord(k) > ord(s)$ to avoid repetitive equations and equations (51-52) are formulated when $k \neq s$ to avoid non-sense equations.

Disjunction (9) is also converted to a MINLP assuming that the toxic release is produced in an installed facility. The following equations are generated:

$$\mathrm{x_s} = \sum_{\alpha} x_{i,s,\alpha}, \forall i \in ri(i,r) \tag{2.59}$$

$$y_{\mathrm{s}} = \sum_{\alpha} y_{i,s,\alpha}, \forall i \in ri(i,r) \tag{2.60}$$

$$\mathrm{s}_{\mathrm{k}}^{\Delta \mathrm{y}} (y_{i,s,\alpha} - B_{i,s,\alpha} y_i) \ge 0, \forall i \in ri(i,r) \tag{2.61}$$

$$\mathrm{s}_{\mathrm{k}}^{\Delta x} (x_{i,s,\alpha} - B_{i,s,\alpha} x_i) \ge 0, \forall i \in ri(i,r) \tag{2.62}$$

$$\mathrm{s}_{\mathrm{k}}^{\Delta x} (y_{i,s,\alpha} - B_{i,s,\alpha} y_i) \le \mathrm{s}_{\mathrm{k}}^{\Delta x} m_{\alpha} (x_{i,s,\alpha} - B_{i,s,\alpha} x_i), \forall i \in ri(i,r) \tag{2.63}$$

$$\mathrm{s}_{\alpha}^{\Delta x} (y_{i,s,\alpha} - B_{i,s,\alpha} y_i) \ge \mathrm{s}_{\alpha}^{\Delta x} m_{\alpha - 1} (x_{i,s,\alpha} - B_{i,s,\alpha} x_i), \forall i \in ri(i,r) \tag{2.64}$$

$$\sum_{\alpha} B_{i,s,\alpha} = 1 \tag{2.65}$$

$$x_{i,s,\alpha} \geq 0,\ y_{i,s,\alpha} \geq 0,\ \ \forall i \in ri(i,r) \tag{2.66}$$

$$x_{i,s,\alpha} \leq B_{i,s,\alpha}(Lx - st - \frac{Lx_s}{2}),\ \forall i \in ri(i,r) \tag{2.67}$$

$$y_{i,s,\alpha} \leq B_{i,s,\alpha}(Ly - st - \frac{Ly_s}{2}),\ \forall i \in ri(i,r) \tag{2.68}$$

where $x_{i,s,\alpha}$ and $y_{i,s,\alpha}$ are the disaggregated variables and $B_{i,s,\alpha}$ are the binary variables from which the only one binary whose value is one indicates the slice direction of the position of facility *s* respect to the releasing facility *i*.

Above equations may require corrections when the slope in the slice includes an infinite value. If this is the case and the value for the binary variable is cero, i.e. facility s is not laying in that direction respect to *i*, then there will be a multiplication of type infinite times zero. To avoid this situation, equation (2.63) is restricted to $m_\alpha \neq \infty$ and $m_\alpha \neq -\infty$ whereas equation (2.64) is restricted to $m_{\alpha-1} \neq \infty$ and $m_{\alpha-1} \neq -\infty$. In fact, these equations are redundant for the slices where they are omitted.

Finally, equation (2.11) is modified to incorporate the binary variables and omit the variable. Thus, the equation can be written as,

$$P_{death_{i,r,s}} = \sum_{\alpha} B_{i,s,\alpha} a_{i,r,\alpha} \cdot e^{-b_{i,r,\alpha} d_{i,s}} \tag{2.69}$$

It should be notice that $\alpha *$ is not included in (2.69) to allow the appropriate use of the binary. The following section shows the case study results.

2.5 Results and Discussion

In this section, the proposed approach is applied to a case study. All examples are solved using the GAMS modeling system [90] using several of NLP and MINLP solvers in a PC Intel® Pentium® M processor 2.00GHz.

The problem consists on finding the best layout in a rectangular land of 250 m in the North-direction and 500 m in the East-direction. Two facilities, *FA* and *FB*, are already installed where facility *FA* can have "chlorine release" from the center point and the respective centers are in *(15, 10)* and *(12.5, 27.5)*, respectively. Two new facilities, *NA* and *NB*, and the control room, *CR*, are desired to be sited in the land. The size of all facilities is given in Table 2.1. In addition, facilities *NA* and *FA* are interconnected as well as *NA* and *NB*. The estimated cost of piping is 196.8 \$/m whereas the cost of land is 6 \$/m^2. The layout is geographically situated in Corpus Christi.

Table 2.1. Dimensions of installed and siting facilities.

Facility	Lx_s, m	Ly_s, m
FA	20	10
FB	15	15
NA	10	30
NB	30	15
CR	15	15

The case study was initially solved assuming no toxic release. Initial values for the center point of the siting facilities correspond to the *(0,0)* in all cases. Using the combination of solvers DICOPT-CONOPT-CPLEX from GAMS to solve the corresponding MINLP, NLP and MILP subproblems, the optimal distribution was achieved in *0.73* s and the total occupied area is *3,025* m^2. By using the combination DICOPT-MINOS-CPLEX, achieving the optimal solution took *0.69* s and the total occupied area decreased to *3,000* m^2. Finally, using the combination BARON-MINOS-CPLEX took 90 s to achieve the optimal and the resulting occupied area is 2625 m^2. Figure 2.6 shows the three resulting layouts. The difficulty of this problem is highlighted with these results since the three solutions are optimal though they correspond to local minima. Therefore, using a global solver may result convenient but the time required achieving the solution increases substantially.

It is worth mentioning that the non-global solvers were enforced to achieve the global solution through appropriate modeling. It can be observed that all nonlinear terms are contained in the equality constraints, which can be incorporated in the objective function:

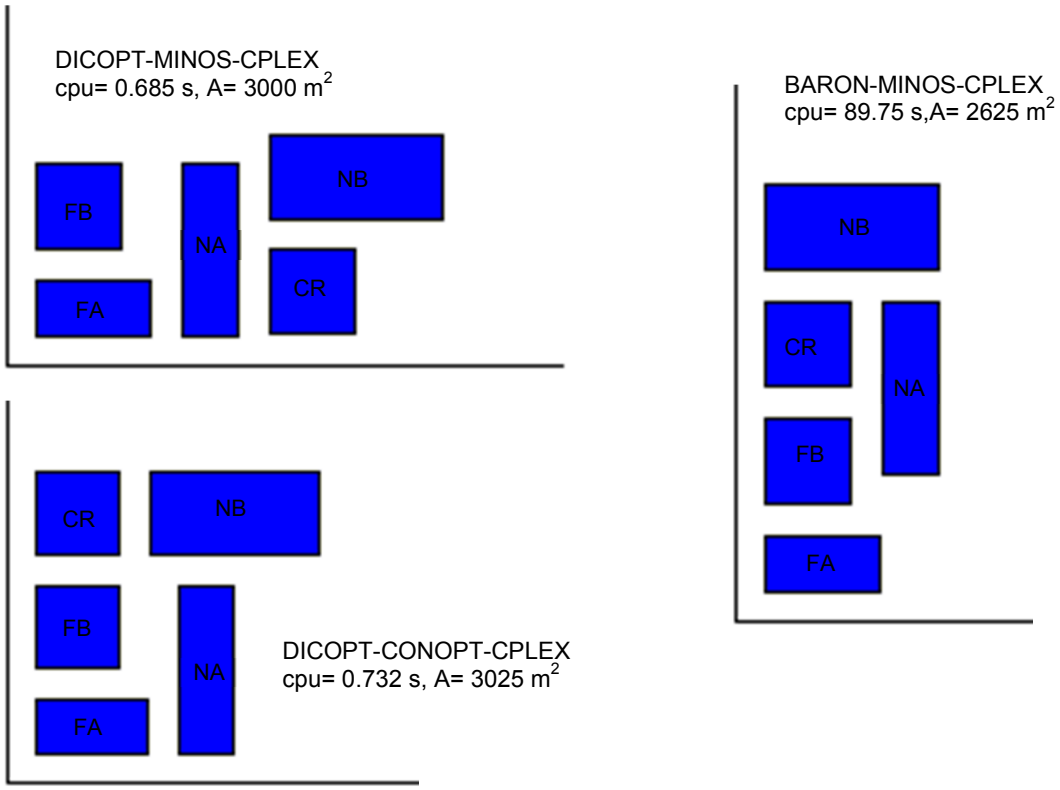

Fig. 2.6. Optimal layouts without toxic release.

$$min\ c_l A_x A_y + \sum_{(i,j)\in M_{ij}} C_p d_{i,j} + \sum_{\alpha} B_{i,s,\alpha} a_{i,r,\alpha} \cdot e^{-b_{i,r,\alpha} d_{i,s}} \tag{2.70}$$

Thus, the problem is reduced to a highly nonlinear objective function with linear inequality constraints. The same global solution obtained with BARON was achieved with the combinations DICOPT-CONOPT-CPLEX and DICOPT-MINOS-CPLEX.

The model developed in this work has been used to solve the facility layout problem with the toxic release incorporated in the already installed *FA* facility. The scenario for the release is described as follows. It is assumed that chlorine is continuously released from *FA* according to the case study given in [65]. Thus the release

is assumed to occur at *1* m height with a rate of *3.0* kg/s and frequency $5.8x10^{-4}$ /year following a Gaussian plume distribution. The surface factor roughness is *1* m and the exposure time *10* min. The same reference provides the following probit function:

$$\Pr = -8.29 + 0.92\ln(C^2 t) \tag{2.71}$$

Monte Carlo simulation was performed to calculate average concentrations every meter, from 1 m to *400* m, in *36* directions for the 360º. Thus, the angular direction was divided in *36* slices of *10º*. Then the exponential decay function was used to fit the calculated values. The expected population in all facilities is denied except in the control room where the expectancy of pupil working in the facility is *10*. Other parameters include *45* years for the expected life of the layout, the street size is considered as *5* m, and the compensation cost is 10^7 $/person [91]. Then, using experimental values for wind direction, wind velocity, etc., as indicated before, the resulting Weibull parameters and probabilities of stability classes calculated for each interval is given in Tables 2.2 and 2.3 for day and night, respectively. Finally, Table 2.4 shows the fitted parameters. In these tables, the angles of 0º, 90º, 180º and 270º correspond to the East, North, West and South directions, respectively. Also, all digits used in this work are included in the tables for the sake of reproducibility of our results.

Table 2.2. Weibull parameters and stability class during the day in Corpus Christi, 1981-1990.

Wind direction	Weibull parameters		Stability class probability			
	Shape	Scale	A	B	C	D
10	2.2741	5.0371	0.000	0.170	0.321	0.509
20	2.3480	4.8354	0.031	0.172	0.336	0.461
30	2.6533	4.5024	0.017	0.133	0.370	0.480
40	2.6050	4.5012	0.019	0.191	0.298	0.493
50	2.6811	4.869	0.018	0.146	0.318	0.518
60	2.7053	5.2755	0.015	0.115	0.336	0.534
70	2.7233	5.7547	0.011	0.102	0.260	0.628
80	2.7924	6.4591	0.004	0.077	0.262	0.657
90	2.6186	6.8634	0.007	0.068	0.250	0.675
100	2.7644	7.9109	0.001	0.042	0.203	0.753
110	2.9488	8.5593	0.002	0.027	0.180	0.791
120	3.1254	8.6449	0.002	0.021	0.165	0.813
130	3.1677	8.2737	0.002	0.019	0.164	0.815
140	3.1275	7.8299	0.002	0.019	0.170	0.809
150	2.9283	7.1950	0.003	0.035	0.194	0.768
160	3.0578	6.7344	0.003	0.045	0.216	0.736
170	3.3563	6.6409	0.005	0.046	0.197	0.751
180	3.2550	6.6034	0.005	0.048	0.222	0.725
190	3.0076	6.4991	0.005	0.075	0.223	0.697
200	2.9051	6.2882	0.001	0.087	0.203	0.709
210	2.7645	6.1306	0.005	0.072	0.227	0.696
220	2.7597	6.5711	0.003	0.058	0.176	0.763
230	2.9595	6.7281	0.004	0.052	0.151	0.793
240	2.8997	6.5811	0.003	0.033	0.199	0.765
250	2.8577	6.7605	0.004	0.041	0.186	0.770
260	2.8074	6.5410	0.000	0.044	0.197	0.759
270	2.7790	6.7461	0.002	0.052	0.167	0.779
280	2.6637	6.9016	0.003	0.040	0.162	0.795
290	2.6043	6.9176	0.003	0.035	0.197	0.766
300	2.4984	7.3041	0.005	0.030	0.183	0.782
310	2.2616	6.9187	0.008	0.047	0.215	0.729
320	2.1017	6.7788	0.005	0.068	0.249	0.678
330	2.1698	6.0327	0.007	0.097	0.264	0.632
340	2.3192	5.2260	0.006	0.091	0.337	0.566
350	2.2416	5.0102	0.000	0.206	0.206	0.588
360	2.3463	4.5294	0.008	0.191	0.298	0.504

Table 2.3. Weibull parameters and stability class during the night in Corpus Christi, 1981-1990.

Wind direction	Weibull parameters		Stability class probability		
	Shape	Scale	D	E	F
10	3.1108	3.2890	0.104	0.422	0.474
20	2.9777	3.1963	0.085	0.326	0.589
30	3.4187	3.0728	0.094	0.278	0.627
40	2.9249	3.4367	0.130	0.381	0.488
50	2.8764	3.3791	0.152	0.393	0.455
60	2.6841	3.6085	0.205	0.317	0.478
70	2.7927	3.7292	0.204	0.343	0.453
80	2.6320	3.9803	0.234	0.342	0.424
90	2.3839	4.6549	0.345	0.344	0.311
100	2.2517	5.4266	0.434	0.342	0.224
110	2.3453	5.7919	0.511	0.314	0.175
120	2.4227	5.8248	0.552	0.297	0.151
130	2.4436	5.5825	0.511	0.312	0.177
140	2.4649	5.2240	0.466	0.340	0.194
150	2.4448	4.8816	0.434	0.340	0.227
160	2.5473	4.6407	0.410	0.337	0.252
170	2.7414	4.4628	0.379	0.385	0.236
180	2.5796	4.4648	0.429	0.337	0.234
190	2.4536	4.6508	0.454	0.330	0.217
200	2.3056	4.7554	0.488	0.310	0.202
210	2.2222	5.1407	0.573	0.247	0.180
220	2.2970	5.9635	0.678	0.215	0.106
230	2.4418	6.1343	0.712	0.204	0.084
240	2.4315	6.1616	0.681	0.228	0.090
250	2.3634	6.0492	0.667	0.229	0.104
260	2.2340	6.2093	0.662	0.220	0.118
270	2.3698	6.0081	0.652	0.241	0.107
280	2.1534	5.7207	0.579	0.249	0.172
290	2.0995	5.5174	0.547	0.263	0.189
300	2.1123	5.3682	0.540	0.247	0.213
310	1.9774	5.3582	0.480	0.288	0.232
320	2.0445	4.6957	0.362	0.341	0.297
330	2.6486	3.6576	0.201	0.343	0.457
340	2.9541	3.3799	0.145	0.325	0.530
350	3.0427	3.3011	0.097	0.374	0.529
360	3.2045	3.1968	0.073	0.348	0.579

Table 2.4. Parameters for the exponential decay model, $P_\alpha(d_{r,\alpha}) = a_\alpha \cdot e^{-b_\alpha d_{r,\alpha}}$.

Angle, º	*a*	*b*	Angle, º	*a*	*b*
10	0.029197	0.020654	190	0.11643	0.012345
20	0.033666	0.019243	200	0.1094	0.015803
30	0.043151	0.019414	210	0.12335	0.014073
40	0.058328	0.021643	220	0.13943	0.01159
50	0.036068	1.9977	230	0.15254	0.011456
60	0.060453	0.31112	240	0.15506	0.012738
70	0.10547	0.080694	250	0.1529	0.013635
80	0.16368	0.033326	260	0.14245	0.011556
90	0.2646	0.022263	270	0.12469	0.010012
100	0.39906	0.018084	280	0.11427	0.011646
110	0.50906	0.016308	290	0.091316	0.012353
120	0.54443	0.016263	300	0.068746	0.010601
130	0.49927	0.016065	310	0.053675	0.0095219
140	0.37822	0.014920	320	0.040917	0.0097168
150	0.28116	0.015945	330	0.02948	0.0098091
160	0.195	0.014816	340	0.02277	0.0095465
170	0.14738	0.011996	350	0.01954	0.0097283
180	0.12714	0.012345	360	0.022943	0.015462

The results in this case indicate that both combinations DICOPT-CONOPT-CPLEX and DICOPT-MINOS-CPLEX gave the same solution. The total occupied area is *3,025* m^2 with a total cost of *$23,432* having no appreciable cost in the financial risk component and laying out the control room in the region *5*. Using DICOPT-MINOS-CPLEX took *1.9 s* whereas using DICOPT-CONOPT-CPLEX took 3.1 s. The combination BARON-MINOS-CPLEX couldn't achieve the optimal solution because the memory was not enough, i.e. another machine is suggested to solve the problem. However, the solution reported might be the real global solution with a total cost of *$23,409* but having a component of *$640* in financial risk and using a total area of *3,000* m^2 while the control room is located in region *3*. Figure 2.6 shows the arrangement of the calculated layout in all cases. BARON ratifies its capabilities of global optimization

but high computational cost to produce solutions. However, the results may also be arguable in the sense that non-global solvers have produced negligible financial risk.

2.6 Conclusions

A new approach for the optimal plant layout including toxic release in installed facilities has been described in this chapter. The importance of considering the wind effect is clearly demonstrated by comparing layouts without toxic release with layouts with toxic release. The problem is numerically difficult but current packages such as GAMS can achieve the solution. The calculation of all optimal layouts is strongly suggested since a local optimum result may be more convenient. In the case study the local optimal could be more acceptable since the financial risk is negligible though the total cost is lower than the one in the global optimal solution.

CHAPTER III

OPTIMAL FACILITY LAYOUT FOR TOXIC GAS RELEASE SCENARIOS USING DENSE GAS DISPERSION MODELING*

3.1 Introduction

The arrangement of process equipment and buildings can have a large impact on plant economics. In effort to maximize plant efficiency, the design of plant layout should facilitate the production process, minimize material handling and operating cost, and promote utilization of manpower. The overall layout development should incorporate safety considerations while providing support for operations and maintenance. Good layout should also consider space for future expansion as well as access for installation, and thereby prevent design rework later. In plant layout, process units that perform similar functions are usually grouped within a particular block on the site. Each group is often referred to as a facility. In this chapter, the concept of facility is referred to any building or occupied unit such as control room and trailer (portable building), where operators can be exposed to any unsafe situation. In general, more land, piping, and cabling will increase the construction and operating costs, and can affect the plant economics. However, additional space tends to enhance safety. Therefore there is a need to integrate costs and safety into the optimization of plant layout.

---

*Reprinted with permission from "An Approach for Risk Reduction (methodology) based on Optimizing Facility Layout and Siting in Toxic Gas Release Scenarios" by S. Jung, D. Ng, J. Lee, R. Vázquez, and M. S. Mannan, Journal of Loss Prevention in the Process Industries 23 (2010) 139-148. © 2010 by Elsevier B.V.

One of the major causes of the accident in Flixborough (1974), which resulted in 28 fatalities, and Pasadena Texas (1989), which led to 24 fatalities, was due to inadequate separation distances between occupied buildings (control rooms) and the nearby process equipment [2]. The siting of a hazardous plant near a densely populated area has resulted in fatal disasters, most notably in Seveso (1976) and Bhopal (1984) [3]. In the toxic gas released in Bhopal incident, major victims were not only workers within the plant but also residents who lived in the surrounding area [92]. Therefore, civilians who didn't partake in the risk assessment during the layout development should be considered in the stages of process design. The four of aforementioned incidents have similarity in contributing cause that the management can learn from. A preliminary identification of various hazards during early stages of layout development may substantially minimize the severity of damage. The aftermath of industrial disasters has shown that facility layout is an important element of process safety. Incidents associated to facility layout in chemical plants have brought material losses, environmental damage, and endangered human life.

From the safety viewpoint, plant layout is largely constrained by the need to maintain minimum safe separation distances between facilities. Adequate separation is often done by grouping facilities of similar hazards together. However, space among facilities is limited and will increase the capital costs (more land, piping, etc.) and operating costs as units are separated. If future plant modifications are anticipated which might impact separation distances, consideration should be given to employing larger initial separation distance and applying protection devices. Therefore, it is essential to

determine minimum distances at which costs can be integrated in the plant layout optimization.

In this work, the facility layout optimization for the toxic gas release scenario has been examined using a mixed-integer nonlinear programming (MINLP). Dense gas (DEGADIS) model was used to account the prevailing wind direction and atmospheric conditions, and to illustrate the flow of toxic gases to the occupied buildings (e.g., control room). The applicability of this approach was further demonstrated in 4 illustrated scenarios of the chlorine gas leak incident at Beaumont, TX. Results generated from this approach will enhance process safety in the conceptual design and layout stages of plant design. The computed value under this stochastic approach for the expected risk becomes useful information for emergency planning in highly populated areas.

The approaches suggested in this methodology can be used to aid decision makers for low-risk layout structures and determining whether the proposed plant could safely and economically be installed in a nearby residential area.

3.2 Problem Statement

In this chapter, the site occupied by facilities was assumed to be a rectangular footprint, with dimensions *Lx* (length) and *Ly* (depth). Similarly, a rectangular shaped was also used to represent a layout design of each facility. The existing facilities ($e \in E$) were fixed on x-y plane in order to configure the placement of new facilities ($n \in N$) in a given site.

Here the population is assumed to be concentrated only in the central point of a facility. It was assumed that a toxic gas release occurs from either one of the existing facilities or the new facilities or from both facilities. Another consideration in the layout design is the minimum separation distances (*st*) between facilities to allow access for maintenance and emergency response. Others include parameters to calculate the probability of death due to toxic gas release. Prior to the optimization step, these parameters were obtained from Monte Carlo simulations by estimating the effects of a toxic release using gas dispersion model and real meteorological conditions. Results from Monte Carlo were later incorporated into the optimization formulation. Finally, optimization program, GAMS (General Algebraic Modeling System) was used to achieve optimal positions of new facilities (x and y) and total cost associated with optimized plant layout. Furthermore, CFD model (computational fluid dynamics) was used to illustrate the gas releases scenario in some layouts. Fig 3.1 shows the simplified scheme of the methodology.

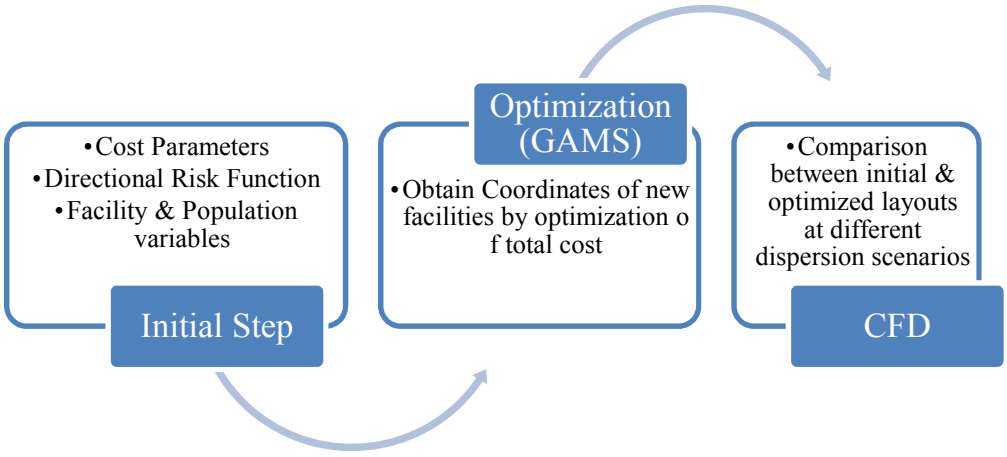

Fig. 3.1. Simplified scheme of the methodology.

3.3 Mathematical Formulation

This section describes the objective function and constraints used in the layout simulations.

3.3.1 Land Constraints

Based on the geometric characteristics, both existing and new facilities are separated by a street (*st*), which is defined as a minimum spacing distance. The center point of a new facility is determined by:

$$\frac{Lx_N}{2} + st \;\leq\; x_N \leq\; Lx - \left(\frac{Lx_N}{2} + st\right) \tag{3.1}$$

$$\frac{Ly_N}{2} + st \;\leq\; y_N \leq\; Lx - \left(\frac{Ly_N}{2} + st\right) \tag{3.2}$$

3.3.2 Non-overlapping Constraints

To avoid overlapping problems in the layout configuration, we had previously proposed a disjunctive model by considering two facilities, *i* and *j*. As shown in Fig. 3.2, a new facility *j* with respect to facility *i* can be accommodated by expanding the footprint of facility *i* by the street size. Then, facility *j* could be placed anywhere on region "*L*", left hand side, anywhere on region "*R*", right hand side or at the center in which case it would lay either in region "*A*", above or "*D*", downward. Details of this work can be found elsewhere [93].

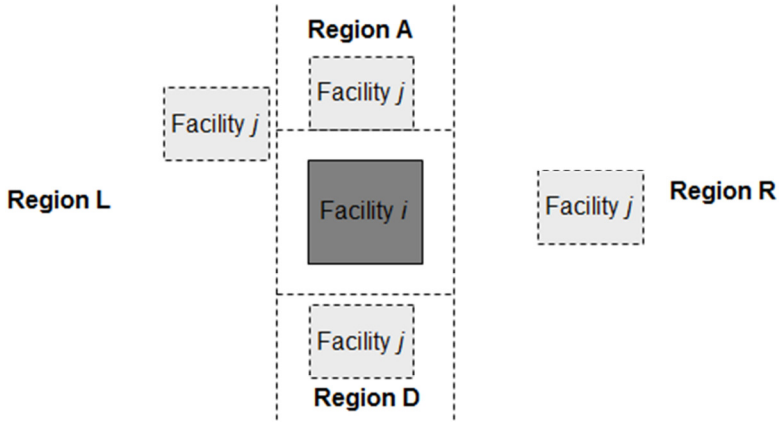

Fig. 3.2. Schematic drawing of new facility placement in the layout design.

3.3.3 Objective Function

The objective function is to minimize the total cost associated with facility layout by considering: land costs, piping costs, and risk associated costs (potential injury costs and protection device costs). Because the scope of this work focused on toxic gas release, the equipment damage will not be considered in the risk cost estimation.

3.3.3.1 Land Cost

The land cost consists of the area occupied by the facilities and the area around the facilities for future expansion. For a given land, the area can be calculated by multiplying the limit lines of facilities. The land cost is determined by:

$$Land\ \ Cost = L_c \times (Max(x_i + \frac{1}{2}Lx_i) + st) \times (Max(y_i + \frac{1}{2}Ly_i) + st)_{ij} \tag{3.3}$$

where L_c is a unit land cost and *st* is the width of street.

3.3.3.2 Piping Cost

Piping cost depends significantly on the layout. The piping cost is given by:

$$Piping\ \ Cost = \sum M_{ij} \times C_p \times d_{ij} \tag{3.4}$$

where M_{ij} is a binary integer to express the connectivity between facility *i* and *j*. If facility *i* is connected to facility *j*, then M_{ij} is 1. If no interconnection is made between facility *i* and *j*, then M_{ij} is 0. C_p is a unit pipe cost. It should include operation cost and maintenance cost. d_{ij} is the distance between the center of facilities, *i* and *j* and it is calculated from:

$$d_{ij}^2 = (x_i - x_j)^2 + (y_i - y_j)^2 \tag{3.5}$$

3.3.3.3 Potential Injury Cost (PIC)

Accidental releases of hazardous gasses can present a threat to a worker's safety and to the communities around the plant. In spill incidents arising from tank trucks, rail

car, and other common container, the human health effects of breathing the toxic *gas* depend on its *concentration* and the *exposure time*. Based on these parameters, the potential injury cost can be expressed as:

$$PIC = Frequency\ of\ incident\ X\ plant\ lifetime\ X\ population\ X\ the\ cost\ willing\ to\ avoid\ a\ fatality\ X\ probability\ of\ death \quad (3.6)$$

The frequency of plant could be obtained from historical data (Anand, Keren, Tretter, Wang, O'Connor, & Mannan, 2006) or through Fault Tree Analysis, the method chosen in this chapter. Frequency of incident is reported as a number of occurrences per year. Plant lifetime has a unit of year. By multiplying frequency of incidence and plant lifetime, the number of incidents during a plant lifetime can be obtained. Population referred to the number of people affected by the incident. There are some acceptable methods to estimate the value of human life in fatality risk, such as Willingness-to-Pay method, Human Capital method, and value of a statistical life approach [94]. In this chapter, the cost of willing to avoid a fatality has been chosen to determine PIC. The cost willing to avoid a fatality is often referred as the cost people are willing to pay to avert fatality. According to API 581, the estimated cost is $ 10,000,000 per death [91]. The probability of death is obtained from directional risk function which is a combination of gas dispersion modeling and Monte Carlo simulations of the affected area.

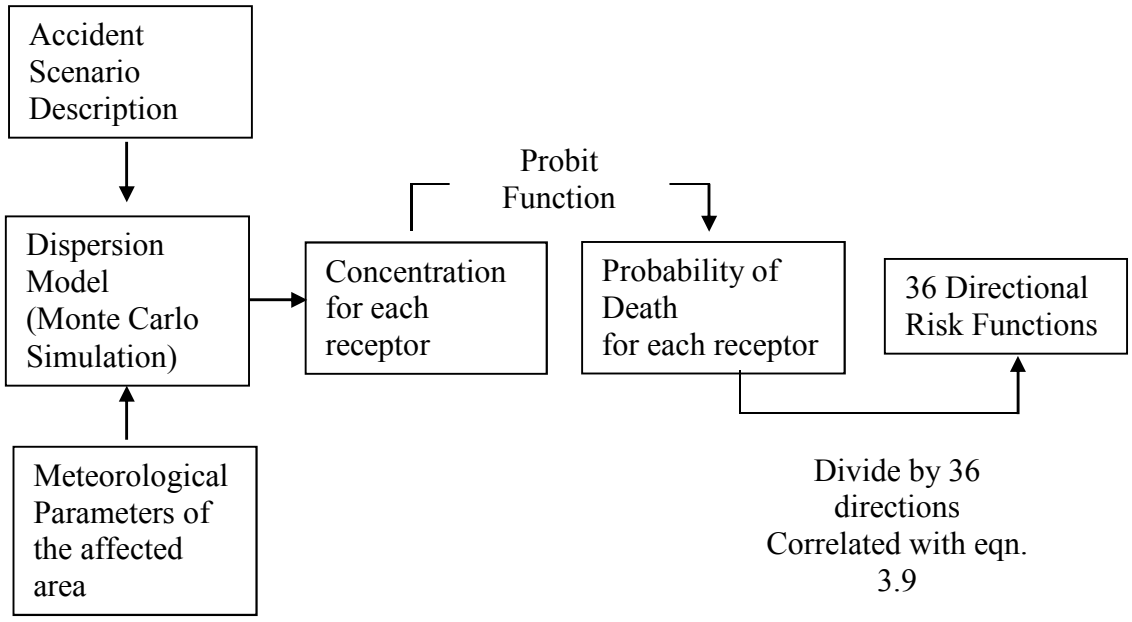

Fig. 3.3. Simplified scheme to obtain Directional Risk Function.

Fig. 3.3 shows the steps to obtain directional risk function. Here directional risk function is used as approximation of the vulnerability maps by considering risk affected by meteorological variables and incorporating them into the optimization program to be used with disjunction formulations.

For toxic gas release, it is important to consider the stochastic uncertainty of meteorological parameters such as wind speed and direction, temperature, humidity, and air stability. Since the natural variability of the weather affects the air diffusion of toxic gas, it is difficult to obtain a direct observation of release characteristics and atmospheric conditions during the accidental release. Therefore, an approach based on the stochastic nature of meteorological parameters can be helpful as they provide information on its probability distribution. The hourly meteorological data for the time period of 10 years

was obtained from the Meteorological Resource Center (The Meteorological Resource Center)[95]. In the 10 years period, there are 87,000 data sets that can be used in the Monte Carlo simulation. By sampling a thousand numbers out of 87,000 data sets with random numbers and inputting the data set (wind direction, wind speed, temperature, etc) into a dispersion model, the concentration of receptors at every point apart from 5 meters on the given plane can be calculated. After simulations, averaged values of concentration in each receptor were used to get the directional risk functions. In order to calculate the concentration of each receptor, there is a need to introduce a dispersion model. Two types of dispersion model have been introduced, light gas and dense gas models. For a light gas such as ammonia (vapor density of 0.59), the Gaussian model has been widely used to model the gas dispersion. For a heavy gas such as chlorine (vapor density of 2.48), DEGADIS has been chosen to simulate the atmospheric dispersion at ground-level. It gives the estimate short-term concentrations and the expected area of exposure [96]. In this work, the DEGADIS model code from EPA was converted from FORTRAN to C# code for Monte Carlo simulation. After generating 1,000 random wind directions accompanying with other data sets, such as wind speed, temperature, humidity and stability class, each receptor was then integrated into the calculated concentration. As such, the average concentrations of all receptors were obtained by dividing the total of integrated concentrations by 1,000.

The probit value is calculated by inputting the calculated concentration of toxic gas from DEGADIS, C and exposure time, t into the following equation:

$$\Pr = k_1 + k_2 \ln(C^2 \times t) \quad [97] \tag{3.7}$$

where k_1 and k_2 are probit parameters used for toxic chemicals. These concentrations can be converted from probit value to the probability of death [81]. By following this step, every receptor/point in the plane will have its own probability of death, and we can choose values on every 10 degrees line to get 36 directional risk functions by correlating with eqn. (3.8).

In the dense gas model, the simulation results of probability of death fitted well to the sigmoid function,

$$y = \frac{a}{1 + \exp\{-(\frac{x - x_0}{b})\}} \tag{3.8}$$

where y is the probability of death of one direction, x is the distance from the release center, and a, b, and x_0 are the correlated parameters. Fig. 3.4 (b) has shown that the correlation result for a direction of 10° and Table 3.1 has presented correlated parameters for 36 directions.

On the other hand, there is another issue for indoor protection. Up to this point, the model described above has assumed that the individual is outside the facilities and left unprotected. For those who stay inside the facilities and exposed through inhalation of toxic gaseous, it is recommended to multiply the probability of death to the factor of 0.1 [98]. Statistical analysis could be accompanied with the percentage of people being outside during the day or inside their residential areas during night time.

3.3.4 Protection Device Cost

The protection devices can be divided into two types: prevention and mitigation. The prevention system such as relief valve, interlocks, system are used to reduce the frequency of accidents. Mitigation system such as water curtain can lessen damages done to a facility or to a residential area when an accident does occur [99]. By applying the protection devices on the identified hazards, the risk posed by personnel in the workplace will be significantly reduced.

To treat this term reasonably, there is a need to provide a detail risk analysis based on hazard identification. After deciding the types of protection devices will be equipped, PIC is decreased and has the form:

$$Decreased \quad PIC = PIC \times \left(1 - RR_k \times B_k\right) \tag{3.9}$$

where RR_k is a risk reduction factor, which has a value between 0 and 1. This value is related to the efficiency or performance of the protection device k. B_k is an integer variable that equals to 1 if a protection device k is installed.

Finally, the total cost is defined as follows:

$$Total\ Cost =$$

$$Land\ Cost + Piping\ Cost + Decreased\ PIC + Protection\ Device\ Cost \tag{3.10}$$

3.3.5 Computational Fluid Dynamics (CFD) Modeling

Following the layout optimization, CFD was used to simulate the toxic gas dispersion from one of the existing facilities or new facilities, or from both facilities. CFD was also used to compare the results from the initial and the optimized layouts

given the potential release scenario. In the CFD modeling, we assumed a worst –case scenario such as wind speed of 1.5 m/s and direct wind direction from the release source to the target facility (i.e. control room). Another advantage of using CFD is the 3-D view, which allows an observation of toxic dispersion in direction of inhabited spaces. In this work, ANSYS-CFX-11 was used to perform the CFD modeling of case studies.

3.4 Illustrative Case Study

The following case study demonstrates the application of proposed methodology on a simplified plant with a chlorine release from the rail tank car loading facility in Beaumont, Texas. The scenario of incident was taken from the Center for Chemical Process Safety (CCPS) guidelines book [100]. The following data were adapted for this study: frequency of small liquid leakage with 12.7 mm hole size at 5.8×10^{-4}/year, estimated liquid discharge rate of 3.0 kg/s, and a leak duration of 10 minutes. Given these information, we set up parameters for directional risk function of the affected area. Because chlorine is heavier than air, DEGADIS was chosen for modeling the toxic dispersion. Fig. 3.4 shows the graph of simulated result at 10 degrees direction obtained from the directional risk function. By applying the correlation function in the risk contour map, we obtained 36 regression coefficients (a, b, x_0) for 36 directional risk functions. These coefficients are tabulated in Table 3.1 and were later incorporated in the optimization formulation. Given the plant lifetime of 45 years and plant population for each case study scenario, the cost of potential injury can be determined.

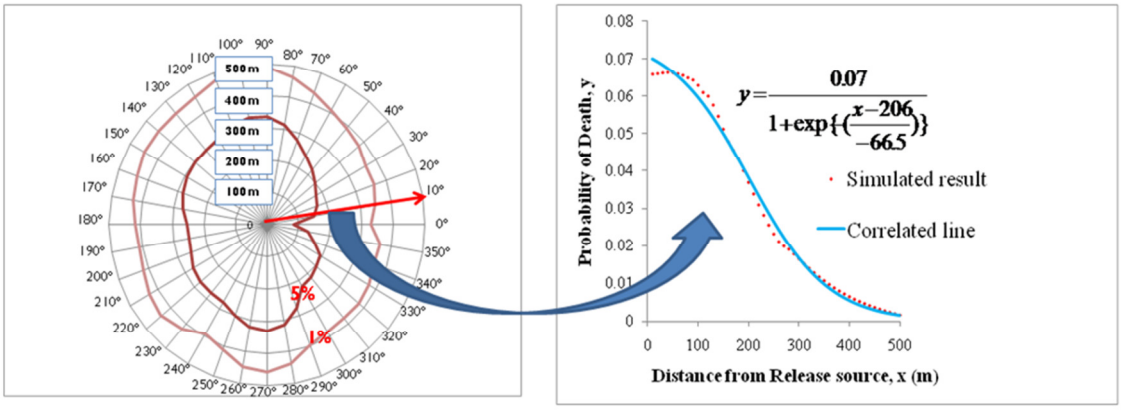

(a) (b)

Fig. 3.4. (a) Risk contours of Beaumont (1%, 5%) and (b) an example plot of DEGADIS correlated result at10° direction.

Table 3.1. List of parameters (a, b, x_0) obtained from DEGADIS model.

Deg.	a	b	x_0	Deg.	a	b	x_0	Deg.	a	b	x_0	Deg.	a	b	x_0
10	0.070	-66.5	206	**100**	0.286	-74.0	207	**190**	0.178	-76.9	181	**280**	0.217	-62.9	229
20	0.094	-81.1	165	**110**	0.275	-73.7	202	**200**	0.179	-76.7	181	**290**	0.171	-60.7	210
30	0.108	-80.5	155	**120**	0.253	-73.5	197	**210**	0.180	-75.3	186	**300**	0.121	-67.2	198
40	0.135	-81.6	144	**130**	0.225	-72.2	199	**220**	0.186	-75.4	184	**310**	0.108	-68.8	200
50	0.186	-83.2	127	**140**	0.209	-72.8	202	**230**	0.229	-69.6	172	**320**	0.100	-71.3	200
60	0.239	-82.0	128	**150**	0.199	-74.9	200	**240**	0.258	-57.9	184	**330**	0.087	-68.1	211
70	0.266	-79.4	153	**160**	0.188	-74.5	198	**250**	0.247	-57.4	207	**340**	0.071	-68.0	213
80	0.280	-77.6	182	**170**	0.181	-76.6	188	**260**	0.242	-63.7	223	**350**	0.064	-71.1	215
90	0.286	-75.9	202	**180**	0.176	-78.3	181	**270**	0.231	-66.8	229	**360**	0.064	-82.0	174

After obtaining the correlated parameters, geometric variables needed to optimize the layout are given as follows. The total land was assumed to be 250 m wide and 500 m long. A total of five facilities were configured in the given land. The width of

roads around facilities was assumed to be 5 meters. In order to set the starting point of the layout, it was assumed that 2 existing facilities, A and B, were fixed at coordinates (15, 10) and (12.5, 27.5), respectively. 2 new facilities and 1 new control room were later added in the given site. The size of all facilities was tabulated in Table 3.2.

Table 3.2. Size of facilities.

Facility	L_x**, meters**	L_y **, meters**
A	20	10
B	15	15
New C	10	30
New D	30	15
Control Room	15	15

Other assumptions include a unit land cost of \$6/m^2 and a unit piping cost of \$98.4/m. Facility A and new Facility C will be connected together with pipes, and likewise, new facilities C and D will be linked together with pipes. Table 3.3 summarizes general inputs into GAMS program for optimization.

Table 3.3. General parameters used in case study.

Location	Beaumont, TX
Unit land cost	\$ 6 / m^2
Given land size	250 m (x)*500 m (y)
Fire road size	5 m
Unit piping cost	\$ 98.4 / m
Pipe connections	A-C, C-D
Number of facilities	5 (2 fixed, 3 new)

The case study was initially solved without the toxic release scenario and only considered land cost and piping cost among facilities. The combination of BARON-MINOS-CPLEX solvers in GAMS was used to obtain the initial layout. The occupied area is now 3,200 m^2, the cost of piping and land (total cost) is $25,380, and the coordinates of each facility are as follows: New Facility C (30, 40), New facility D (20, 67.5), Control Room (12.5, 47.5). Fig. 3.5 shows the block layout concept derived for the cost optimization without the PIC. From the economics viewpoint, this initial layout was well squeezed to keep facilities as close as possible with the lowest sum of distances between A-C-D in order to minimize piping costs. It is important to note that the calculated total cost excludes any hazard from the surrounding distance between the hazardous facility and the occupied building. If a release point of chlorine gas was originated from the center of Facility A, and there were 10 people in Control Room (CR), the total cost would have risen to over five hundred forty thousand dollars in which the injury risk cost contributes over five hundred thousand dollars of the total cost. Moreover, the separation distance between A-CR was 38 meters in a 90° direction, which indicates a high potential injury cost due to prevailing wind directions. Overall, this optimization result did not give the best optimal layout from the viewpoint of risk management.

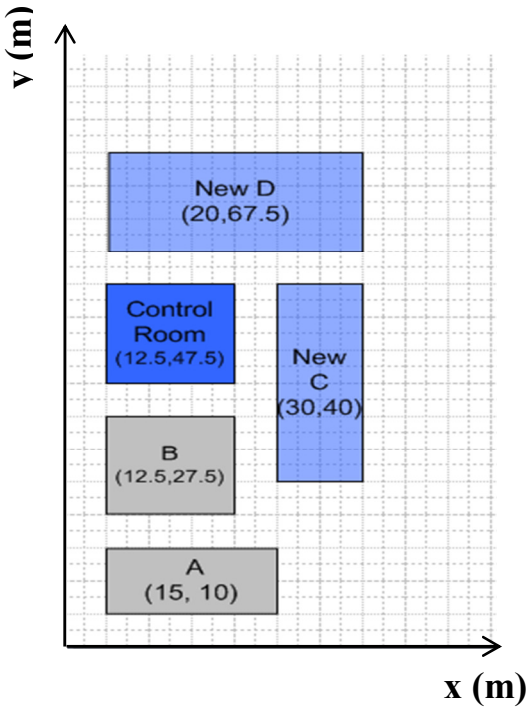

Fig. 3.5. Initial layout.

3.4.1 Case Study 1: One Release Point, One Occupied Building

Here the simplified plant consists of facility A as a release point and the control room as the only occupied unit. Based on this configuration, potential injury cost (PIC) due to toxic gas release was considered in the total cost optimization. As inferred from equation of directional risk function, large separation distance will reduce PIC and eventually minimize the total cost.

Fig. 3.6 shows the layout result incorporated with directional risk functions obtained from DEGADIS. Table 3.4 shows the net costs for this example. In this layout, the control room has been moved to all the way to the right-hand side (east) of the plot plan to decrease PIC despite of increasing land cost, therefore it gave much lower total

cost than the initial layout without toxic release. The separation distance between Facility A and the control room is now 218 meters.

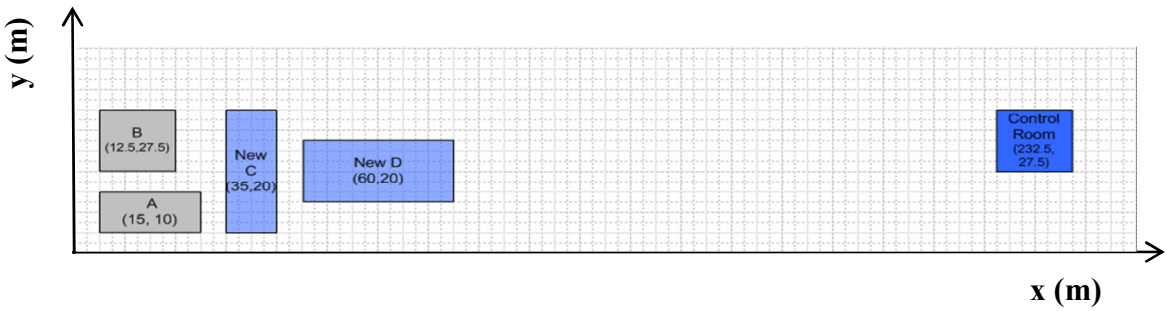

Fig. 3.6. Layout with 1 release source in A and 1 control room.

Table 3.4. Costs for 1st case study.

Element	**Net Costs**
Land cost	58,800
Piping cost	4,660
PIC	82,859
Total cost	146,319

3.4.2 Case Study 2: Two Release Points and One Occupied Building

Here, both Facility A and new Facility C were simulated as source of chlorine release. These facilities assumed the release frequency of 0.00058/yrs at their center points. Due to this arrangement, injuries associated with toxic releases will rise

drastically, which consequently increased the injury risk. Results from the GAMS solver showed the location of control room was moved to the end of east side of the given land (Fig. 3.7). It was shown that the control room has almost the same coordinate with the first case due to the limited space to accommodate in a given land. In addition, the wind direction from 0 to 10 degrees has a lower probability of risk distribution.

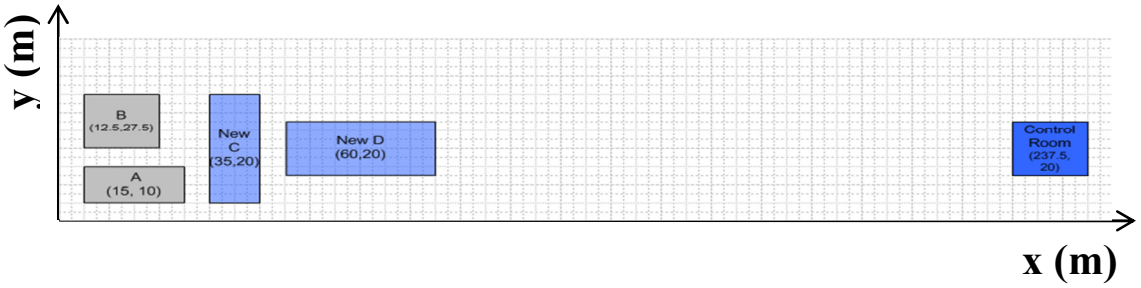

Fig. 3.7. Layout with 2 release sources (A,C) and 1 control room.

Table 3.5. Costs for 2nd case study.

Element	Net Costs
Land cost	60,000
Piping cost	4,660
PIC	176,884
Total cost	241,544

3.4.3 Case Study 3: One Release Point, One Occupied Building with Protection Devices

In this example, five different protection devices were applied to the first case study (one release point in the center of A and one occupied building (control room)).

The price of these devices and its risk reduction factors were presumably set and are shown in Table 3.6.

Table 3.6. Protection devices and total cost.

Protection device	Price ($)	Risk reduction factor	Total Cost ($)
A	20,000	0.9	61,170
B	15,000	0.7	89,328
C	10,000	0.5	115,690
D	5,000	0.3	141,700
E	1,000	0.1	131,580

After applying the protection devices into layout formulation, we found that device A gives the lowest cost $ 61,170, as seen in Table 3.7. Relationship between costs of protection device and corresponding total costs is shown in Fig. 3.8. With protection device A, the separation distance was reduced from 218 m (first case study) to 27.6 m (Fig. 3.9). The total cost was decreased from $ 151,820 to $ 61,170 and the layout is given in Fig. 3.9.

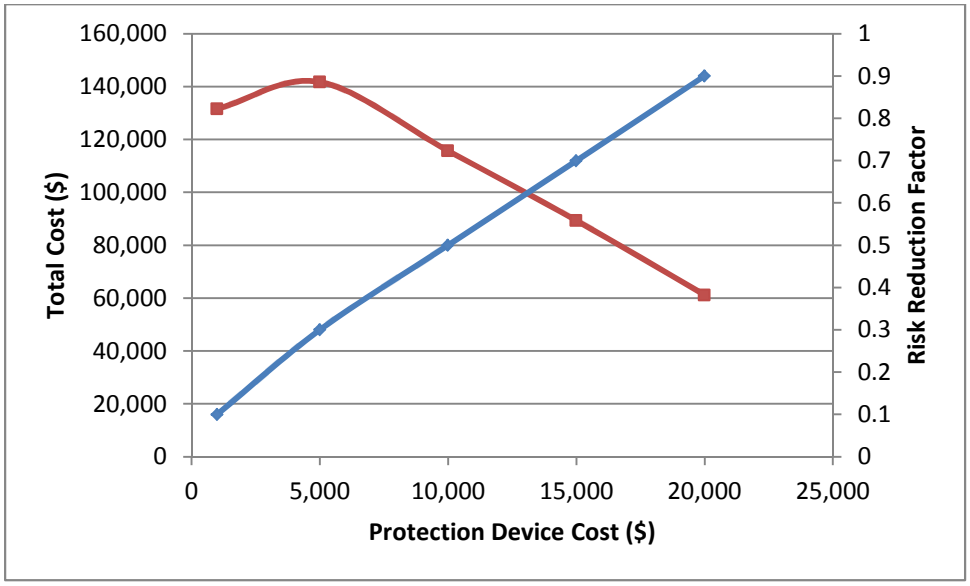

Fig. 3.8. Relationship between costs of protection device and corresponding total costs.

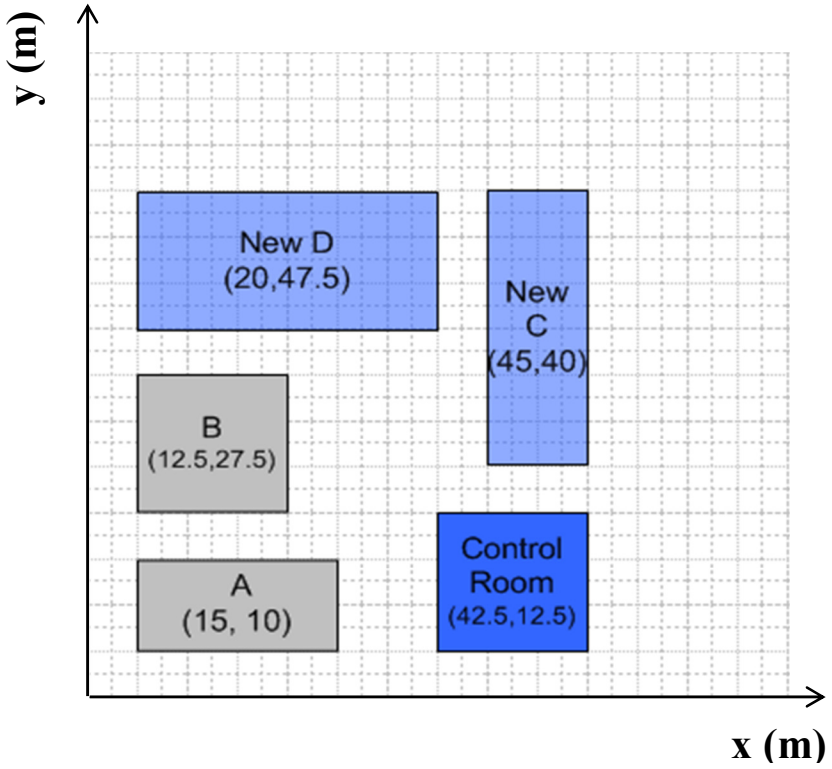

Fig. 3.9. Layout with 1 release source (A) and 1 control room equipped with protection device A.

Table 3.7. Costs for 3rd case study.

Element	Net Costs
Land cost	16,500
Piping cost	6,743
Protection Device cost	20,000
PIC	17,927
Total cost	61,170

3.4.4 Case Study 4: One Release Point (New Facility C) around the Residential Area

Here the case study was used to obtain the optimum layout for the plant that is sited near the residential areas. There are one release source in New Facility C, one occupied building (control room), and residential areas outside of the given land. The placement of New Facility C is very critical as it may pose hazards to the nearby populated areas. To evaluate this scenario, the residential areas were simulated near the plant location. For simplicity, it was assumed that 10 people were living at one location, defined as a village. It was assumed that there were three villages with the following coordinates: (20,550), (40,550), and (60,550). In this example, the potential injury cost was calculated as the sum of injury cost of workers in the control room and civilians in the villages. The layout result of this case is presented in Fig. 3.10 with the New Facility C was located further from the control room and further away from the villages.

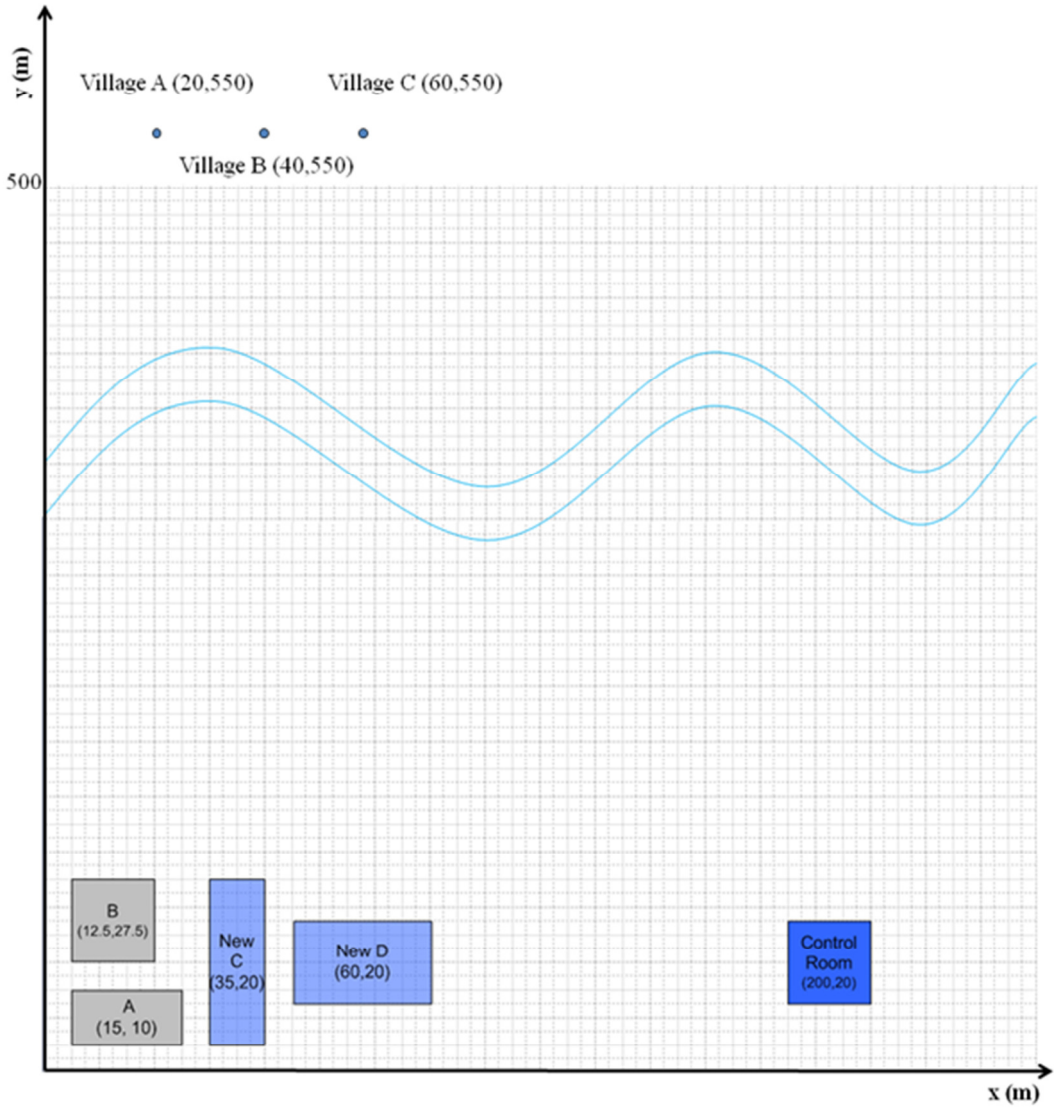

Fig. 3.10. Layout with 1 release source (A) and 1 control room near residential area.

Table 3.8. Costs for 4th case study.

Element	Net Costs
Land cost	43,105
Piping cost	4,660
PIC	140,736
Total cost	188,501

3.5 Discussion

As stated above, multiple case studies were simulated to illustrate the risk optimization model in solving facility layout and siting problems. Case scenario developments were presented to express the desired level of safety based on the total cost optimization. As inferred from the first two cases (case 1 and 2), the cost of land arises from the needs to separate the occupied building(s) from the release point(s). At larger distance from the release point, the gas concentration is lower due to dilution with the atmosphere. While in case 3, applying protection devices in facilities reduce the risk cost with a lower total cost. Such risk levels should also reflect on the level of design and operational function of the protection device. Because major accidents associated with toxic gas release affect the population outside the plant, societal risk should be included in the plant layout to minimize risk levels outside the plant boundaries. As illustrated in Case 4, the distance between the plant site and the residential area may be inadequate. Therefore, potential offsite impacts involving the general public cannot be avoided, which was confirmed by the higher risk cost than other case scenarios.

On the other hand, if it was assumed that Facility A is the release point for Figs. 3.5 and 3.6, one might argue risk levels should be decreased when obstacle features are present in the plot plan of initial layout (Fig. 3.5), which in turn has lower land cost and chlorine exposure on the control room than Fig. 3.6. This question represents the weak point of the 2-D model of the plot plan.

To solve this problem, we performed CFD modeling to simulate the facilities around the release point and the gas concentration. As shown in Fig. 3.11, chlorine released from the center of Facility A was compared with the corresponding layout in Figs. 3.5 and 3.6. The concentration of chlorine on the control room (shown as a black dot) on Fig. 3.11(b) had a longer separation distance than the initial layout (Fig. 3.11(a)). This result was simulated at the following conditions: wind speed 1.5 m/s, direct wind direction from the source to the control room, and all facilities have heights of 1.5 meters. These colored plane represent the concentrations of 1.6 meters from the ground level. It showed that the chlorine concentration was decreased from 6,070 ppm to 1,880 ppm, indicating that the obstacle feature has less effect on the gas dilution than the distance effect.

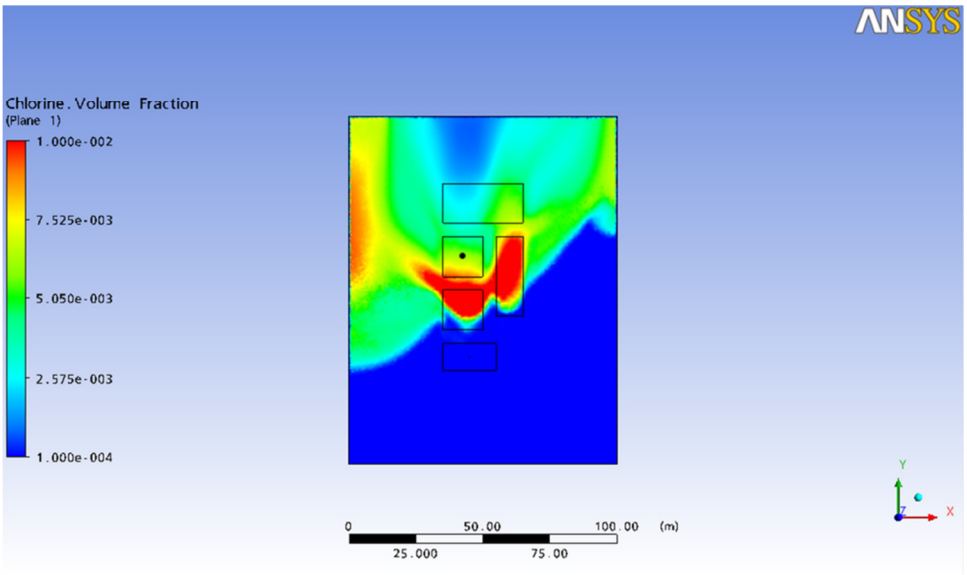

(a) Initial layout

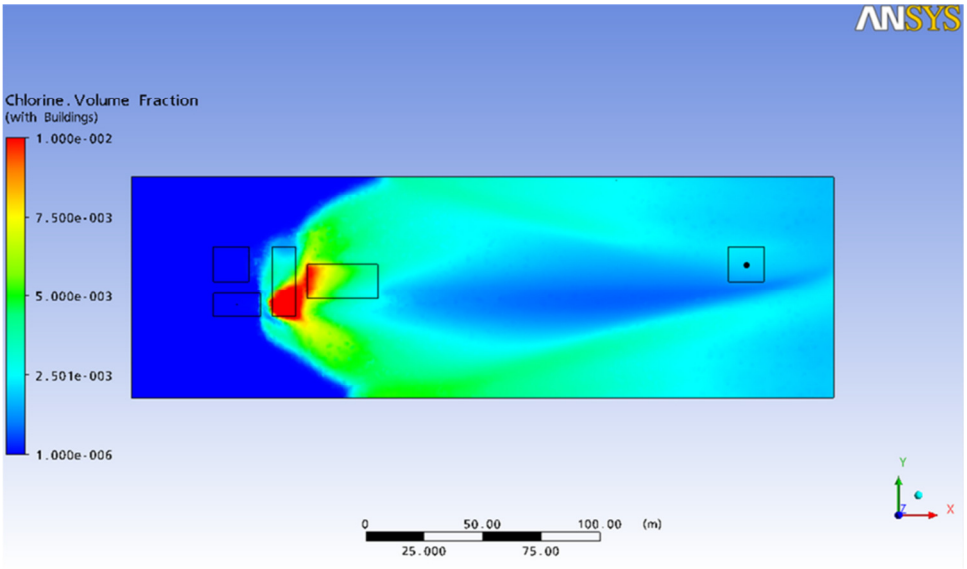

(b) Layout from 1st case study

Fig. 3.11. CFX results for (a) initial layout & (b) layout from 1st case study.

For the 1st case study, we generated CFD modeling without buildings (obstacles) around the release point in Fig. 3.12. When it is simulated without obstacles around the

release facility, the concentration is 2400 ppm for the receptor in the control room (232.5, 27.5, 1.6). The factor of obstacle effect is around 20 % of the concentration, which means buildings around the release facility can decrease 20 % of the concentration in the control room.

However, this information is not available to be included to modify directional risk function because this is caused from the plant layout for this specific result. To be reasonably used in modifying directional risk function, the facility of releasing itself should have a real shape with 3-D, then the decreased factor could be addressed to control directional risk function.

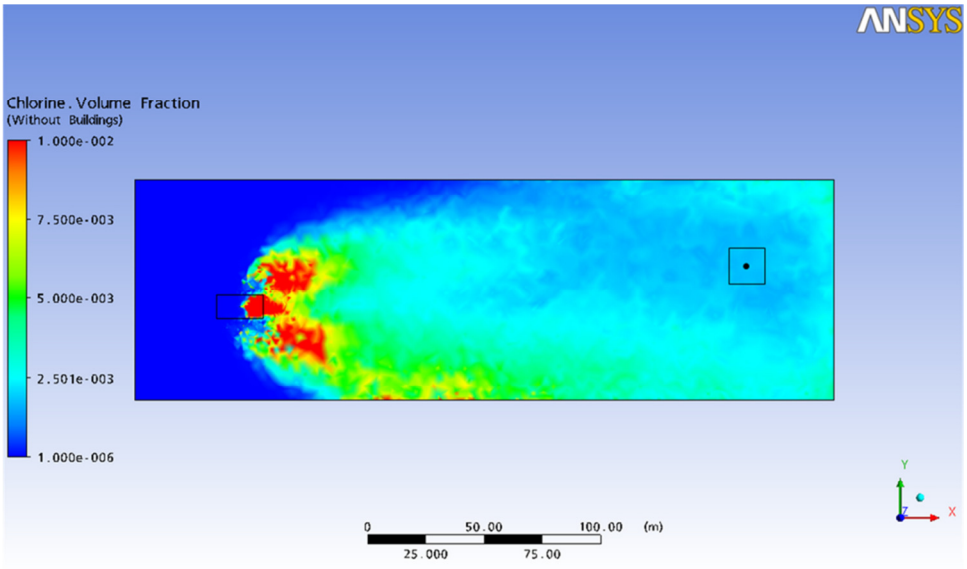

Fig. 3.12. CFX result for layout from 1st case study without surrounding facilities.

Also the simplified model presented here has some limitations with assuming people are all at the center of the control room or villages. Future work should focus on population scattered around the facility by generating many different points in the residential area. The other limitation is that this suggested method cannot expect to appropriately work for unplanned accommodations after the plant is built as happened in Bhopal incident. In order to prevent unforeseen situations, QRA should be performed periodically even after plant is built, thus it will complement this methodology.

3.6 Conclusions

In this research, we presented a new approach in integrating safety and economic decisions into the optimization of plant layout for toxic gas release scenario. The concept of personal injury cost was introduced for the potential injury risk associated with toxic release. The stochastic approach based on the real meteorological conditions and dense gas dispersion (DEGADIS) modeling was integrated to understand the directional risk function on personal injury. Finally, GAMS simulation was used to obtain coordinates of new facilities and total costs associated with optimized layout. The optimization problem was formulated as a mixed integer nonlinear programming problem (MINLP) where the integer variables define the existence of protection devices.

Future works will focus on the optimization of facilities with flammable gas scenario and to expand the proposed optimization tool for risk of equipment damage to acquire a safer layout. This study aims in providing information that can be used to assist in risk assessment and advice for emergency preparedness and accident management.

CHAPTER IV

OPTIMAL FACILITY SITING AND LAYOUT FOR FIRE AND EXPLOSION SCENARIOS

4.1 Introduction

High-profile incidents such as Buncefield (2005) and Texas City (2005) have prompted the urgency to assess the risks associated with process plant buildings and the protection they offer to building occupants [101]. To date, facility siting and layout have become one of the most scrutinized subjects when designing new plant layout or integrating new facilities into the existing plant. The needs for facility siting assessment also arise from a number of escalated incidents due to inadequate analysis of blast impact on the process plant buildings. The Texas City refinery explosion on March 2005 has highlighted concerns for facility siting of temporary buildings. Inadequate separation distances between trailers and the isomerization process unit was identified as the contributing causes of fatalities [1]. Similar accidents due to improper siting of occupied buildings and adjacent process units have been observed in the Flixborough accident (1974), which resulted in 28 fatalities, and in Pasadena, Texas (1989), which led to 24 fatalities [2].

The aftermath of industrial disasters has pointed out that facility siting is an important element in process safety and has been addressed in the Occupational Safety and Health Administration (OSHA)'s Process Safety Management regulation. To enforce this regulation, OSHA has issued approximately 93 citations from 1992 to 2004

to process industries for the following reasons: (1) no record of facility siting had been performed; (2) facility siting study had not been carried out; (3) inadequate analysis of facility siting study; and (4) the existing layout and spacing of buildings do not meet the current standards/recommended practices [102]. Based on these findings, OSHA identified that facility siting study should assess the following major subjects [102]: (1) location of buildings with high occupant density such as control room and administrative building; (2) location of other less occupant density units (including utility and maintenance buildings); (3) layout of process units such as reactors, reaction vessels, large inventories, or potential ignition sources; (4) installation of monitoring/warning devices; and (5) development of emergency response plans.

The current guidance and recommended practices, such as the Dow Fire and Explosion Index (Dow F&EI), Industrial Risk Insurance (IRI)'s General Recommendations for Spacing, American Petroleum Institute (API) Recommended Practice (RP) 752 and 753, has been adopted as guidelines for facility siting studies and evaluations in the process industries [18, 103, 13]. Dow F&EI is the leading hazard index recognized by the process industry to quantitatively measure the safe separation distance from the hazardous unit by considering the potential risk from a process and the properties of the process materials under study [13]. This index has also been incorporated in a risk analysis tool for evaluating the layout of new and existing facilities [14]. Additionally, API RP 752 and 753 provides some guidelines to manage hazards associated with the siting of both permanent and temporary occupied buildings, however both RPs only provides conceptual guidelines to address facility siting without specific

recommendations for layout and spacing of occupied buildings. Generally, it is often difficult to deduce a common separation distance and spacing criteria for particular process units without a proper risk assessment. Thus there is a need to develop new methodologies for facility siting and layout assessment.

Several studies have been performed to solve the complex plant layout problem using heuristic methods and focused only on the economic viability of the plant, however little work has addressed safety issues directly into their formulations. In recent years, the use of optimization methods has gained increasing attention in facility siting study as it determines the optimal location of a facility. Such method has been demonstrated in the layout configuration of pipeless batch plants [104]. Subsequently, Penteado et al. developed a Mixed Integer Non-Linear Programming (MINLP) model to account for a financial risk and a protection device into their layout formulation, and configured the new facilities with circular footprints [11]. This model was further evaluated using a MILP model by adopting rectangular-shaped footprints and rectilinear distances [12]. Both works used the equivalent TNT model to obtain the risk costs due to particular accidents with a simple risk assessment approach.

For the purpose of incorporating safety concept into the facility layout, it is essential to combine a detailed risk analysis called Quantitative Risk Analysis (QRA) and optimization. In this work, risk analysis was utilized in site selection and location relative to other plants or facilities. Three approaches to configure facility layout based on optimization methodology have been proposed in order to guide the development of optimal facility siting and layout for fire and explosion scenarios. In the first approach,

facility layout using fixed distances (recommended separation distances) was configured to minimize the objective function, *i.e.,* the sum of land cost and interconnection cost between facilities. In the second approach, the layout was formulated without the recommended separation distances; however it includes the risk cost derived from the probability of structural damage caused by blast overpressures. Finally, the above two approaches were integrated to form a layout whose objective function minimizes the land, interconnection and risk costs along with weighting factors. The weighting factor is introduced to account for the building occupancy and the likelihood of domino effect. In these three approaches, the overall problem was modeled as a disjunctive program to achieve the layout of rectangular-shaped facilities, then, the convex hull approach was used to reformulate the problem as a Mixed Integer Non-Linear Program (MINLP) model to identify potential layouts. Consequence modeling program, PHAST (ver. 6.53.1), was used to measure the overpressure around the process plant unit and the result was further studied to obtain the risk cost. The applicability of the proposed approaches was further demonstrated in the illustrated case study of hexane leak incident. Results generated from each approach were compared and evaluated using 3D explosion simulator program, Flame Acceleration Simulator (FLACS) for evaluating the congestion and confinement effects in the plant in order to provide substantial guidance for deciding the final layout. The proposed methodology can aid in decision making process for facility siting and layout in early design stage as well as provide assessment of the existing layout against fire and explosion scenarios.

4.2 Problem Statement

There are two types of layout formulation, grid based and continuous plane. Some of the disadvantages associated with the grid-based approach have been identified by previous researchers, such as the configured grid locations tend to be larger than the facilities, leading to a coarse grid and require the use of sub-optimal solution; or the units may cover multiple grid locations thereby generating a more complex formulation and requiring excessive computer time [105]. Another drawback of grid-based approach is that sizes of facility are often difficult to be accommodated in the formulation because the units must be allocated in predetermined discrete grids or locations [106]. In order to overcome the limitations of grid-based approach, the continuous-plane formulation has been adopted and highlighted in various studies [56, 58, 107].

In this chapter, the site occupied by the facilities was assumed to be a rectangular footprint, with dimensions *Lx* (length) and *Ly* (depth) in a continuous plane. Similarly, a rectangular shape was also used to represent a design of each facility. All new facilities ($n \in N$) are to be allocated on a given site, on an x-y plane, including hazardous units ($r \in N$). It was assumed that a flammable gas release occurs from one of the hazardous facilities. Another consideration in the layout design is the minimum separation distances ($D_{i,j}$, *st*) between facilities to allow access for maintenance and emergency response. Other considerations include parameters to calculate the probability of structural damage due to flammable gas release. Prior to the optimization step, these parameters were obtained from Quantitative Risk Analysis (QRA) by estimating the consequences of a flammable gas release. Given a set of facilities and their building

costs and dimensions, unit land cost, cost of interconnection between facilities, and minimum separation distance of facilities from the property boundary along with the conditions mentioned above, the overall problem was then solved with the optimization program GAMS (General Algebraic Modeling System) to determine optimal locations of facilities (x and y) and the lowest total cost associated with optimized plant layout.

As mentioned above, three approaches in layout formulation were proposed in this chapter. For the distance-based and integrated approaches, the distance matrix was used as a constraint for determining the minimum separation distance. Subsequently, a list of potential incidents caused by a hazardous process unit was employed for risk cost estimation in the overpressure-based and integrated approaches.

4.3 Methodology

Fig. 4.1 shows the overall scheme of proposed methodology for optimizing the layout formulation. The proposed methodology can be classified into three folds: QRA, optimization and layout validation using FLACS. For the QRA stage, we assumed the worst case scenario for flammable gas release, *i.e.,* fire and explosion in process plant buildings. The resulting consequences were estimated using PHAST (ver. 6.53.1).

One of the main challenges before the optimization stage is to obtain accurate estimates of risk cost for realistic and reliable risk assessment. The risk cost was calculated from the probability of structural damage due to blast overpressures. Furthermore, a 3D explosion simulator based on CFD (computational fluid dynamics)

code, FLACS, was used to simulate the explosion scenario in the optimized layouts for selecting the final layout.

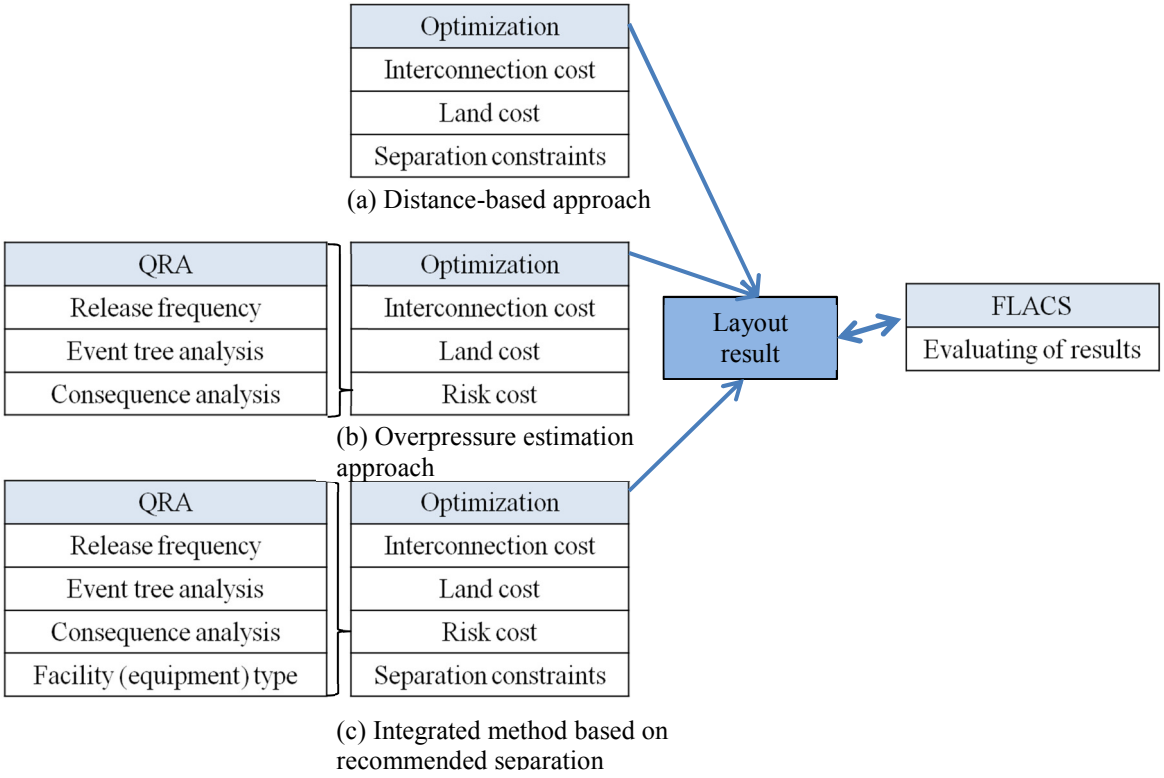

Fig 4.1. Scheme of the proposed methodology.

4.4 Case Study

The case study used to demonstrate the proposed methodology is a hexane distillation unit, which consists of an overhead condenser, reboiler, accumulator and several pumps and valves [65]. In addition to this process unit, several new facilities are to be configured in the layout formulation. For the worst-case scenario of flammable gas release, BLEVE (Boiling Liquid Expanding Vapor Explosion) and VCE (Vapor Cloud Explosion) are identified as potential accidents in the hexane distillation unit. Table 4.1

shows the dimension of each facility along with its recommended distances from the property boundary and the building cost. Based on the distance from property boundary, several occupied buildings such as the control room, administrative building and warehouse tend to be located closer to the process unit.

Table 4.1. Dimension, distance from the property boundary and building cost for each facility.

Facility (i)	Type of Facility	Length (m-m)	Distance from property boundary (m)	Facility cost, FC_i ($)
1	Control room (non-pressurized)	10-10	30	1,000,000
2	Administrative building	20-15	8	300,000
3	Warehouse	5-10	8	200,000
4	High pressure storage sphere	10-10	30	150,000
5	Atmospheric flammable liquid storage tank 1	4-4	30	100,000
6	Atmospheric flammable liquid storage tank 2	4-4	30	100,000
7	Cooling tower	20-10	30	500,000
8	Process unit	30-40	30	.

4.4.1 Distance-based Approach

In the distance-based approach, the objective function is to minimize the total cost of land and interconnection, and can be written as follows.

$$Total\ cost = Land\ Cost + \sum Interconnection\ cost_{i,j} \quad (4.1)$$

$$Land\ cost = UL \times Max(x_i + 0.5Lx_i) \times Max(y_i + 0.5Ly_i) \quad (4.2)$$

$$Interconnection\ cost = UIC_{i,j} \times d_{i,j} \quad (4.3)$$

$$d_{i,j}^2 = (x_i - x_j)^2 + (y_i - y_j)^2 \quad (4.4)$$

st . Non-overlapping constraint

where UL is a unit land cost and $UIC_{i,j}$ is a unit interconnection cost between facilities i and j. The interconnection cost includes costs for maintenance or physical connection such as piping or cabling. It was assumed that the interconnection cost between occupied facilities is 0.1 $ / m and a similar amount was also assumed for the storage units. Additionally, preliminary areas and spacing for site layout from Mecklenburgh [21] were used to define a minimum separation distance between facilities. Table 4.2 shows the interconnection cost and separation distances for each facility. The distance between tanks (#5 and #6) is assumed to be equal to its diameter.

Table 4.2. Unit interconnection costs and minimum separation distances between facilities.

Facility (i)	Unit interconnection cost, $UIC_{i,j}$ ($ / m)							
Minimum separation distance between facilities (m)	1	0.1	0.1	10	10	10	10	10
	5	2	0.1	0	0	0	0	0
	5	5	3	0.1	0.1	0.1	0.1	0.1
	30	60	60	4	0.1	0.1	100	0
	60	60	60	10	5	0.1	100	0
	60	60	60	10	4	6	100	0
	30	30	30	30	30	30	7	100
	30	60	60	15	5	5	30	8

To avoid overlapping problems in the layout configuration, we had previously proposed a disjunctive model by considering two facilities, *i* and *j*. As shown in Fig. 4.2, a new facility *j* with respect to facility *i* can be accommodated by expanding the footprint of facility *i* by the street size. Then, facility *j* could be placed anywhere on region "*L*" (left hand side); or anywhere on region "*R*" (right hand side); or at the center in which case it would lay either in region "*A*" (above) or "*D*" (downward). Details of this work can be found elsewhere [108].

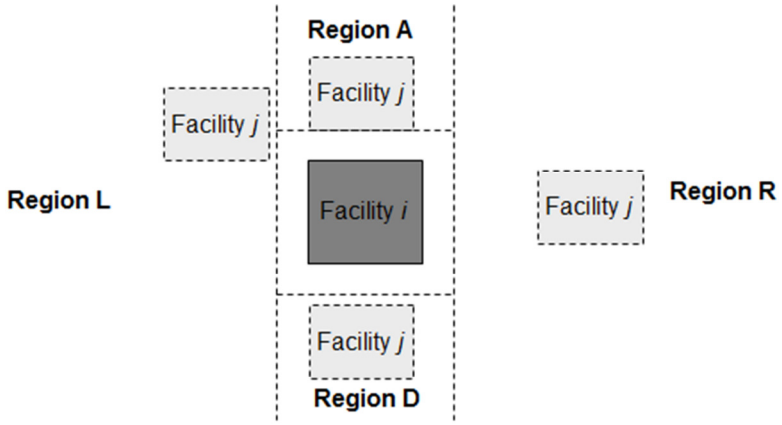

Fig. 4.2. Schematic drawing of new facility placement in the layout design.

The above disjunction model can be formulated as follows:

(4.5)

where:

——— (4.6)

——— (4.7)

Table 4.3 and Fig. 4.3 show the optimized result using the DICOPT solver. As seen in the layout result, facilities #4, #5, #6, and #7 are allocated closely to the process unit. Among the occupied buildings, facility #1, control room, has been closely located to the process unit because of the high interconnection cost.

Table 4.3. Optimized cost from the distance-based approach.

Type of Cost	Cost ($)	Remarks
Interconnection	3840.232	Between all facilities
Land	52275	$5 / m^2
Total	56115.232	

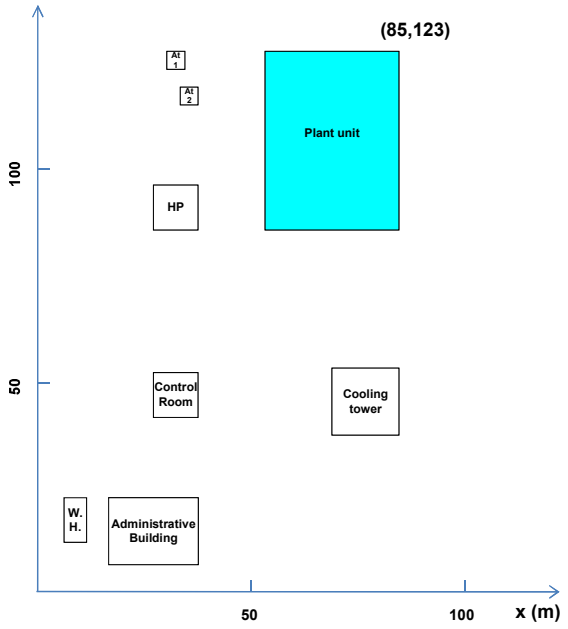

Fig. 4.3. Layout result for distance-based optimization model.

4.4.2 Overpressure Estimation Approach

According to the CPQRA (Chemical Process Quantitative Risk Analysis) book, BLEVE (Boiling Liquid Expanding Vapor Explosion) and VCE (Vapor Cloud Explosion) are identified as potential accidents in the hexane distillation unit [65]. To assess the likelihood and consequence of BLEVE, PHAST ver. 6.53.1 was used to

estimate the distance to certain overpressures following ignition of a flammable vapor cloud. In this work, the term BLEVE is reserved for only the explosive rupture of a pressure vessel and the flash evaporation of liquefied gas. The resulting fireball formation will not be taken into account. The mass of released gas was assumed to be 28,000 kg of hexane and later used as an input for predicting blast overpressures of BLEVE and VCE. There are three models for analyzing the VCE in PHAST: TNT-equivalency model, multi-energy explosion model, and Baker-Strehlow-Tang (BST) model. We used the BST model to account for the congestion and confinement effects in layout formulation. Parameters such as medium material reactivity, flame expansion 1, high obstacle density and 2 ground reflection factor were also selected when using this model. In addition, a wind speed of 1.5 m/s and F-class stability were also assumed to obtain an overpressure profile from the explosion center.

The probit value was calculated from the data of overpressure using the following equation (AICHE/CCPS, 1999).

$$\Pr = k_1 + k_2 \ln(p) \tag{4.8}$$

where k_1 and k_2 are probit parameters used for estimating structural damage and values are -23.8 and 2.92, respectively [3]. The probability of structural damage can be converted from the probit function. The resulting probability of structural damage fitted well with the sigmoid function, and is given by:

$$y = \frac{a}{1 + \exp\{-(\frac{x - x_0}{b})\}} \tag{4.9}$$

where y is the probability of structural damage, x is the distance from the explosion center, and a, b, and x_0 are the sigmoid function parameters. Both BLEVE and VCE follow the sigmoid function profile agreeably, and these parameters are presented in Table 4.4.

Table 4.4. Correlated sigmoid function parameters for BLEVE and VCE.

	a	b	x_0
BLEVE	1.000	-8.009	64.694
VCE	1.006	-64.887	513.220

Potential Structural Damage Cost (PSDC) for i-th facility is defined as follows.

$PSDC_i$ = Plant lifetime × Incident outcome frequency × probability of structural damage × FC_i (4.10)

$$Total\ cost = Land\ Cost + \sum Interconnection\ cost_{i,j} + \sum PSDC_i, r \neq i \quad (4.11)$$

where: FC_i is i-th facility cost assumed in Table 4.1.

For overpressure-based approach, non-overlapping constraints in eqns. (4.6) and (4.7) have been changed to eqns. (4.12) and (4.13) in order to have fixed separation distance between facilities, st.

$$D_{i,j}^{NO,x} = \frac{Lx_i + Ly_j}{2} + st \quad (4.12)$$

$$D_{i,j}^{NO,y} = \frac{Ly_i + Ly_j}{2} + st \quad (4.13)$$

where st is assumed to be 5 meters.

The plant lifetime was assumed to be 50 years. Other assumptions include incident outcome frequencies of 5.7 x 10^{-6} / year for BLEVE and 7.8 x 10^{-6} / year for VCE in the distillation unit [65]. In the overpressure estimation approach, the total cost is also a function of PSDC as seen in eqn. (4.11). This overpressure approach does not consider the recommended separation distance, but it includes the property boundary line for each facility.

In order to enable access for emergency response and maintenance, each facility is separated by a street of 5 meters and this is simply formulated by changing $D_{i,j}$ to st (5 meters). After running the optimization program, the total cost was obtained and showed in Table 4.5. The land cost has been decreased as compared to the result obtained from the distance-based approach due to no separation distance constraints. The PSDC is very low because incident outcome frequencies are very small. The layout result is shown in Fig. 4.4.

Table 4.5. Optimized cost from the overpressure-based approach.

Type of Cost	**Cost ($)**	**Remarks**
Interconnection	1921.319	Between all facilities
Land	30000	\$5 / m^2
Risk	1174.978	
Total	33096.297	

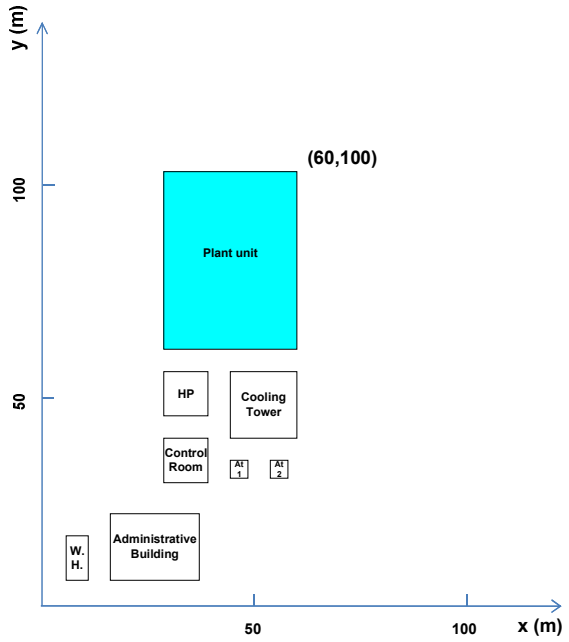

Fig. 4.4. Layout result for overpressure-based optimization model.

4.4.3 Integrated Method based on Recommended Separation Distance and Overpressure

In this approach, the recommended separation distance and PSDC are considered in the layout formulation. In addition to equations and constraints used in the first two approaches, here weighting factors and different probit parameters are taken into account to solve the complex optimization problem. Weighting factors shown in Table 4.6 were derived from population data of occupied buildings and potential domino effects caused by a pressurized vessel and atmospheric tanks containing flammable liquid.

Table 4.6. Population data and weighting factor for each facility.

Facility (i)	Type of Facility	Population	Weighting Factor, WF_i
1	Control room (non-pressurized)	10	100
2	Administrative building	15	150
3	Warehouse	2.5	25
4	High pressure storage sphere	0	20
5	Atmospheric flammable liquid storage tank 1	0	10
6	Atmospheric flammable liquid storage tank 2	0	10
7	Cooling tower	0	1

A number of probit models have been developed for different types of process equipment for the prediction of probability of equipment damage caused by blast overpressures [109]. In this approach, it was assumed that all units can be grouped into 3 types of facilities or equipment, such as a general building, a pressurized vessel, and an atmospheric vessel. Specific probit functions were used to calculate the damage cost for different types of facilities [109]. Subsequently, different types of facilities may have different impacts from the resulting overpressure, thus, the probability of structural

damage represented by the sigmoid equation may have different parameters. These parameters were calculated for different types of explosion as shown in Table 4.7.

Table 4.7. Probit function and sigmoid equation parameters for different types of facility.

Facility (i)	Type of Facility	Probit function	Type of Explosion	Sigmoid parameters		
				a	b	x_0
1	General Building	$-23.8+2.92\ln(p^0)$	BLEVE	1.000	-8.009	64.694
2			VCE	1.006	-64.890	513.220
3						
4	Pressurized vessel	$-42.44+4.33\ln(p^0)$	BLEVE	1.005	-2.558	33.838
			VCE	1.014	-23.220	208.780
5	Atmospheric Vessel	$-18.96+2.44\ln(p^0)$	BLEVE	1.019	-10.050	66.186
6			VCE	1.002	-74.530	524.120
7						

$PSDCW_i$ = Plant lifetime × Incident outcome frequency × probability of structural damage × $FC_i \times WF_i$ (4.14)

$$Total\ cost = Land\ Cost + \sum Interconnection\ cost_{i,j} + \sum PSDCW_i\ , \quad r \neq i \quad (4.15)$$

As seen in eqns. (4.14) and (4.15), PSDCW (Probability of Structural Damage Cost with Weighting factors) has been multiplied with the weighting factor for each facility. After including the same separation constraints used in the distance-based

approach, the optimized total cost and final layout are shown in Table 4.8 and Fig. 4.5, respectively. The land size has slightly increased as compared to the result obtained in Fig. 4.3, similarly, the distance between the process unit and the control room is also increased. The main difference in the result of the integrated approach is the location of administrative building, which has been moved to the furthest location from the process unit due to high occupancy. Therefore, the integrated approach offers the best solution for creating a safer plant layout. Table 4.9 summarizes each layout coordinate based on the proposed formulations.

Table 4.8. Optimized cost from the integrated approach.

Type of Cost	**Cost ($)**	**Remarks**
Interconnection	4009.319	Between all facilities
Land	52700	5 $ / m^2
Risk	44285.798	
Total	100995	

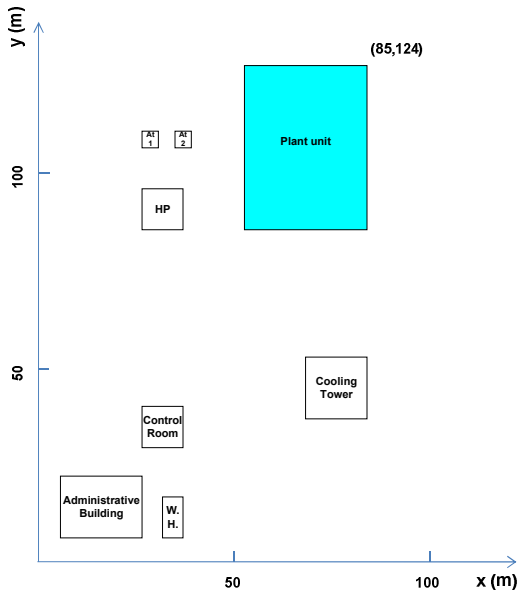

Fig. 4.5. Layout result for the integrated optimization model.

Table 4.9. Coordinates of all facilities based on the proposed approaches.

Facility (i)	Type of Facility	Distance-based approach		Overpressure-based approach		Integrated approach	
		x (m)	y (m)	x (m)	y (m)	x (m)	y (m)
1	Control room (non-pressurized)	35	46	35	35	35	35
2	Administrative building	30	15.5	28	15.5	20	15.5
3	Warehouse	12.5	18	10.5	13	37.5	13
4	High pressure storage sphere	35	88	35	50	35	88
5	Atmospheric flammable liquid storage tank 1	35	121	47	33	32	105
6	Atmospheric flammable liquid storage tank 2	38	113	56	33	40	105
7	Cooling tower	77.5	45.5	52.5	47.5	77.5	46.5
8	Process unit	70	103	45	80	70	104

4.4.4 Evaluation of Layout Result Using FLACS

In order to evaluate the accuracy of optimized layouts in terms of congestion and confinement and its corresponding explosion overpressures, a CFD-based fire and explosion simulator, FLACS was employed in this study to provide more comprehensive risk analysis. In our first attempt to simulate the explosion scenario for the generated layouts, it was observed that some low overpressures in the FLACS results might be due to the low obstacle density, attributed by the simple geometry proposed from the case study. To avoid this simple geometry problem, we imported a real geometry obtained from the laser scanning, which is stored in the RealityLINx software. Using the RealityLINx software, the user can create a 3D object to accurately represent the existing or "as-built" plant conditions from laser scan data. In this chapter, the geometry generated by the software was imported to FLACS and used to evaluate the optimized layout. Fig. 4.6 shows the imported image from RealityLINx to FLACS to represent a process plant.

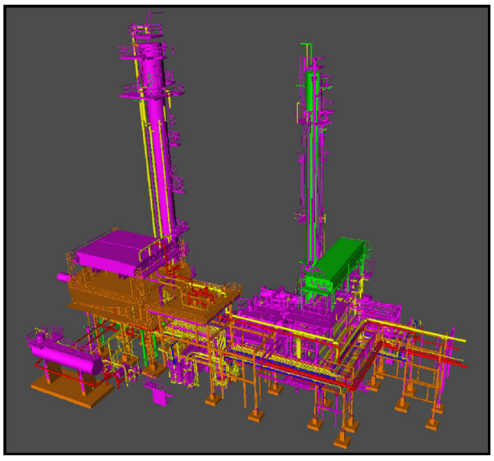

Fig. 4.6 Geometry of process plant used in FLACS simulation.

Fig. 4.7 depicts the maximum overpressure and temperature distribution around the process unit using the FLACS simulation. The flame region was assumed to cover the process unit space, and the ignition source was assumed to be the center of the process plant. Overpressure of the locations having the center coordinates of each facility was monitored and its height was assumed to be 1 meter. According to the simulation results, the overpressure values around the process plant for all optimized layouts are between 0.086 barg and 0.355 barg, as shown in Table 4.10.

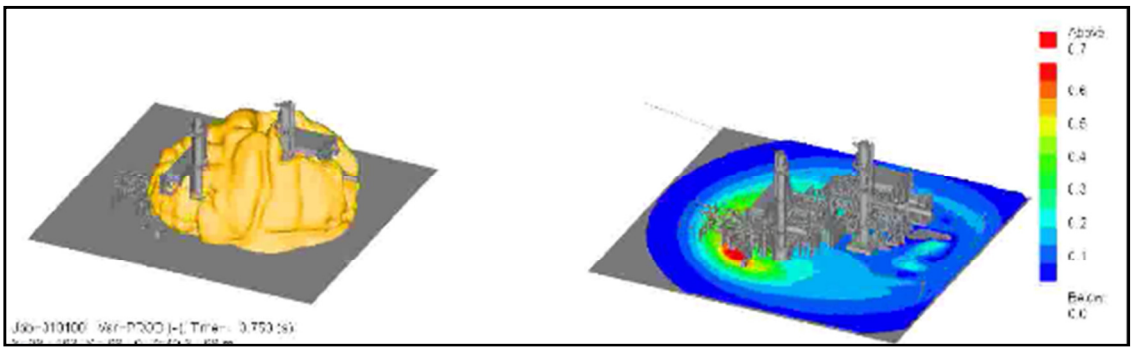

Fig. 4.7 FLACS simulation result showing overpressures (left) and temperature distribution (right) around the process plant.

Table 4.10. Overpressure results from FLACS simulations.

Facility #, i	Overpressure of the layout using distance-based approach (barg)	Overpressure of the layout using overpressure-based approach (barg)	Overpressure of the integrated layout (barg)
1	0.130	0.185	0.113
2	0.092	0.131	0.089
3	0.086	0.116	0.091
4	0.218	0.241	0.215
5	0.233	0.207	0.226
6	0.254	0.225	0.269
7	0.170	0.355	0.170

As seen in Table 4.10, the overpressure results generated from the distance-based and integrated layouts are relatively lower than that of the overpressure-based approach. In both distance-based and integrated approaches, lower overpressures are especially observed in the occupied buildings (facilities #1 - #3) as compared to the overpressure-based approach. Moreover, in the integrated approach, a slightly higher overpressure has been obtained for the warehouse (facility #3), which is attributed by the close proximity to the process unit and the low occupancy of facility #3. The high overpressures as indicated in facilities #5 and #6 in the integrated approach are due to the close proximity

to the ignition source. The probit function of atmospheric vessel (facilities #5 and #6) was found to generate lower impact of overpressures as compared to the probit function for general buildings, and thus these facilities can be placed closer to the process unit.

The overpressure-based approach has a relatively higher overpressure results because of the close distances of facilities from the process unit as depicted in Fig. 4.4. Among the three approaches described in here, the integrated approach has more considerations about occupancy and domino effect thereby allow more important facilities to be allocated in a safer place. Therefore, the integrated approach is found to generate the safest layout among three optimized layouts.

4.5 Conclusions

The method proposed in this chapter demonstrates a systematic technique to integrate QRA in the optimization of plant layout. The use of QRA allows better estimation of potential consequences under study. Three different approaches to allocate facilities for a flammable gas release scenario were developed: fixed distance (recommended separation distance) approach, overpressure-based approach, and the integration of first two approaches with weighting factors to account for building occupancy and domino effect. The optimized layouts from each approach were further evaluated by measuring overpressures in order to provide guidance to select the final layout. According to the prediction results obtained from FLACS, lowest overpressures were observed in the locations of occupied building of the integrated approach result, whereas a slight increase in overpressures and highest overpressures were observed in

almost all facilities covered by the fixed distance and overpressure-based approaches, respectively.

The use of FLACS and real geometry from the RealityLINx software can enhance process safety in the conceptual design and layout stages of plant design. The computed value under this deterministic approach for the expected risk becomes useful information for siting consideration. The approaches suggested in this methodology can be used to aid decision makers in creating low-risk layout structures and determining whether the proposed plant could be safely and economically configured in a particular area.

CHAPTER V

FACILITY SITING OPTIMZATION BY MAPPING RISKS ON A PLANT GRID AREA *

5.1 Introduction

Facility siting focuses on identifying hazard scenarios that could have significant impacts on process plant buildings and building occupants. Such studies include identifying vulnerable locations for occupied buildings such as a control room and temporary buildings, spacing between the adjacent facilities, and spacing between equipment and potential ignition sources. Typically, facility siting is conducted for evaluating the location of existing process plant buildings to minimize the impact of onsite hazards. Likewise, facility siting has been performed as an initial site screening and evaluation for placement of new facilities early in the process design phase. Despite continuous efforts done to regulate facility siting in the process industry, major industrial incidents due to improper siting continue to occur.

One of the contributing factors in major industrial accidents is due to improper siting of occupied buildings near the processing facilities. For instance, the Texas City refinery explosion (2005) was attributed to insufficient spacing between trailers and the isomerization process unit [1].

---

*Reprinted with permission from "A New Approach to Optimizing Facility Layout by Mapping Risk Estimates on Plant Area, Monetizing and Minimizing" by S. Jung, D. Ng, C.D. Laird, and M. S. Mannan, Journal of Loss Prevention in the Process Industries accepted in 2010 © 2010 by Elsevier B.V.

Another incident in Pasadena, Texas (1989) originated from releases of isobutene and ethylene and resulted in an explosion that destroyed the entire facility, including the control room and administration building (Dole, 1990). Similar incidents involving chemical releases and the impacted buildings have also been observed in La Mede, France (1992) [110], Norco, Louisiana (1988) [111], and Flixborough, United Kingdom (1974) [112]. The aforementioned incidents have resulted in many fatalities and industrial losses, which prompt the need to create acceptable guidelines of facility siting in the process industry and establish research initiatives to optimize the placement of occupied facilities while considering potential fire and explosion scenarios. Several publications have been developed to provide guidelines on facility siting and keep its minimum spacing criteria for the process plant. This includes Guidelines for Facility Siting and Layout by Center for Chemical Process Safety/AIChE [5], Process plant layout by Mecklenburgh [21], and Design of Blast Resistant Buildings in Petrochemical Facilities by American Society of Civil Engineers [113]. The recommended spacing criteria here are meant to reduce the impact of fire and explosion on major equipment and facilities, including adjacent process units and buildings. In addition, API 752 and 753 are the two most referred guidelines developed by American Petroleum Institute to assess the siting of permanent and temporary buildings from external fires, explosions, and toxic releases [103, 114]. Facility siting and layout are also addressed in Process Hazard Analysis (PHA) to meet the applicable requirements of OSHA‘s Process Safety Management standard [92]. During a PHA study, the hazard identification should assess the possible impacts of fires and explosions on equipment, structures, and occupant safety on the existing facilities or

proposed facilities. From a research perspective, several mathematical models have been proposed to tackle the complex layout problem. Previous attempts have showed satisfactory results in optimizing the facility layout in combination with some safety considerations using Mixed Integer Non Linear Programming (MINLP), however these findings do not guarantee the global optimum solution [11]. Similarly, numerous publications for the facility layout based on toxic gas release scenarios have also not provided globally optimal solutions [107, 108, 115]. Thus, it is imperative to develop a new methodology to achieve global optima in the facility layout problem with fire, explosion, and toxic release scenarios.

In this chapter, a mathematical formulation using Mixed Integer Linear Programming (MILP) in combination with a quantitative risk analysis (QRA) approach for facility layout is proposed. The proposed methodology addresses trade-offs between risks and capital costs. In the first stage, the entire plant area is discretized into grids. A risk calculation is performed for each grid to account for the risk of having the existing/potential facilities near the hazardous process unit. This grid forms a risk map. The MILP formulation needs to find an optimal layout of facilities in order to reduce the overall costs associated with the risk for each occupied grid, and the capital costs. Finally, the proposed work is accompanied with a case study to illustrate the fire and explosion scenarios in the facility processing heptanes and hexanes. Results from this chapter can be used to provide guidance for facility siting in the process industry and to address the impacts of fire and explosion to process plant buildings and building occupants.

5.2 Problem Statement

The present chapter attempts to address the following questions: "How to manage siting risks when limited space is available?" and "What types of inherently safer design measures should be applied to determine plant layout given a tight cost constraint?" There are two basic problem formulations for layout, continuous plane and grid-based methods [105]. In the continuous plane method, discrete non-linear formulations have been incorporated to solve the optimization problem for different hazardous scenarios, however, the complexity of its algorithms make it difficult to achieve a globally optimum solution [107]. In grid-based methods, two different approaches have often been addressed. The first approach assumes that each facility occupies a single grid of a fixed size. The other approach allows one facility to cover multiple grid locations. In this chapter, the single occupied grid assumption will be employed in this chapter to solve layout problems. The proposed methodology can be divided into two sections, risk mapping on grids and optimization. Risk mapping was used to obtain risk scores around a unit processing flammable chemicals (simply termed the process unit), while the optimization technique was employed for determining safer locations of other facilities. In the initial phase of study, the plant area was divided into 'n' discrete grids (G_k) having coordinates, x_k, y_k. The location of the process unit is assumed to be known and fixed at the center of the available land. New facilities such as storage tanks, control rooms, and buildings are to be allocated in available spaces as depicted by square-shaped grids. AMPL was used to formulate the optimization problem to minimize the total costs, the sum of converted risks and other cost-related variables such as piping, cable, and

maintenance by determining the optimal location of each facility in reference to the fixed process unit.

Overall, the proposed methodology can be divided into 4 steps:

1. Identify hazards from the unit processing flammable chemicals
2. Compute risk scores in terms of probability of structural damage for all grids
3. Set up cost parameters and generate a function for the total cost
4. Determine the optimal locations of each facility based on optimized total cost

5.3 Mathematical Formulation

5.3.1 Risk Score Determination Using Consequence Modeling

Given the close proximity of a unit processing flammable chemicals and the location of other facilities, two types of worst-case release scenarios will be considered: BLEVE (boiling liquid expanding vapor explosion) and VCE (vapor cloud explosion). BLEVE overpressures can be estimated from the amount of released material, temperature and pressure. Blast overpressures from a BLEVE usually yield a circular impact zone around the explosion point. Thus, calculating overpressures for each grid at a given site depends on distances from the explosion point. Here, the consequence modeling program PHAST (v. 6.53.1) was used for overpressure calculations. In the case of a VCE, the flammable vapor is dispersed throughout the plant site while mixing with air. Flammable vapors are often heavier than air and are transported with the wind until the vapor cloud meets an ignition source. Therefore, the explosion center cannot be assumed to be at the point of release, rather it is more rational to use a wind rose to

account for directional effects. A challenge in this approach is that a large number of uncertain parameters such as wind speed, wind direction, air stability, temperature, pressure, humidity of the area, and time delay to ignition must be incorporated in the mathematical formulation. The latter is fixed at 180 seconds in this work for simplification of the calculations. Monte Carlo simulations were used to provide distributions of uncertain variables in the risk analysis. In the Monte Carlo simulation, values are sampled at random from the input probability distributions. Each set of samples is called an iteration, and the resulting outcome from that sample is recorded. After one thousand samplings, the average size of vapor cloud at ignition was determined and the VCE overpressures in the pressure range of interest were estimated using the TNT equivalency method. Finally, the average overpressure due to VCE for each grid can be estimated. Using the TNT equivalency model, the equivalent mass of TNT explosion strength can be estimated as follows:

$$W = \eta M \frac{E_c}{E_{cTNT}} \tag{5.1}$$

where W is an equivalent mass of TNT (kg), M is an actual mass of hydrocarbon, η is an empirical explosion efficiency and the value varies between 1% and 10 % in most flammable cloud estimates [3], here we assumed 10 % for conservative estimation. *Ec* is the heat of combustion of hydrocarbon, and E_{cTNT} is the heat of combustion of TNT (4.6 X 10^6 J/kg).

Subsequently, the overpressure values of BLEVE and VCE were then translated into the probability of structural damage using a probit function [97]:

$$\Pr = -23.8 + 2.92\ln(p^o) \tag{5.2}$$

where p^o is the peak overpressure (N/m^2). By following these steps, every grid in the plane will have its own probability of structural damage, which is defined as risk score (index) in the proposed methodology.

5.3.2 Constraints

5.3.2.1 Non-overlapping Constraints

The non-overlapping constraints ensure n facilities are assigned to K grids without collision. The binary variable B_{ik} is introduced and given by [8]:

$$B_{ik} = 0 \text{ or } 1 \begin{cases} k = 1,2,3,\dots,K \\ i = 1,2,\dots,n \end{cases}$$

$$B_{ik} = \begin{cases} 1 \text{ if facility i is located in the site area} \\ 0 \text{ otherwise} \end{cases}$$

$$\forall k \in \text{all grids on the plane}$$

$$\sum_{k=1}^{K} B_{ik} = 1 \,, \forall i \in \text{New facilities} \tag{5.3}$$

$$\sum_{i=1}^{n} B_{ik} \leq 1 \tag{5.4}$$

5.3.2.2 Distance Constraints

The distance between facilities and the process unit was taken to be rectilinear rather than Euclidean, making it more applicable to industrial conditions. RD_k is defined

to be the distance of the k-th grid from the fixed process unit. These distances can be pre-calculated and supplied as data into the optimization formulation. However, the problem may also have separation constraints between facilities since the location of the facilities are optimization variables, these cannot be precalculated. Equations (5.5) and (5.6) are big-M constraints that define the x-y coordinates of facility i based on its current grid location (defined through the B_{ik} variables);

$$-M(1 - B_{ik}) \leq x_k - x_i \leq M(1 - B_{ik}) \quad (5.5)$$

$$-M(1 - B_{ik}) \leq y_k - y_i \leq M(1 - B_{ik}) \quad (5.6)$$

where x_k is the x coordinate of k-th grid, y_k is the y coordinate of k-th grid, and M is a fixed upper bound on the distance. The coordinates x_k, y_k will be used to calculate the costs of interconnection between i-th facility and the process unit as well as separation distances between new facilities.

5.3.2.3 Separation Distance Constraints

In addition to the process unit, there may be some facilities such as storage tanks and occupied buildings which should not be configured close to each other to minimize the risk of accidental release. Here we establish a separation distance constraint which is given by:

$$|x_i - x_j| + |y_i - y_j| \geq D_{i,j} \quad (5.7)$$

This equation can also be modeled using big-M constraints as follows:

$$(x_i - x_j) + (y_i - y_j) \geq D_{ij} \cdot sepB1_{ij} - M(1 - sepB1_{ij}) \quad (5.8)$$

$$(x_i - x_j) - (y_i - y_j) \geq D_{ij} \cdot sepB2_{ij} - M(1 - sepB2_{ij}) \quad (5.9)$$

$$-(x_i - x_j) + (y_i - y_j) \geq D_{ij} \cdot sepB3_{ij} - M(1 - sepB3_{ij}) \quad (5.10)$$

$$-(x_i - x_j) - (y_i - y_j) \geq D_{ij} \cdot sepB4_{ij} - M(1 - sepB4_{ij}) \quad (5.11)$$

$$sepB1_{ij} + sepB2_{ij} + sepB3_{ij} + sepB4_{ij} \geq 1 \quad (5.12)$$

$$sepB1_{ij};\ sepB2_{ij};\ sepB3_{ij}; sepB4_{ij} \in \{0, 1\}$$

where i represents occupied buildings, j represents storage tanks, x_i, y_i are x, y coordinates of i-th facility and x_j, y_j are x, y coordinates of j-th facility. $D_{i,j}$ is the minimum separation distance between i-th facility and j-th facility. $sepB1_{i,j}$ to $sepB4_{i,j}$ are binary variables to decide the location of i-th facility and j-th facility. M is an appropriate distance upper bound.

On the other hand, similar types of facilities should be placed closer for maintenance and operation purposes. For instance, it is more cost effective to have a group of storage tanks located at some part of the plant area, as depicted in equation (5.13).

$$|x_i - x_j| + |y_i - y_j| \leq m_{ij} \quad (5.13)$$

Equation (5.13) is then modeled using big-M constraints as follows.

$$x_i - x_j + y_i - y_j \leq m_{ij} \quad (5.14)$$

$$x_i - x_j - y_i + y_j \leq m_{ij} \quad (5.15)$$

$$-x_i + x_j + y_i - y_j \leq m_{ij} \quad (5.16)$$

$$-x_i + x_j - y_i + y_j \leq m_{ij} \quad (5.17)$$

where $m_{i,j}$ is the limitation distance among similar facilities and i,j ∈ occupied buildings or i,j ∈ storage tanks.

5.3.3 Objective Function

The objective is to determine the layout of the facilities that minimizes the total cost, which includes the interconnection cost and the probable cost of property damage due to fires or explosions. For simplicity, the unit processing hazardous materials was assumed to be located in the center of the given land (center grid). The objective function is given by

$$\text{Min} \quad \sum_{i=1}^{n} \sum_{k=1}^{K} \left\{ RS_k \times FC^i + RD_k \times UP^i \right\} \times B_{ik} \tag{5.18}$$

where RS_k is the risk score of k-th grid measured from the center of fixed process unit, RD_k is the rectilinear distance of k-th grid calculated from the center of fixed process unit, FC^i is the facility building cost of i-th facility, and UP^i is the unit piping (or interconnection) cost between i-th facility and the center of fixed process unit. These parameters are all pre-calculated based on the grids. The only optimization variables in the objective function are the binary variables Bik. In addition, this objective function is subject to the non-overlapping, and the minimum–maximum separation distance constraints as given in equations (5.3)-(5.12).

5.4 Case Study

The proposed methodology is demonstrated through a case study of hexane-heptane separation in a distillation tower, which was taken from the CCPS-*Chemical Process Quantitative Risk Assessment* book [65]. Here we assumed that there is a single process unit, that this is the hazardous unit for the purposes of the risk map, and that the location of this unit was fixed prior to the optimization. The set of facilities to be placed

refers only to facilities other than the hazardous process unit. Prior to the consequence analysis, three major incident scenarios associated with the distillation process unit were identified, such as catastrophic failure of a component, a liquid or a vapor release from a hole in the pipe. The first scenario can result in explosion and destroy the entire distillation unit. Such catastrophic failure can occur in a case of failure of one of the vessels or a failure of a full bore line rupture. In such cases it is assumed that the entire contents of the column, reboiler, condenser, and accumulator are lost instantaneously. Subsequently, catastrophic failure can also occur due to the failure of some components in the distillation system or a full-bore rupture of pipelines. If it is assumed that approximately 25 m of 0.5 m-diameter pipe and 55 m of 0.15 m-equivalent diameter pipe involved in this accident, the incident frequencies associated with each scenario can be determined and is shown in Table 5.1. Fig. 5.1 shows the potential outcomes of accident scenarios, which was generated from the event tree analysis [65].

Table 5.1. Incident frequency.

Incident	**Frequency (yr^{-1})**
Catastrophic rupture of distillation system	6.5×10^{-6}
Full-bore rupture of a 55 m long pipe	$25 \times 2.6 \times 10^{-7} = 6.5 \times 10^{-6}$
Full-bore rupture of a 25 m long pipe	$25 \times 8.8 \times 10^{-8} = 2.2 \times 10^{-6}$
Sum of release frequency	1.5×10^{-5}

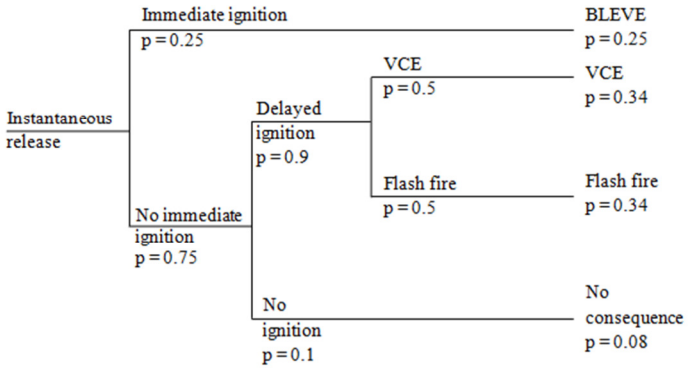

Fig. 5.1. Event tree analysis [65].

Using the incident outcome probability obtained from event tree analysis and release frequency calculation, the incident outcome frequency (yr^{-1}) can be calculated and is shown in Table 5.2.

Table 5.2. Incident outcome frequency.

Incident outcome	Incident frequency (yr^{-1})	Incident outcome probability	Incident outcome frequency
BLEVE	1.5×10^{-5}	0.25	3.8×10^{-6}
VCE	1.5×10^{-5}	0.34	5.1×10^{-6}
Flash fire	1.5×10^{-5}	0.34	5.1×10^{-6}

Since the damage to the process plant buildings due to blast overpressures is the main concern in this study, particular attention will focus on estimating the risk scores caused by BLEVE and VCE. For the simplicity, flash fire is not considered here and will

be the subject of future work. Prior to identifying the risk score for each facility, other information such as the size of plant and the number of grids to be allocated in the given area are needed. Fig. 5.2 shows the risk map with a total area of 10,000 m^2 and its corresponding grids. Each grid in the risk map has a size of 10 m x 10 m. The distillation unit is assumed to be located in the center of the map, marked with black area.

G01	G02	G03	G04	G05	G06	G07	G08	G09	G10
G11	G12	G13	G14	G15	G16	G17	G18	G19	G20
G21	G22	G23	G24	G25	G26	G27	G28	G29	G30
G31	G32	G33	G34	G35	G36	G37	G38	G39	G40
G41	G42	G43	G44	Proc		G47	G48	G49	G50
G51	G52	G53	G54			G57	G58	G59	G60
G61	G62	G63	G64	G65	G66	G67	G68	G69	G70
G71	G72	G73	G74	G75	G76	G77	G78	G79	G80
G81	G82	G83	G84	G85	G86	G87	G88	G89	G90
G91	G92	G93	G94	G95	G96	G97	G98	G99	G100

Fig. 5.2. Grids on the given area.

Blast overpressure of each grid was calculated using PHAST based on the distance from the center point (explosion point) of the process unit. Fig. 5.3 shows the distance to overpressures caused by BLEVE. The calculated result does not consider the wind effect because BLEVE happens instantaneously after releasing. Subsequently, the

overpressure values were then converted to the probability of structural damage via the probit function. For example, the distance between Grid 01 (G_{01}) and the explosion center is 63.6 m, if BLEVE occurs in the center of the process unit, the calculated overpressure using PHAST is 0.20 barg. If this overpressure value is converted to the probability of structural damage via the probit function, it gives 52.7%. If it is assumed that the frequency of BLEVE is 3.8 x 10^{-6} yr^{-1} (taken from Table 5.2) and the lifetime of a plant is 50 years, then the probability of structural damage caused by BLEVE for the entire lifetime on the particular facility sited on Grid 01 is 0.0101 %. This value was multiplied by the weighting factor of 100, and the result is called a risk score. Risk scores for all grids were calculated in this way and given in Fig. 5.4.

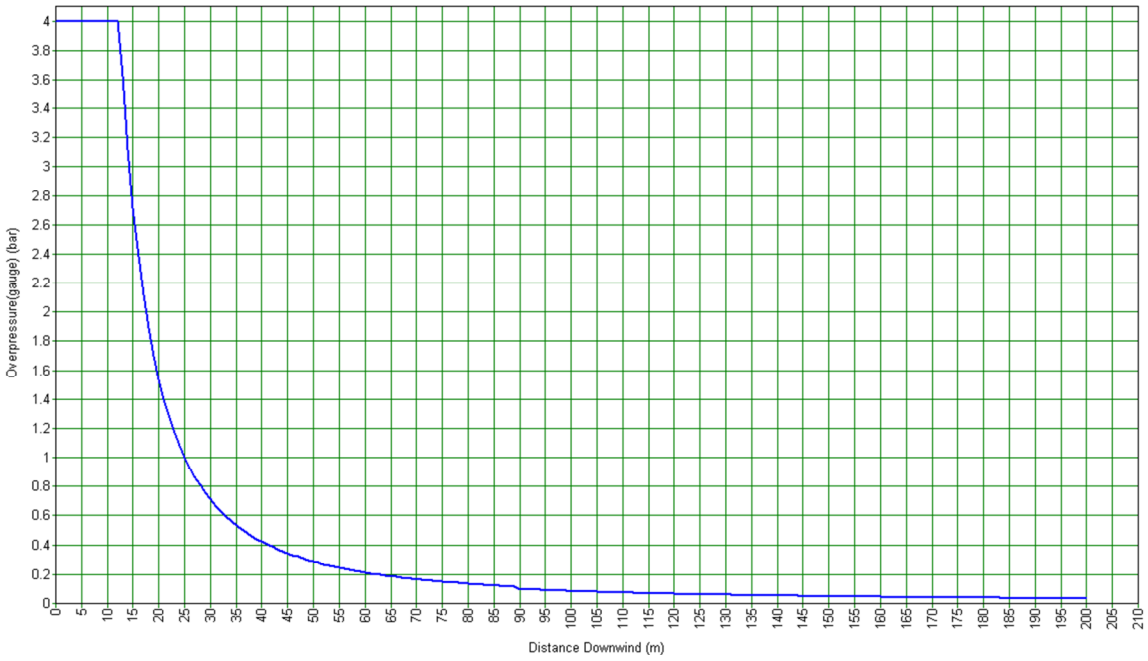

Fig. 5.3. BLEVE overpressure vs. Distance.

0.0101	0.0137	0.0159	0.0170	0.0175	0.0175	0.0170	0.0159	0.0137	0.0101
0.0137	0.0165	0.0178	0.0183	0.0185	0.0185	0.0183	0.0178	0.0165	0.0137
0.0159	0.0178	0.0185	0.0188	0.0189	0.0189	0.0188	0.0185	0.0178	0.0159
0.0170	0.0183	0.0188	0.0189	0.0190	0.0190	0.0189	0.0188	0.0183	0.0170
0.0175	0.0185	0.0189	0.0190	Proc		0.0190	0.0189	0.0185	0.0175
0.0175	0.0185	0.0189	0.0190			0.0190	0.0189	0.0185	0.0175
0.0170	0.0183	0.0188	0.0189	0.0190	0.0190	0.0189	0.0188	0.0183	0.0170
0.0159	0.0178	0.0185	0.0188	0.0189	0.0189	0.0188	0.0185	0.0178	0.0159
0.0137	0.0165	0.0178	0.0183	0.0185	0.0185	0.0183	0.0178	0.0165	0.0137
0.0101	0.0137	0.0159	0.0170	0.0175	0.0175	0.0170	0.0159	0.0137	0.0101

Fig. 5.4. Risk scores from BLEVE overpressures.

In the case of VCE, the blast overpressures were calculated using the TNT-equivalency model by assuming an ignition delay time of 180 seconds. The C# program was used to perform the Monte Carlo simulation for a 1,000 meteorological data set in Beaumont, TX [95, 116]. DEGADIS model was used for the dispersion modeling and later incorporated into the TNT-equivalency model for each weather data set. After 1,000 times of simulation, overpressures of each point were averaged, and then the average overpressures were converted to probability of structural damage via probit function. For example, the distance between Grid 01 (G_{01}) and the explosion center is 63.6 m. The simulated value of overpressure was then converted to the probability of structural damage via the probit function and combined with the incident frequency of VCE, the

plant lifetime, and the weighting factor (100). Finally this value is defined as VCE risk score. Using this method, risk scores for all grids were calculated and shown in Fig. 5.5.

0.0054	0.0057	0.0062	0.0063	0.0062	0.0063	0.0057	0.0053	0.0049	0.0042
0.0058	0.0062	0.0066	0.0070	0.0068	0.0068	0.0060	0.0055	0.0048	0.0043
0.0057	0.0066	0.0072	0.0075	0.0076	0.0069	0.0063	0.0055	0.0049	0.0041
0.0059	0.0066	0.0076	0.0083	0.0083	0.0075	0.0064	0.0057	0.0048	0.0042
0.0059	0.0066	0.0075	0.0083	Proc		0.0059	0.0053	0.0046	0.0041
0.0058	0.0064	0.0072	0.0079			0.0057	0.0051	0.0046	0.0041
0.0058	0.0063	0.0068	0.0072	0.0073	0.0068	0.0058	0.0052	0.0046	0.0040
0.0055	0.0059	0.0063	0.0065	0.0067	0.0062	0.0055	0.0050	0.0044	0.0039
0.0051	0.0055	0.0057	0.0061	0.0060	0.0057	0.0053	0.0047	0.0043	0.0038
0.0047	0.0050	0.0054	0.0055	0.0055	0.0052	0.0050	0.0047	0.0041	0.0037

Fig. 5.5. Risk scores from VCE overpressures.

After obtaining the risk scores from different incidents (BLEVE and VCE) separately, next we combine the two risk maps and the resulting two risk indices is called the integrated risk score, as shown in Fig. 5.6.

0.0155	0.0194	0.0221	0.0233	0.0237	0.0237	0.0227	0.0212	0.0186	0.0143
0.0195	0.0228	0.0244	0.0253	0.0253	0.0253	0.0243	0.0233	0.0213	0.0180
0.0217	0.0245	0.0257	0.0263	0.0265	0.0258	0.0251	0.0241	0.0227	0.0201
0.0229	0.0250	0.0264	0.0272	0.0273	0.0265	0.0253	0.0244	0.0231	0.0212
0.0234	0.0251	0.0264	0.0273	Proc		0.0249	0.0242	0.0231	0.0216
0.0232	0.0250	0.0261	0.0269			0.0247	0.0240	0.0231	0.0216
0.0228	0.0246	0.0256	0.0262	0.0263	0.0258	0.0248	0.0240	0.0229	0.0211
0.0214	0.0237	0.0248	0.0253	0.0256	0.0250	0.0243	0.0235	0.0223	0.0199
0.0189	0.0220	0.0235	0.0244	0.0245	0.0242	0.0237	0.0226	0.0208	0.0176
0.0149	0.0187	0.0213	0.0225	0.0230	0.0226	0.0220	0.0206	0.0178	0.0138

Fig. 5.6. Integrated risk scores, with the process unit sited in the center location.

In this case study, it is assumed that there exists one main control room, one office building, one maintenance building, three storage tanks (one is larger than 38 m^3, two are smaller than 38 m^3), and one utility facility. Table 5.3 shows the recommended separation distances between each facility [5]. Some distances of interest were extracted for this case study, as shown in Table 5.4.

Table 5.3. Typical spacing requirements for on-site buildings [5].

On-Site Building	Utilities	Atmospheric & Low Pressure Flammable & Combustible Storage Tanks (up to 1 atm) < 38 m^3	Atmospheric & Low Pressure Flammable & Combustible Storage Tanks (up to 1 atm) > 38 m^3	High Pressure Flammable Storage
Office, Lab, Maintenance, Warehouse	30 m	15 m	76 m	107 m
Substation, Motor Control-More than One Unit	30 m	30 m	76 m	76 m
Substation, Motor Control-One Unit	30 m	15 m	76 m	76 m
Control Room-Main	30 m	30 m	76 m	107 m
Control Room-More than One Unit	30 m	30 m	76 m	107 m
Control Room-One Unit	30 m	15 m	76 m	76 m

Table 5.4. Minimum separation distances between facilities

	4. (Large storage)	5. (Small storage)	6. (Small storage)	7. (Utility)
1. (Main control room)	76 m	30 m	30 m	30 m
2. (office)	76 m	15 m	15 m	30 m
3. (Maintenance building)	76 m	15 m	15 m	30 m

It is assumed that each facility has different facility building cost and interconnection cost with the center process unit, as depicted in Table 5.5.

Table 5.5. Facility cost and unit piping cost of each facility.

Num.	Type	Facility Cost ($)	UP cost ($/ m)
1	Main control room	1,000,000	10
2	Office	300,000	0.1
3	Auxiliary building for maintenance	200,000	2
4	Large volume storage tank (> 38 m^3)	150,000	100
5	Small volume storage tank 1 (< 38 m^3)	100,000	100
6	Small volume storage tank 2 (< 38 m^3)	100,000	100
7	Utility	500,000	50

As mentioned earlier, similar facilities such as #1,#2,#3 for occupied buildings and #4,#5,#6 for storage need to be located closer for operation and maintenance purposes, thus the maximum separation distance is set at 30 m for each facility. After including all separation distance constraints and cost information into the optimization formulation, the problem is solved with CPLEX and the final layout is shown in Fig. 5.7.

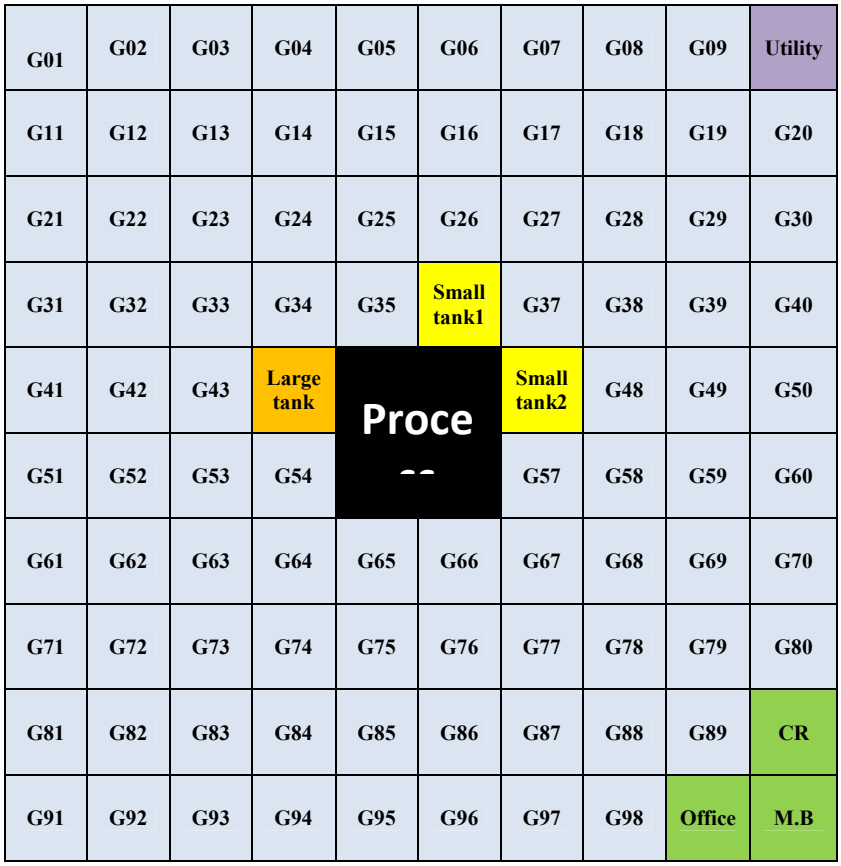

Fig. 5.7. Final layout for the case study.

As seen from Fig. 5.7, all occupied facilities have been located in the bottom-right area which may have smallest overpressure impacts by considering the direction of wind and the location of the distillation unit. This result is also supported by the VCE risk score as shown in Fig. 5.5. Due to the minimum separation distances between storage and occupied buildings, storage areas are far from the control room, however, they are positioned closer to the process unit because of high interconnection costs. Moreover, maximum separation distance constraints allow each similar facility to be positioned within 30 m. The utility area has been assigned to block G10, which is far

from the occupied areas and has a relatively low risk score as shown in Fig. 5.6. In this case study the process unit has been located in the center of the given plot in order to avoid getting close to potential properties outside of the plant site.

5.5 Conclusions

In this chapter, we present a systematic approach to integrate safety and economic analyses in the optimization of plant layout for fire and explosion scenarios. Using the grid-based approach with a single occupied grid assumption, the fixed process unit and new facilities have been configured according to the optimizations of risk score, cost, and separation distance constraints. The risk map, which represents potential accident outcomes such as BLEVE and VCE, was generated to account for the impacts of blast overpressures on process plant buildings. The use of Monte Carlo simulation in VCE overpressure estimation also allows a more realistic representation of meteorological condition associated with the flammable gas release from the fixed process unit. The proposed approach aims in obtaining a globally optimum solution using the grid-based approach and has been successfully demonstrated in a layout planning of hexane-heptane separation unit. The optimization problem was formulated as a mixed integer linear programming problem (MILP) that was formulated in AMPL and solved with CPLEX Thus similar approach here can also be applied to handle irregular shaped facilities.

Nevertheless, the grid-based approach presented here has some limitations such as the configured grid locations tend to be larger than the facilities, the units may cover

multiple grid locations thereby generating a more complex formulation and sizes of facility are often difficult to be accommodated in the formulation because the units must be allocated in predetermined discrete grids or locations. Future work should focus on solving allocation spaces in the grid, sizes of facility stated above and apply the proposed methodology into more complex layout such as acrylic acid production, LPG storage tanks, and LNG terminals in order to expand the proposed optimization tool for developing safer layouts. Results from this chapter can be used to assist in risk assessment of new or existing facilities and to provide guidance in emergency preparedness and accident management at industrial facilities.

CHAPTER VI

CONCLUSIONS AND FUTURE WORKS

6.1 Conclusions

In this dissertation, we explored how to have a better and safer plant layout. New approaches for optimal plant layout, including various risk scenarios, have been described. Different types of scenarios in facility layout haven been separately addressed because toxic gases and flammable gases have different impacts on people or buildings near the plant area. Formulations for MILP and MINLP have been developed for the two dimensional process plant layout problems based on continuous plane approaches and a uniform area discretization approach. QRA has been combined with optimization theory in order to obtain reasonable facility layouts, as well as CFD simulations.

The importance of considering the wind effect is clearly demonstrated by comparing layouts in toxic release cases (Chapters II and III). In these two chapters, I presented a new approach for integrating safety and economic decisions into the optimization of plant layout for toxic gas release scenarios. Although it is not guaranteed that there will be global optimization solutions, it has been suggested several local optimums which gave us room to compare. The concept of personal injury cost was introduced for the potential injury risk associated with toxic release. Gaussian modeling, or dense gas dispersion (DEGADIS) modeling for gases, was integrated to help understand the directional risk function on personal injury.

In Chapters IV and V, facility layout optimizations against fire and explosion scenarios have been solved using QRA approaches, and showed the applicability of using FLACS code for evaluating the layout results. The use of FLACS and real geometry from the RealityLINx software can enhance process safety in the conceptual design and layout stages of plant design. The computed value under this deterministic approach for the expected risk becomes useful information for siting consideration. Especially in Chapter V, a grid-based approach is used with a single occupied grid assumption, the fixed process unit and new facilities have been configured according to the optimizations of risk score, cost, and separation distance constraints. This new concept for risk mapping has been suggested to represent potential accident outcomes such as BLEVE and VCE, and to account for the impacts of blast overpressures on process plant buildings.

Another noticeable development in these approaches is the use of Monte Carlo simulations in gas dispersion estimations, which allows for a more realistic representation of meteorological condition associated with gas releases from a fixed process unit. Other typical consequence modeling studies had only used simple weather concepts, for instance, simply dividing 8 or 16 directions of prevailing wind data to address the local specific weather, but in this dissertation several years of much more extensive wind data have been used to reflect the meteorological data thoroughly.

The approaches suggested in this dissertation can be used to aid decision makers in creating low-risk layout structures and determining whether the proposed plant could be safely and economically configured in a particular area.

6.2 Future Works

Based on the results and difficulties of this dissertation, there are many possible directions future work could be taken.

First of all, consequence modeling studies such as BLEVE estimation or VCE estimation have been developed in process safety research. For BLEVE, there has been a model assuming non-isentropic expansion for the non-ideal gas different from the model I have used in this dissertation. For VCE modeling, the importance of confinement or congestion has been increased instead of using an unconfined explosion approach. For example, API 752 has recommended not using TNT-equivalency modeling for VCE, which has been employed in Chapter V. Therefore, a future work will use the real geometry and FLACS code in order to have a better estimation on VCE and obstacle effects. Considering the Domino effect on the plant area is another issue which cannot be neglected because accidents caused by the domino effect are more serious than any other accidents. It is very difficult to accurately decide general causes and consequences because the domino effect is affected by many nonlinear factors[117].

Future works will focus on the optimization of facilities with flammable gas scenarios and to expand the proposed optimization tool for risk of equipment damage to acquire a safer layout, because the chemical and petrochemical industry has more interest in facility siting against fire and explosion incidents. For continuous plane approach, the way to achieve global optimums will be developed using various techniques such as using rectilinear distance for interconnection cost, separating intervals of non-linear functions, and using global solvers (BARON). For grid-based

plane approach, it is important to make a model realistic as pointed out in discussion of Chapter V. In order to do that, the model needs to improve the formulation of occupying multi-grid for one facility and having multi-hazardous facilities in the given land from the view of optimization. Adequate weighting factors for different occupancy level and various type of building also need to be incorporated in the model with consideration of process safety point of view. Overall, this study will aim to provide information that can be used to assist in risk assessment and give advice for emergency preparedness and accident management.

REFERENCES

1. Baker, J. A.; Erwin, G.; Priest, S.; Tebo, P. V.; Rosenthal, I.; Bowman, F. L.; Hendershot, D.; Leveson, N.; Wilson, L. D.; Gorton, S.; Wiegmann, D. A. *The Report of the BP U.S. Refineries Independent Safety Review Panel*; 2007.
2. Dole, E.; Scannell, G. F. *Phillips 66 Company Houston Chemical Complex Explosion and Fire*; 1990.
3. Crowl, D. A.; Louvar, J. F., *Chemical process safety*. 2nd ed.; Prentice Hall PTR: Upper Saddle River, NJ, 2002.
4. Joseph, G.; Kaszniak, M.; Long, L., Lessons after Bhopal: CSB a catalyst for change *Journal of Loss Prevention in the Process Industries* **2005,** *18*, (4-6).
5. AICHE/CCPS, *Guidelines for facility siting and layout.* American Institute of Chemical Enginers: New York, 2003.
6. Mannan, M. S., *Lees' Loss prevention in the process industries: Hazard identification, assessment and control*. 3rd ed.; Vol. 1,2,3; Elsevier Butterworth-Heinemann: Amsterdam, 2005.
7. Mecklenburgh, J. C., *Plant layout: A guide to the layout of process plant and sites*. Wiley: New York, 1973.
8. Georgiadis, M. C.; Macchietto, S., Layout of process plants: A novel approach. *Computers & Chemical Engineering* **1997,** *21*, (1), 337-342.
9. S. Jayakumar; Reklaitis, G. V., Chemical plant layout via graph partitioning-l. Single level,. *Computers & Chemical Engineering* **1994,** *18*, (5), 441-458.

10. S. Jayakumar; Reklaitis, G. V., Chemical plant layout via graph partitioning-II. Multiple levels. *Computers & Chemical Engineering* **1996,** *20*, (5), 563-578.

11. Penteado, F. D.; Ciric, A. R., An MINLP approach for safe process plant layout. *Industrial and Engineering Chemistry Research* **1996,** *35*, (4), 1354-1361.

12. Patsiatzis, D. I.; Papageorgiou, L. G., Optimal multi-floor process plant layout. *Computers & Chemical Engineering* **2002,** *26*, (4-5), 575-583.

13. AIChE, *Dow's fire & explosion index hazard classification guide*. 7th ed.; American Institute of Chemical Engineers: New York, 1994.

14. Patsiatzis, D. I.; Knight, G.; Papageorgiou, L. G., An MILP approach to safe process plant layout. *Trans IChemE Part A: Chemical Engineering and Design* **2004,** *82*, (5), 579-586.

15. Cozzani, V.; Tugnoli, A.; Salzano, E., Prevention of domino effect: From active and passive strategies to inherently safer design. *Journal of Hazardous Materials* **2007,** *139*, (2), 209-219.

16. Paterson, K.; Tam, V. H. Y.; Moros, T.; Ward-Gittos, D., The design of BP ETAP platform against gas explosions. *Journal of Loss Prevention in the Process Industries* **2000,** *13*, (1), 73-79.

17. Sanders, R. E., Designs that lacked inherent safety: case histories. *Journal of Hazardous Materials* **2003,** *104*, (1-3), 149-161.

18. American Petroleum Institute, *Management of hazards associated with locations of process plant permant buildings*. American Petroleum Institute: Washington DC, 2009.

19. Peters, M. S.; Timmerhaus, K. D.; West, R. E., *Plant design and economics for chemical engineers*. 5th ed.; McGraw Hill: New York, 2003.

20. Tompkins, J. A.; White, J. A.; Bozer, Y. A.; Frazelle, E. H.; Tanchoco, J. M. A.; Treviño, J., *Facility planning*. 2nd ed.; John Wiley & Sons, Inc: New York, 1996.

21. Mecklenburgh, J. C., *Process plant layout*. John Wiley & Sons: New York, 1985.

22. Singh, S. P.; Sharma, R. R. K., A review of different approaches to the facility layout problems *International Journal of Advanced Manufacturing Technology* **2006,** *30*, (5-6), 425-433.

23. Moore, J. M., *Plant layout and design*. Macmillan: New York, 1962.

24. Armour, G. C.; Buffa, E., A heuristic algorithm and simulation approach to relative location of facilities. *Management Science* **1963,** *9*, 294-309.

25. Newell , R. G. Algorithms for the design of chemical plant layout and pipe routing. Ph.D., Imperial College, London, 1973.

26. Goetschalckx, M., An interactive layout heuristic based on hexagonal adjacency graphs. *European Journal of Operational Research* **1992,** *63*, (2), 304-321.

27. Abdinnour-Helm, S.; Hadley, S. W., Tabu search based heuristics for multi-floor facility layout. *International Journal of Production Research* **2000,** *38*, 365-383.

28. Watson, K. H.; Giffin, J. W., The Vertex Splitting Algorithm for facilities layout. *International Journal of Production Research* **1997,** *35* (9), 2477-2492.

29. Huang, X.; Lai, W.; Sajeev, A. S. M.; Gao, J., A new algorithm for removing node overlapping in graph visualization. *Information Sciences* **2007,** *177*, (14), 2821-2844.

30. Foulds, L. R.; Hamacher, H. W.; Wilson, J. M., Integer programming approaches to facilities layout models with forbidden areas *Annals of Operations Research* **1998,** *82*, (0), 405-418.

31. Evans, G. W.; Wilhelm, M. R.; Karwowski, W., A layout design heuristic employing the theory of fuzzy sets. *International Journal of Production Research* **1987,** *25*, (10), 1431-1450.

32. Mavridou, T. D.; Pardalos, P. M., Simulated annealing and genetic algorithms for the facility layout problem: A survey. *Computational Optimization and Applications* **1997,** *7*, (1), 111-126

33. Castell, C. M. L.; Lakshmanan, R.; Skilling, J. M.; Bañares-Alcántara, R., Optimisation of process plant layout using genetic algorithms. *Computers & Chemical Engineering* **1998,** *22*, (1), 993-996.

34. Verweij, B.; Ahmed, S.; Kleywegt, A. J.; Nemhauser, G.; Shapiro, A., The sample average approximation method applied to stochastic routing problems: A computational study. *Computational Optimization and Applications* **2003,** *24*, 289-333.

35. Martens, J., Two genetic algorithms to solve a layout problem in the fashion industry. *European Journal of Operational Research* **2004,** *154*, (1), 304-322.

36. Wu, X.; Chu, C. H.; Wang, Y.; Yan, W., A genetic algorithm for cellular manufacturing design and layout. *European Journal of Operational Research* **2007,** *181*, (1), 156-167.

37. Bortfeldt, A., A genetic algorithm for the two-dimensional strip packing problem with rectangular pieces. *European Journal of Operational Research* **2006,** *172*, (3), 814-837.

38. Gomes-de-Alvarenga, A.; Negreiros-Gomes, F. J.; Mestria, M., Metaheuristic methods for a class of the facility layout problem. *Journal of Intelligent Manufacturing* **2000,** *11*, (4), 421-430.

39. Balakrishnan, J.; Cheng, C. H.; Wong, K. F., FACOPT: a user friendly FACility layout OPTimization system. *Computers & Operations Research* **2003,** *30*, (11), 1625-1641.

40. McKendall, A. J. R.; Shang, J.; Kuppusamy, S., Simulated annealing heuristics for the dynamic facility layout problem. *Computers & Operations Research* **2006,** *33*, (8), 2431-2444.

41. Balakrishnan, J.; Cheng, C. H., A note on "A hybrid genetic algorithm for the dynamic plant layout problem". *International Journal of Production Economics* **2006,** *103*, 87-89.

42. Amaral, A. R. S., On the exact solution of a facility layout problem. *European Journal of Operational Research* **2006,** *173*, 508-518.

43. Koopmans, T. C.; Beckmann, M., Assignment Problems and the Location of Economic Activities. *Econometrica* **1957,** *25*, (1), 53-76.

44. Pardalos, P. M.; Rentl, F.; Wolkowicz, H., The quadratic assignment problem: A survey and recent developments, *American Mathematical Society* **1994**, *16*, 1-42.

45. Sahni, S.; Gonzalez, T., P-Complete Approximation Problems. *Journal of the Association for Computing Machinery* **1976,** *23*, (3), 555-565.

46. Christofides, N.; Mingozzi, A.; Toth, P., Contributions to the quadratic assignment problem. *European Journal of Operational Research* **1980,** *4*, (4), 243-247.

47. Francis, R. L.; McGinnis, L. F.; White, J. A., *Facility layout and location : an analytical approach*. 2nd ed.; Prentice-Hall International Series in Industrial and Systems Engineering: Englewood Cliffs, NJ, 1992.

48. Kelachankuttu, H.; Batta, R.; Nagi, R., Contour line construction for a new rectangular facility in an existing layout with rectangular departments. *European Journal of Operational Research* **2007,** *180*, (1), 149-162.

49. Savas, S.; Batta, R.; Nagi, R., Finite-Size Facility placement in the presence of barriers to rectilinear travel. *Operations Research* **2002,** *50*, 1018 - 1031.

50. Urban, T. L., A multiple criteria model for the facilities layout problem. *International Journal of Production Research* **1987,** *25*, (12), 1805-1812.

51. Rosenblatt, M. J., The facilities layout problem: a multi-goal approach. *International Journal of Production Research* **1979,** *17,* (4), 323-332.

52. Montreuil, B. In *A modeling framework for integrating layout design and flow network design*, Proceedings of the Material Handling Research Colloquium, Hebron, 1990.

53. Heragu, S. S.; Kusiak, A., Efficient models for the facility layout problem. *European Journal of Operational Research* **1991,** *53*, (1), 1-13.

54. Lacksonen, T. A., Preprocessing for static and dynamic facility layout problems. *International Journal of Production Research* **1997,** *35*, (4), 1095-1106.

55. Lacksonen, T. A., Static and dynamic layout problems with varying areas. *Journal of Operational Research Society* **1994,** *45*, (1), 59-69.

56. Xie, W.; Sahinidis, N. V., A branch-and-bound algorithm for the continuous facility layout problem. *Computers & Chemical Engineering* **2007**, doi:10.1016/j.compchemeng.2007.05.003.

57. Barbosa-Póvoa, A. P.; Mateus, R.; Novais, A. Q., Optimal 3D layout of industrial facilities. *International Journal of Production Research* **2002,** *40*, (7), 1669-1698.

58. Papageorgiou, L. G.; Rotstein, G. E., Continous-domain mathematical models for ooptimal process plant layout. *Industrial and Engineering Chemistry Research* **1998,** *37*, (9), 3631-3639.

59. Barbosa-Póvoa, A. P.; Mateus, R.; Novais, A. Q., Optimal two-dimensional layout of industrial facilities. *International Journal of Production Research* **2001,** *39*, (12), 2567-2593.

60. Westerlund, J.; Papageorgiou, L. G.; Westerlund, T., A MILP Model for N-dimensional allocation. *Computers & Chemical Engineering* **2007**, *31*, (12), 1702-1714.

61. Guirardello, R.; Swaney, E., Optimization of process plant layout with pipe routing. *Computers & Chemical Engineering* **2005,** *30*, (1), 99-114.

62. Sherali, H. D.; Fraticelli, B. M. P.; Meller, R. D., Enhanced model formulations for optimal facility layout. *Operations Research* **2003,** *51*, 629-644.

63. Hendershot, D. C., Tell me why. *Journal of Hazardous Materials* **2007,** *142*, (3), 582-588.

64. Kletz, T., *What went wrong? Case histories of process plant disasters*. Gulf Publishing Co: Houston, 1985.

65. AICHE/CCPS, *Guidelines for chemical process quantitative risk analysis*. American Institute of Chemical Engineers: New York, 2007.

66. Modarres, M., *Risk analysis in engineering, tecniques, tools, and trends*. Taylor & Francis: Boca Raton, FL, 2006.

67. Scenna, N. J.; Cruz, A. S. M. S., Road risk analysis due to the transportation of chlorine in Rosario City. *Reliability Engineering & System Safety* **2005,** *90*, (1), 83-90.

68. Godoy, S. M., STRRAP system-A software for hazardous materials risk assessment and safe distances calculation. *Reliability Engineering & System Safety* **2007,** *92*, 847-857.

69. EPA Technology Transfer Network Support Center for Regulatory Atmospheric Modeling.
http://www.epa.gov/scram001/metobsdata_databases.htm (05/15/2007),

70. DC-NOAA Sunrise/Sunset Calculator.
http://www.srrb.noaa.gov/highlights/sunrise/sunrise.html (05/15/2007),

71. Wiekema, B. J., Vapour cloud explosions-An analysis based on accidents Part I. *Journal of Hazardous Materials* **1984,** *8*, 295-311.

72. Wiekema, B. J., Vapour cloud explosions-An analysis based on accidents Part II. *Journal of Hazardous Materials* **1984,** *8*, 313-329.

73. Conradsen, K.; Nielsen, L. B.; Prahm, L. P., Review of Weibull statistics for estimation of wind speed distributions. *Journal of Applied Meteorology* **1984,** *23*, 1173-1183.

74. EPA, *Meteorological monitoring guidance for regulatory modeling applications*: Environmental Protection Agency, Research Triangle Park, NC, 2000.

75. Turner, D. B., A diffusion model for an urban area. *Journal of Applied Meteorology* **1964,** *3*, (1), 83-91.

76. Fairhurst, S.; Turner, R. M., Toxicological assessments in relation to major hazzards. *Journal of Hazardous Materials* **1993,** *33*, 215-227.

77. Vilchez, J. A.; Montiel, H.; Casal, J.; Arnaldos, J., Analytical expressions for the calculation of damage percentage using the probit methodology. *Journal of Loss Prevention in the Process Industries* **2001,** *14*, 193-197.

78. Franks, A. P.; Harper, P. J.; Bilo, M., The relationship between risk of death and risk of dangerous dose for toxic substances. *Journal of Hazardous Materials* **1996,** *51*, (1-3), 11-34.

79. Bliss, C. I., The method of probits--A correction. *Science, New Series* **1934,** *79*, (2053), 409-410.

80. Bliss, C. I., The method of probits. *Science, New Series* **1934,** *79*, (2037), 38-39.

81. Finney, D. J., *Probit analysis*. Cambridge University Press: Cambridge, 1971.

82. Beaumont, N., An algorithm for disjunctive programs. *European Journal of Operational Research* **1990,** *48*, (3), 362-371.

83. Lee, S.; Grossmann, I. E., New algorithms for nonlinear generalized disjunctive programming. *Computers and Chemical Engineering* **2000,** *24*, 2125-2141.

84. Grossmann, I. E.; Lee, S., Generalized disjunctive programming: nonlinear convex hull relaxation and algorithms. *Computational Optimization and Applications* **2003,** *26*, 83-100.

85. Grossmann, I. E., Review of nonlinear mixed-integer and disjunctive programming techniques. *Optimization and Engineering* **2002,** *3*, 227-252.

86. McCormick, G. P., *Nonlinear programming, theory, algorithms and applications*. John Wiley & Sons: New York, 1982.

87. Williams, H. P., *Model building in mathematical programming*. John Wiley & Sons: New York, 1985.

88. Raman, R.; Grossmann, I. E., Relation between MILP modeling and logical inference for chemical process synthesis. *Computers and Chemical Engineering* **1991,** *15*, (2), 73-84.

89. Robles-Agudo, O.; Vázquez-Román, R.; Grossmann, I. E.; Iglesias-Silva, G., A multiperiod planning model for the oil and gas production system *Computers & Chemical Engineering* **2007,** sent for publishing.

90. Brooke, A.; Kendrick, D.; Meeraus, A.; Raman, R., *GAMS- a user guide*. Washington DC: GAMS Development Corporation: 1998.

91. American Petroleum Institute, *API 581 - Risk-based inspection.* American Petroleum Institute: Washington DC, 2000.

92. Kaszniak, M.; Holmstrom, D., Trailer siting issues: BP Texas City. *Journal of Hazardous Materials* **2008,** *159*, (1), 105-111.

93. Vazquez-Roman, R.; Lee, J. H.; Jung, S.; Mannan, M. S., Designing plant layouts with toxic releases based on wind statistics. In *IASTED International Conference on Modelling and Simulation*, Quebec, 2008.

94. Ayyub, B. M., *Risk analysis in engineering and economics*. CHAPMAN & HALL/CRC: Boca Raton, FL, 003.

95. The_Meteorological_Resource_Center, *accessed in December, 2008* http://www.webmet.com/State_pages/met_tx.htm

96. AICHE/CCPS, *Guidelines for use of vapor cloud dispersion models*. American Institute of Chemical Engineers: New York, 1996.

97. AICHE/CCPS, *Guidelines for consequence analysis of chemical releases*. American Institute of Chemical Engineers: New York, 1999.

98. Haag, P. A. M. U. d.; Ale, B. J. M., *Guideline for quantitative risk assessment (Purple Book)*. Committee for the Prevention of Disasters (CPR): Apeldoorn, 1999.

99. Dandrieux, A. l.; Dusserre, G.; Ollivier, J., Small scale field experiments of chlorine dispersion. *Journal of Loss Prevention in the Process Industries* **2002,** *15*, 5-10.

100. AICHE/CCPS, *Guidelines for chemical process quantitative risk analysis*. 2nd ed.; American Institute of Chemical Engineers: New York, 2000.

101. Mannan, M. S.; West, H. H.; Berwanger, P. C., Lessons learned from recent incidents: Facility siting, atmospheric venting, and operator information systems. *Journal of Loss Prevention in the Process Industries* **2007,** *20*, 644-650.

102. Dreux, M. S., Defending OSHA facility siting citations: Issues and recommendations. *Process Safety Progress* **2005,** *24*, (2), 77-78.

103. American Petroleum Institute, *Management of hazards associated with location of process plant portable buildings*. American Petroleum Institute: Washington DC, 2007.

104. Realff, M. J.; Shah, N.; Pantelides, C. C., Simultaneous design, layout and scheduling of pipeless batch plants. *Computers & Chemical Engineering* **1996,** *20*, (6-7), 869-883.

105. Ozyurt, D. B.; Realff, M. J., Geographic and process information chemical plant layout problems. *AIChE J.* **1999,** *45*, 2161-2174.

106. Georgiadis, M. C.; Schilling, G.; Rotstein, G. E.; Macchietto, S., A general mathematical programming approach for process plant layout. *Computers & Chemical Engineering* **1999,** *23*, (7), 823-840.

107. Jung, S.; Ng, D.; Lee, J. H.; Vazquez-Roman, R.; Mannan, M. S., An approach for risk reduction (methodology) based on optimizing the facility layout and siting in toxic gas release scenarios. *Journal of Loss Prevention in the Process Industries* **2010,** *23*, 139-148.

108. Vazquez-Roman, R.; Lee, J. H.; Jung, S.; Mannan, M. S., Optimal facility layout under toxic release in process facilities: A stochastic approach. *Computers and Chemical Engineering* **2009,** *34*, (1), 122-133.

109. Cozzani, V.; Salzano, E., The quantitative assessment of domino effects caused by overpressure: Part I. Probit models. *Journal of Hazardous Materials* **2004,** *107*, (3), 67-80.

110. Heller, S. I., Overview of major incidents. In *the NPRA National Safety Conference*: Houston, 1993.

111. Hagar, R., Most Norco units shut down in wake of blast. *Oil & Gas Journal* **1988,** *32*.

112. Marshall, V. C., The siting and protection of buildings in hazardous areas. In *Major Chemical Hazards*, Ellis Horwood Limited: Sussex, 1987.

113. ASCE, *Design of blast resistant buildings in petrochemical facilities*. American Society of Civil Engineers: New York, 1997.

114. American Petroleum Institute, *Management of hazards associated with locations of process plant buildings*. American Petroleum Institute: Washington DC, 2003.

115. Diaz-Ovalle, C.; Vazquez-Roman, R.; Mannan, M. S., An approach to solve the facility layout problem based on the worst-case scenario. *Journal of Loss Prevention in the Process Industries* **2010,** Accepted Manuscript.

116. The_Meteorological_Resource_Center, *accessed in July, 2009* http://www.webmet.com/State_pages/met_tx.htm

117. Lee J.; Kim, H. S., Yoon, E. S., A new approach for allocating explosive facilities in order to minimize the domino effect using NLP *Journal of Chemical Engineering of Japan,* **2006,** *39*, (7), 731-745.

APPENDIX A

GAMS CODE FOR CHAPTER III

```
*******************************************************************************
sets
i  Installed facilities   /"Facility A","Facility B", "Residential A", "Residential B", "Residential C"/

s  Release Facilitie for siting  /"New A", "New B", "Control Room"/

r  Release types                                /"cl release" /

*ri(i,r)  Installed facilities having release     /"Facility A"."cl release" /


**Removed because no new facility is having toxic release
rs(s,r)  Siting facilities having release     /"New A"."cl release" /


* There are 36 intervals of 10?each
angle Number of intervals related to wind direction /1*36/


alias (s,saux);
sets
MIS(s,i) Pipes connecting installed-siting facilities /"New A"."Facility A"/
MSS(s,saux) Pipes connecting siting facilities /"New A"."New B"/
;
parameters
Pupil(s) Population in siting facility
    /"New A"  0, "New B"   0, "Control Room"   10/
Pupil2(i) Population in installed facility
    /"Facility A" 0, "Facility B" 0, "Residential A" 10, "Residential B" 10, "Residential C" 10/



parA(s,r,angle) Parameter to calculate the probability of death
                        /"New A"."cl release"."1" 0.069676

                         "New A"."cl release"."2" 0.093931

                         "New A"."cl release"."3" 0.108214

                         "New A"."cl release"."4" 0.135176

                         "New A"."cl release"."5" 0.18611

                         "New A"."cl release"."6" 0.239302

                         "New A"."cl release"."7" 0.265774
```

"New A"."cl release"."8" 0.279551

"New A"."cl release"."9" 0.286384

"New A"."cl release"."10" 0.286385

"New A"."cl release"."11" 0.274937

"New A"."cl release"."12" 0.252825

"New A"."cl release"."13" 0.225602

"New A"."cl release"."14" 0.209072

"New A"."cl release"."15" 0.199054

"New A"."cl release"."16" 0.187923

"New A"."cl release"."17" 0.180797

"New A"."cl release"."18" 0.175532

"New A"."cl release"."19" 0.178149

"New A"."cl release"."20" 0.179259

"New A"."cl release"."21" 0.180206

"New A"."cl release"."22" 0.18598

"New A"."cl release"."23" 0.228869

"New A"."cl release"."24" 0.258162

"New A"."cl release"."25" 0.24705

"New A"."cl release"."26" 0.241674

"New A"."cl release"."27" 0.231645

"New A"."cl release"."28" 0.217144

"New A"."cl release"."29" 0.17119

"New A"."cl release"."30" 0.121049

"New A"."cl release"."31" 0.108453

"New A"."cl release"."32" 0.100075

"New A"."cl release"."33" 0.086666545

"New A"."cl release"."34" 0.071409654

"New A"."cl release"."35" 0.064410813

"New A"."cl release"."36" 0.064182541

/
parB(s,r,angle) Parameter to calculate the probability of death
/"New A"."cl release"."1" -66.4824

"New A"."cl release"."2" -81.1134

"New A"."cl release"."3" -80.4913

"New A"."cl release"."4" -81.5867

"New A"."cl release"."5" -83.1793

"New A"."cl release"."6" -81.9707

"New A"."cl release"."7" -79.4018

"New A"."cl release"."8" -77.6074

"New A"."cl release"."9" -75.9418

"New A"."cl release"."10" -73.9833

"New A"."cl release"."11" -73.7306

"New A"."cl release"."12" -73.4923

"New A"."cl release"."13" -72.2163

"New A"."cl release"."14" -72.8344

"New A"."cl release"."15" -74.8626

"New A"."cl release"."16" -74.4505

"New A"."cl release"."17" -76.56

"New A"."cl release"."18" -78.3431

"New A"."cl release"."19" -76.9182

"New A"."cl release"."20" -76.6886

"New A"."cl release"."21" -75.3455

"New A"."cl release"."22" -75.4216

"New A"."cl release"."23" -69.645

"New A"."cl release"."24" -57.8696

"New A"."cl release"."25" -57.4273

"New A"."cl release"."26" -63.6342

"New A"."cl release"."27" -66.7632

"New A"."cl release"."28" -62.9143

"New A"."cl release"."29" -60.6511

"New A"."cl release"."30" -67.2007

"New A"."cl release"."31" -68.797

"New A"."cl release"."32" -71.3277

"New A"."cl release"."33" -68.1173379

"New A"."cl release"."34" -68.0154954

"New A"."cl release"."35" -71.1123693

"New A"."cl release"."36" -82.0116129

/

parC(s,r,angle) Parameter to calculate the probability of death
/"New A"."cl release"."1" 206.3742

"New A"."cl release"."2" 164.9547

"New A"."cl release"."3" 154.7033

"New A"."cl release"."4" 144.3328

"New A"."cl release"."5" 127.327

"New A"."cl release"."6" 128.0577

"New A"."cl release"."7" 153.2477

"New A"."cl release"."8" 182.278

"New A"."cl release"."9" 201.7401

"New A"."cl release"."10" 207.4434

"New A"."cl release"."11" 202.3512

"New A"."cl release"."12" 196.5768

"New A"."cl release"."13" 199.3704

"New A"."cl release"."14" 202.2436

"New A"."cl release"."15" 200.2474

"New A"."cl release"."16" 197.924

"New A"."cl release"."17" 188.6714

"New A"."cl release"."18" 180.9315

"New A"."cl release"."19" 180.842

"New A"."cl release"."20" 180.9704

"New A"."cl release"."21" 185.6501

"New A"."cl release"."22" 184.4758

"New A"."cl release"."23" 171.5417

"New A"."cl release"."24" 184.2796

"New A"."cl release"."25" 207.2998

"New A"."cl release"."26" 223.1897

"New A"."cl release"."27" 229.1287

"New A"."cl release"."28" 228.6024

"New A"."cl release"."29" 210.394

"New A"."cl release"."30" 198.0825

"New A"."cl release"."31" 200.3191

"New A"."cl release"."32" 200.0424

"New A"."cl release"."33" 210.8498204

"New A"."cl release"."34" 212.5006148

"New A"."cl release"."35" 214.9089854

"New A"."cl release"."36" 173.5391878

/

Sx(angle) Sign of slope in interval Nangle
/"1" 1, "2" 1, "3" 1, "4" 1, "5" 1, "6" 1, "7" 1, "8" 1, "9" 1

```
   "10" -1, "11" -1, "12" -1, "13" -1, "14" -1, "15" -1, "16" -1, "17" -1, "18" -1
   "19" -1, "20" -1, "21" -1, "22" -1, "23" -1, "24" -1, "25" -1, "26" -1, "27" -1
   "28" 1, "29" 1, "30" 1, "31" 1, "32" 1, "33" 1, "34" 1, "35" 1, "36" 1 /
Sy(angle) Sign of delta y in interval Nangle
    /"1"  1, "2"   1, "3"   1, "4"   1, "5" 1, "6" 1, "7" 1, "8" 1, "9" 1
   "10" 1, "11" 1, "12" 1, "13" 1, "14" 1, "15" 1, "16" 1, "17" 1, "18" 1
   "19" -1, "20" -1, "21" -1, "22" -1, "23" -1, "24" -1, "25" -1, "26" -1, "27" -1
   "28" -1, "29" -1, "30" -1, "31" -1, "32" -1, "33" -1, "34" -1, "35" -1, "36" -1 /
parameters
*xrsd(s,r) Displacement in x to ubicate the release of s  /"New A".  10 /
*yrsd(s,r) Displacement in y to ubicate the release of s  /"New A".  1 /

xrfd(s,r) Displacement in x to ubicate the release of f  /"New A"."cl release"  0/
yrfd(s,r) Displacement in y to ubicate the release of f  /"New A"."cl release"  0/
freq(s,r) "Frequency of the release (times/year)"   /"New A"."cl release" 0.00058/

xi(i)  Position in x of installed facility fi        / "Facility A"     15
                                                      "Facility B"     12.5
                                                      "Residential A"  20
                                                      "Residential B"  40
                                                      "Residential C"  60/
yi(i)  Position in y of installed facility fi      /"Facility A"       10
                                                      "Facility B"     27.5
                                                      "Residential A"  550
                                                      "Residential B"  550
                                                      "Residential C"  550/
Lxi(i)  Length in x of installed facility fi       /"Facility A"       20
                                                     "Facility B"       15/
Lyi(i)  Length in y of installed facility fi       /"Facility A"       10
                                                     "Facility B"       15/
Lxs(s)  Length in x of siting facility s           /"New A"        10
                                                     "New B"        30
                                                     "Control Room" 15/
Lys(s)  Length in y of siting facility s           /"New A"        30
                                                     "New B"        15
                                                     "Control Room" 15/
scalar Lx   Maximum length of land in x direction (m)           /250/
scalar Ly   Maximum length of land in y direction (m)           /500/

scalar st   Size of the street                                  /5/
scalar Cp   "Price per m of pipe ($/m)"                        /196.8/
*scalar Lc   "Price per m2 of land ($/m2)"                      /67.0/
scalar Lc   "Price per m2 of land ($/m2)"                      /6.0/
scalar CostPerLife Cost for each person dead in an accident       /10000000.0/
scalar lyfeLayout  Life time of layout (years)                  /45/
* /0.00058/
*scalar Lc   "Price per m2 of land ($/m2)"                      /1500.0/
*
* Calculated Parameters (but verify the angles)
*
*parameter maxFIx  Minimum x value to calculate the occupied area;
*
parameter Dminx(s,i) Minimum sitting-installed facilities x-separation;
```

```
Dminx(s,i)= (Lxi(i) + Lxs(s))/2.0 + st;
parameter Dminy(s,i) Minimum sitting-installed facilities x-separation;
Dminy(s,i)= (Lyi(i) + Lys(s))/2.0 + st;

parameter Dminsx(s,saux) Minimum sitting-sitting facilities x-separation;
Dminsx(s,saux)= (Lxs(saux) + Lxs(s))/2.0 + st;
parameter Dminsy(s,saux) Minimum sitting-sitting facilities x-separation;
Dminsy(s,saux)= (Lys(saux) + Lys(s))/2.0 + st;

parameter Lxsi(s,i) Minimun separation of siting-installed facilities;
Lxsi(s,i)= (Lxs(s) + Lxi(i))/2.0 + st;
parameter Lysi(s,i) Minimun separation of siting-installed facilities;
Lysi(s,i)= (Lys(s) + Lyi(i))/2.0 + st;

parameter Lxss(s,saux) Constants to evaluate the minimun separation of siting-siting facilities;
Lxss(s,saux)= (Lxs(s) + Lxs(saux))/2.0 + st;
parameter Lyss(s,saux) Constants to evaluate the minimun separation of siting-siting facilities;
Lyss(s,saux)= (Lys(s) + Lys(saux))/2.0 + st;
parameter slope(angle) Slope for every 10?
slope(angle)= sin(PI*ord(angle)/18)/cos(PI*ord(angle)/18);
slope("9")= inf;
slope("27")= -inf;
* Some of the equations must be modified if the angles change
*
*****************************************************************************
***
***                 VARIABLES
***
variables
x(s)        Position in x of siting facility
y(s)        Position in y of siting facility
Dsi(s,i)    "Distance between center-center, siting-fixed facility"
Dss(s,saux)  "Distance between center-center, siting facilities"
PDeath(s,r,saux)  Probability of death because of release in s affecting saux
PDeath2(s,r,i) Probability of death because of release in s affecting i

*
areaX      The extreme side in x direction for the final occupied area
areaY      The extreme side in x direction for the final occupied area
area       The occupied area
costP      Piping cost for facility-siting
costP2     Piping cost for siting-siting
costL      Land cost
costR      Cost for toxic release(NA)-CR
costR2     Cost for toxic release(NA)-FB
cost       Total cost
*
xsiL(s,i)   Convex hull variable for siting-installed facilities
xsiR(s,i)   Convex hull variable for siting-installed facilities
xsiAD(s,i)  Convex hull
ysiA(s,i)   Convex hull variable for siting-installed facilities
ysiD(s,i)   Convex hull variable for siting-installed facilities
ysiLR(s,i)  Convex hull
```

BsiL(s,i) Binary for siting-installed facilities
BsiR(s,i) Binary for siting-installed facilities
BsiAD(s,i) Binary for siting-installed facilities
BsiA(s,i) Binary for siting-installed facilities
BsiD(s,i) Binary for siting-installed facilities
*
xssL(s,saux) Convex hull variable for siting-siting facilities
xssR(s,saux) Convex hull variable for siting-siting facilities
xssAD(s,saux) Convex hull
yssA(s,saux) Convex hull variable for siting-siting facilities
yssD(s,saux) Convex hull variable for siting-siting facilities
yssLR(s,saux) Convex hull
BssL(s,saux) Binary for siting-siting facilities
BssR(s,saux) Binary for siting-siting facilities
BssAD(s,saux) Binary for siting-siting facilities
BssA(s,saux) Binary for siting-siting facilities
BssD(s,saux) Binary for siting-siting facilities
*
DssxL(s,saux) Convex hull variable for siting-siting facilities
DssxR(s,saux) Convex hull variable for siting-siting facilities
DssxAD(s,saux) Convex hull variable for siting-siting facilities
DssyLR(s,saux) Convex hull variable for siting-siting facilities
DssyA(s,saux) Convex hull variable for siting-siting facilities
DssyD(s,saux) Convex hull variable for siting-siting facilities
BssL(s,saux) Binary for siting-siting facilities
BssR(s,saux) Binary for siting-siting facilities
BssAD(s,saux) Binary for siting-siting facilities
BssA(s,saux) Binary for siting-siting facilities
BssD(s,saux) Binary for siting-siting facilities
*
xisAR(i,s,angle) Convex hull variable for angle calculation
yisAR(i,s,angle) Convex hull variable for angle calculation
xsiAR(s,i,angle) Convex hull variable for angle calculation
ysiAR(s,i,angle) Convex hull variable for angle calculation

xssAR(s,r,saux,angle) Convex hull variable for angle calculation
yssAR(s,r,saux,angle) Convex hull variable for angle calculation
xssARa(s,r,angle)
yssARa(s,r,angle)
BisAR(i,s,angle) Binary to indicate the angular region between installed-siting
BssAR(s,r,saux,angle) Binary to indicate the angular region between siting-siting
BsiAR(s,i,angle) Binary to indicate the angular region between siting-installed

diffx(s,saux)
diffy(s,saux)

basura
*
Binary variable BsiL(s,i), BsiR(s,i), BsiAD(s,i), BsiA(s,i), BsiD(s,i),
        BssL(s,saux), BssR(s,saux), BssAD(s,saux), BssA(s,saux),
        BssD(s,saux), BisAR(i,s,angle), BssAR(s,r,saux,angle)
        BsiAR(s,i,angle);

```
*
*  Separation distances
*
Equation eqDsf(s,i)  Distances between siting-installed facilities;
eqDsf(s,i).. Dsi(s,i)=e= sqrt((x(s) - xi(i))*(x(s) - xi(i))
                        +  (y(s) - yi(i))*(y(s) - yi(i)));
Equation eqDss(s,saux)  Distances between siting-siting facilities;
eqDss(s,saux)$(ord(saux) gt ord(s)).. Dss(s,saux)=e=
                          sqrt((x(s) - x(saux))*(x(s) - x(saux))
                        +  (y(s) - y(saux))*(y(s) - y(saux)));
*
*  Non overlapping convex hull for siting-installed facilities
*
Equation eqSF1(s,i)  Non overlapping using convex hull: disaggregation of x(s);
eqSF1(s,i).. x(s) =e= xsiL(s,i) + xsiR(s,i) + xsiAD(s,i);
Equation eqSF2(s,i)  Non overlapping using convex hull: disaggregation of y(s);
eqSF2(s,i).. y(s) =e= ysiA(s,i) + ysiD(s,i) + ysiLR(s,i);
Equation eqSF3(s,i)  Non overlaping left dijunction;
eqSF3(s,i).. xsiL(s,i)=l= (xi(i) - Dminx(s,i))*BsiL(s,i);
Equation eqSF4(s,i)  Non overlaping right dijunction;
eqSF4(s,i).. xsiR(s,i) =g= (xi(i) + Dminx(s,i))*BsiR(s,i);
Equation eqSF5(s,i)  Non overlaping right dijunction ;
eqSF5(s,i).. xsiAD(s,i) =g= (xi(i) - Dminx(s,i))*BsiAD(s,i);
Equation eqSF6(s,i)  Non overlaping right dijunction ;
eqSF6(s,i).. xsiAD(s,i) =l= (xi(i) + Dminx(s,i))*BsiAD(s,i);
Equation eqSF7(s,i)  Non overlaping right dijunction ;
eqSF7(s,i).. ysiA(s,i) =g= (yi(i) + Dminy(s,i))*BsiA(s,i);
Equation eqSF8(s,i)  Non overlaping right dijunction ;
eqSF8(s,i).. ysiD(s,i) =l= (yi(i) - Dminy(s,i))*BsiD(s,i);
Equation eqSF9(s,i)  Non overlaping right dijunction ;
eqSF9(s,i).. BsiL(s,i) + BsiR(s,i) + BsiAD(s,i) =e= 1;
Equation eqSF10(s,i)  Non overlaping right dijunction ;
eqSF10(s,i).. BsiA(s,i) + BsiD(s,i) =e= BsiAD(s,i);
Equation eqSF11(s,i)  Non overlaping right dijunction ;
eqSF11(s,i).. xsiL(s,i) =g= 0.0;
Equation eqSF12(s,i)  Non overlaping right dijunction ;
eqSF12(s,i).. xsiR(s,i) =g= 0.0;
Equation eqSF13(s,i)  Non overlaping right dijunction ;
eqSF13(s,i).. xsiAD(s,i) =g= 0.0;
Equation eqSF14(s,i)  Non overlaping right dijunction ;
eqSF14(s,i).. ysiA(s,i) =g= 0.0;
Equation eqSF15(s,i)  Non overlaping right dijunction ;
eqSF15(s,i).. ysiD(s,i) =g= 0.0;
Equation eqSF16(s,i)  Non overlaping right dijunction ;
eqSF16(s,i).. ysiLR(s,i) =g= 0.0;
Equation eqSF17(s,i)  Non overlaping right dijunction ;
eqSF17(s,i).. xsiL(s,i) =l= (Lx - st - Lxs(s)/2)*BsiL(s,i);
Equation eqSF18(s,i)  Non overlaping right dijunction ;
eqSF18(s,i).. xsiR(s,i) =l= (Lx - st - Lxs(s)/2)*BsiR(s,i);
Equation eqSF19(s,i)  Non overlaping right dijunction ;
eqSF19(s,i).. xsiAD(s,i) =l= (Lx - st - Lxs(s)/2)*BsiAD(s,i);
Equation eqSF20(s,i)  Non overlaping right dijunction ;
eqSF20(s,i).. ysiA(s,i) =l= (Ly - st - Lys(s)/2)*BsiA(s,i);
```

```
Equation eqSF21(s,i)  Non overlaping right dijunction ;
eqSF21(s,i).. ysiD(s,i) =l= (Ly - st - Lys(s)/2)*BsiD(s,i);
Equation eqSF22(s,i)  Non overlaping right dijunction ;
eqSF22(s,i).. ysiLR(s,i) =l= (Ly - st - Lys(s)/2)*(1 - BsiAD(s,i));
*
*  Non overlapping convex hull for siting-siting facilities
*
Equation eqSS1(s,saux)  Non overlapping using convex hull: disaggregation of x(s);
eqSS1(s,saux)$(ord(saux) gt ord(s)).. x(s) =e= xssL(s,saux) + xssR(s,saux) + xssAD(s,saux);
Equation eqSS1A(s,saux)  Non overlapping using convex hull: disaggregation of x(s);
eqSS1A(s,saux)$(ord(saux) gt ord(s)).. x(saux) =e= xssL(saux,s) + xssR(saux,s) + xssAD(saux,s);
Equation eqSS2(s,saux)  Non overlapping using convex hull: disaggregation of y(s);
eqSS2(s,saux)$(ord(saux) gt ord(s)).. y(s) =e= yssA(s,saux) + yssD(s,saux) + yssLR(s,saux);
Equation eqSS2A(s,saux)  Non overlapping using convex hull: disaggregation of y(s);
eqSS2A(s,saux)$(ord(saux) gt ord(s)).. y(saux) =e= yssA(saux,s) + yssD(saux,s) + yssLR(saux,s);
Equation eqSS3(s,saux)  Non overlaping left dijunction;
eqSS3(s,saux)$(ord(saux) gt ord(s)).. xssL(s,saux)=l= xssL(saux,s) - Dminsx(s,saux)*BssL(s,saux);
Equation eqSS4(s,saux)  Non overlaping right dijunction;
eqSS4(s,saux)$(ord(saux) gt ord(s)).. xssR(s,saux) =g= xssR(saux,s) + Dminsx(s,saux)*BssR(s,saux);
Equation eqSS5(s,saux)  Non overlaping right dijunction ;
eqSS5(s,saux)$(ord(saux) gt ord(s)).. xssAD(s,saux) =g= xssAD(saux,s) -
Dminsx(s,saux)*BssAD(s,saux);
Equation eqSS6(s,saux)  Non overlaping right dijunction ;
eqSS6(s,saux)$(ord(saux) gt ord(s)).. xssAD(s,saux) =l= xssAD(saux,s) +
Dminsx(s,saux)*BssAD(s,saux);
Equation eqSS7(s,saux)  Non overlaping right dijunction ;
eqSS7(s,saux)$(ord(saux) gt ord(s)).. yssA(s,saux) =g= yssA(saux,s) + Dminsy(s,saux)*BssA(s,saux);
Equation eqSS8(s,saux)  Non overlaping right dijunction ;
eqSS8(s,saux)$(ord(saux) gt ord(s)).. yssD(s,saux) =l= yssD(saux,s) - Dminsy(s,saux)*BssD(s,saux);
Equation eqSS9(s,saux)  Non overlaping right dijunction ;
eqSS9(s,saux)$(ord(saux) gt ord(s)).. BssL(s,saux) + BssR(s,saux) + BssAD(s,saux) =e= 1;
Equation eqSS10(s,saux)  Non overlaping right dijunction ;
eqSS10(s,saux)$(ord(saux) gt ord(s)).. BssA(s,saux) + BssD(s,saux) =e= BssAD(s,saux);
Equation eqSS11(s,saux)  Non overlaping right dijunction ;
eqSS11(s,saux)$(not sameas(saux,s)).. xssL(s,saux) =g= 0.0;
Equation eqSS12(s,saux)  Non overlaping right dijunction ;
eqSS12(s,saux)$(not sameas(saux,s)).. xssR(s,saux) =g= 0.0;
Equation eqSS13(s,saux)  Non overlaping right dijunction ;
eqSS13(s,saux)$(not sameas(saux,s)).. xssAD(s,saux) =g= 0.0;
Equation eqSS14(s,saux)  Non overlaping right dijunction ;
eqSS14(s,saux)$(not sameas(saux,s)).. yssA(s,saux) =g= 0.0;
Equation eqSS15(s,saux)  Non overlaping right dijunction ;
eqSS15(s,saux)$(not sameas(saux,s)).. yssD(s,saux) =g= 0.0;
Equation eqSS16(s,saux)  Non overlaping right dijunction ;
eqSS16(s,saux)$(not sameas(saux,s)).. yssLR(s,saux) =g= 0.0;
Equation eqSS17(s,saux)  Non overlaping right dijunction ;
eqSS17(s,saux)$(ord(saux) gt ord(s)).. xssL(s,saux) =l= (Lx - st - Lxs(s)/2)*BssL(s,saux);
Equation eqSS17A(s,saux)  Non overlaping right dijunction ;
eqSS17A(s,saux)$(ord(saux) gt ord(s)).. xssL(saux,s) =l= (Lx - st - Lxs(saux)/2)*BssL(s,saux);
Equation eqSS18(s,saux)  Non overlaping right dijunction ;
eqSS18(s,saux)$(ord(saux) gt ord(s)).. xssR(s,saux) =l= (Lx - st - Lxs(s)/2)*BssR(s,saux);
Equation eqSS18A(s,saux)  Non overlaping right dijunction ;
eqSS18A(s,saux)$(ord(saux) gt ord(s)).. xssR(saux,s) =l= (Lx - st - Lxs(saux)/2)*BssR(s,saux);
```

```
Equation eqSS19(s,saux)  Non overlaping right dijunction ;
eqSS19(s,saux)$(ord(saux) gt ord(s)).. xssAD(s,saux) =l= (Lx - st - Lxs(s)/2)*BssAD(s,saux);
Equation eqSS19A(s,saux)  Non overlaping right dijunction ;
eqSS19A(s,saux)$(ord(saux) gt ord(s)).. xssAD(saux,s) =l= (Lx - st - Lxs(saux)/2)*BssAD(s,saux);
Equation eqSS20(s,saux)  Non overlaping right dijunction ;
eqSS20(s,saux)$(ord(saux) gt ord(s)).. yssA(s,saux) =l= (Ly - st - Lys(s)/2)*BssA(s,saux);
Equation eqSS20A(s,saux)  Non overlaping right dijunction ;
eqSS20A(s,saux)$(ord(saux) gt ord(s)).. yssA(saux,s) =l= (Ly - st - Lys(saux)/2)*BssA(s,saux);
Equation eqSS21(s,saux)  Non overlaping right dijunction ;
eqSS21(s,saux)$(ord(saux) gt ord(s)).. yssD(s,saux) =l= (Ly - st - Lys(s)/2)*BssD(s,saux);
Equation eqSS21A(s,saux)  Non overlaping right dijunction ;
eqSS21A(s,saux)$(ord(saux) gt ord(s)).. yssD(saux,s) =l= (Ly - st - Lys(saux)/2)*BssD(s,saux);
Equation eqSS22(s,saux)  Non overlaping right dijunction ;
eqSS22(s,saux)$(ord(saux) gt ord(s)).. yssLR(s,saux) =l= (Ly - st - Lys(s)/2)*(1 - BssAD(s,saux));
Equation eqSS22A(s,saux)  Non overlaping right dijunction ;
eqSS22A(s,saux)$(ord(saux) gt ord(s)).. yssLR(saux,s) =l= (Ly - st - Lys(saux)/2)*(1 - BssAD(s,saux));
*
* Toxic release
*
* Determining the angular position of targets respect to sources
* source: an installed facility
*
Equation diff1(s,saux);
diff1(s,saux)$(ord(saux) ne ord(s)).. diffx(s,saux) =e= x(saux)-x(s);
Equation diff2(s,saux);
diff2(s,saux)$(ord(saux) ne ord(s)).. diffy(s,saux) =e= y(saux)-y(s);

Equation eqSRS1(s,r,saux)  Toxic release using convex hull: disaggregation of diffx(s);
eqSRS1(s,r,saux)$(rs(s,r)and (ord(saux) ne ord(s))).. diffx(s,saux) =e= sum(angle,xssAR(s,r,saux,angle));
Equation eqSRS2(s,r,saux)  Toxic release using convex hull: disaggregation of y(s);
eqSRS2(s,r,saux)$(rs(s,r)and (ord(saux) ne ord(s))).. diffy(s,saux) =e= sum(angle,yssAR(s,r,saux,angle));
Equation eqSRS3(s,r,saux,angle)  Toxic release disjunction Eq 1;
eqSRS3(s,r,saux,angle)$(rs(s,r) and (ord(saux) ne ord(s))).. Sy(angle)*yssAR(s,r,saux,angle) =g= 0.0;
Equation eqSRS4(s,r,saux,angle)  Toxic release disjunction Eq 2;
eqSRS4(s,r,saux,angle)$(rs(s,r) and (ord(saux) ne ord(s))).. Sx(angle)*xssAR(s,r,saux,angle) =g= 0.0;
Equation eqSRS5(s,r,saux,angle)  Toxic release disjunction Eq 3;
eqSRS5(s,r,saux,angle)$((rs(s,r)) and (ord(angle) ne 9) and (ord(angle) ne 27) and (ord(saux) ne ord(s))).
Sx(angle)*
                    yssAR(s,r,saux,angle) =l=
                    Sx(angle)*slope(angle)*xssAR(s,r,saux,angle);
Equation eqSRS6(s,r,saux,angle) Toxic release dijunction 4;
eqSRS6(s,r,saux,angle)$((rs(s,r)) and (ord(angle) ne 10) and (ord(angle) ne 28) and (ord(saux) ne ord(s))).
Sx(angle)*
                yssAR(s,r,saux,angle) =g=
                Sx(angle)*slope(angle - 1)*xssAR(s,r,saux,angle);
Equation eqSRS7(s,r,saux)  Toxic release dijunction;
eqSRS7(s,r,saux)$(rs(s,r) and (ord(saux) ne ord(s))).. sum(angle,BssAR(s,r,saux,angle)) =e= 1;
Equation eqSRS8(s,r,saux,angle)  Toxic release dijunction;
eqSRS8(s,r,saux,angle)$(rs(s,r) and (ord(saux) ne ord(s))).. xssAR(s,r,saux,angle) =g= -
BssAR(s,r,saux,angle)*(Lx - st - Lxs(s)/2);
Equation eqSRS9(s,r,saux,angle)  Toxic release dijunction;
eqSRS9(s,r,saux,angle)$(rs(s,r) and (ord(saux) ne ord(s))).. yssAR(s,r,saux,angle) =g= -
BssAR(s,r,saux,angle)*(Ly - st - Lys(s)/2);
```

```
Equation eqSRS10(s,r,saux,angle)  Toxic release dijunction;
eqSRS10(s,r,saux,angle)$(rs(s,r) and (ord(saux) ne ord(s))).. xssAR(s,r,saux,angle) =l=
BssAR(s,r,saux,angle)*(Lx - st - Lxs(s)/2);
Equation eqSRS11(s,r,saux,angle)  Toxic release dijunction;
eqSRS11(s,r,saux,angle)$(rs(s,r) and (ord(saux) ne ord(s))).. yssAR(s,r,saux,angle) =l=
BssAR(s,r,saux,angle)*(Ly - st - Lys(s)/2);

* Directional Disjunction for NA(Release) - FB(Pupils)
Equation eqSRI1(s,r,i)  Toxic release using convex hull: disaggregation of x(s);
eqSRI1(s,r,i)$rs(s,r).. x(s) =e= sum(angle,xsiAR(s,i,angle));
Equation eqSRI2(s,r,i)  Toxic release using convex hull: disaggregation of y(s);
eqSRI2(s,r,i)$rs(s,r).. y(s) =e= sum(angle,ysiAR(s,i,angle));
Equation eqSRI3(s,r,i,angle)  Toxic release disjunction Eq 1;
eqSRI3(s,r,i,angle)$rs(s,r)..  Sy(angle)*(BsiAR(s,i,angle)*yi(i) - ysiAR(s,i,angle)) =g= 0.0;
Equation eqSRI4(s,r,i,angle)  Toxic release disjunction Eq 2;
eqSRI4(s,r,i,angle)$rs(s,r)..  Sx(angle)*(BsiAR(s,i,angle)*xi(i) - xsiAR(s,i,angle)) =g= 0.0;
Equation eqSRI5(s,r,i,angle)  Toxic release disjunction Eq 3;
eqSRI5(s,r,i,angle)$((rs(s,r)) and (ord(angle) ne 9) and (ord(angle) ne 27))..
Sx(angle)*(BsiAR(s,i,angle)*yi(i) - ysiAR(s,i,angle)) =l=
                    Sx(angle)*slope(angle)*(BsiAR(s,i,angle)*xi(i) - xsiAR(s,i,angle));
Equation eqSRI6(s,r,i,angle) Toxic release dijunction 4;
eqSRI6(s,r,i,angle)$((rs(s,r)) and (ord(angle) ne 10) and (ord(angle) ne 28))..
Sx(angle)*(BsiAR(s,i,angle)*yi(i) - ysiAR(s,i,angle)) =g=
                  Sx(angle)*slope(angle - 1)*(BsiAR(s,i,angle)*xi(i) - xsiAR(s,i,angle));
Equation eqSRI7(s,r,i)  Toxic release dijunction;
eqSRI7(s,r,i)$rs(s,r).. sum(angle,BsiAR(s,i,angle)) =e= 1;
Equation eqSRI8(s,r,i,angle)  Toxic release dijunction;
eqSRI8(s,r,i,angle)$rs(s,r).. xsiAR(s,i,angle) =g= 0;
Equation eqSRI9(s,r,i,angle)  Toxic release dijunction;
eqSRI9(s,r,i,angle)$rs(s,r).. ysiAR(s,i,angle) =g= 0;
Equation eqSRI10(s,r,i,angle)  Toxic release dijunction;
eqSRI10(s,r,i,angle)$rs(s,r).. xsiAR(s,i,angle) =l= BsiAR(s,i,angle)*(Lx - st - Lxs(s)/2);
Equation eqSRI11(s,r,i,angle)  Toxic release dijunction;
eqSRI11(s,r,i,angle)$rs(s,r).. ysiAR(s,i,angle) =l= BsiAR(s,i,angle)*(Ly - st - Lys(s)/2);

*
* Determining the angular position of targets respect to sources
* source: a siting facility
*

*
*  Calculating Risk because of toxic release
*
Equation eqTR1(s,r,saux) Calculate probability of death at this distance;
eqTR1(s,r,saux)$(rs(s,r)and (ord(saux) ne ord(s)))..  PDeath(s,r,saux) =e=
sum(angle,BssAR(s,r,saux,angle)*parA(s,r,angle)/(1+exp(-(Dss(s,saux)-
parC(s,r,angle))/parB(s,r,angle))));
Equation eqTR2(s,r,i) Calculate probability of death at this distance;
eqTR2(s,r,i)$rs(s,r)..  PDeath2(s,r,i) =e= sum(angle,BsiAR(s,i,angle)*parA(s,r,angle)/(1+exp(-(Dsi(s,i)-
parC(s,r,angle))/parB(s,r,angle))));

*
*
```

```
* Other equations
*
* Angles
*
$ontext
Removed because no new facility is having toxic release
Equation eqAngle2(s,saux);
eqAngle2(s,saux)$ ri(i,r).. angless(s,saux) =e= arctan((y(saux) - yi(s))/(x(saux) - xi(s)));
Equation eqAngle3(s,r,i);
eqAngle3(s,i)$ rs(s,r).. anglesi(s,i) =e= arctan((y(i) - yi(s))/(x(i) - xi(s)));
$offtext
*
* Ocupied area:
*
Equation calcX(s) Calculate the maximum x component;
calcX(s).. areaX =g= x(s) + Lxs(s)/2;
Equation calcY(s) Calculate the maximum y component;
calcY(s).. areaY =g= y(s) + Lys(s)/2;
Equation AreaCalculation;
AreaCalculation.. area=e= areaX*areaY;
*
* Constraints on positions
*
Equation eqOnL1(s)  All siting facilities must layout inside the land;
eqOnL1(s)..  x(s) =g= Lxs(s)/2 + st;
Equation eqOnL2(s)  All siting facilities must layout inside the land;
eqOnL2(s)..  x(s) =l= Lx - (Lxs(s)/2 + st);
Equation eqOnL3(s)  All siting facilities must layout inside the land;
eqOnL3(s)..  y(s) =g= Lys(s)/2 + st;
Equation eqOnL4(s)  All siting facilities must layout inside the land;
eqOnL4(s)..  y(s) =l= Ly - (Lys(s)/2 + st);
*
* Defining the objective function
*
Equation eqLC  Building land cost: surface area occupied by units and piperack (eq 2);
eqLC.. costL =e= Lc*area;
Equation eqPC  Piping cost for siting-installed facilities;
eqPC.. costP =e= 0.5*Cp*(sum(MIS(s,i),Dsi(s,i)));
Equation eqPC2 Piping cost for siting-siting facilities;
eqPC2.. costP2=e= 0.5*Cp*(sum(MSS(s,saux)$(ord(saux) gt ord(s)), Dss(s,saux)));
Equation eqRC Calculate cost of death at this distance;
eqRC..  costR =e= sum((s,r,saux)$(rs(s,r)and (ord(saux) ne ord(s))),freq(s,r)*PDeath(s,r,saux)*
                        CostPerLife*lyfeLayout*Pupil(saux));
Equation eqRC2 Calculate cost of death at this distance;
eqRC2..  costR2 =e= sum((s,r,i)$rs(s,r),freq(s,r)*PDeath2(s,r,i)*
                       CostPerLife*lyfeLayout*Pupil2(i));
Equation totalCost Includes all costs;
totalCost.. cost=e= costP + costP2 + costL + sum((s,r,saux)$rs(s,r),freq(s,r)*PDeath(s,r,saux)*
                         CostPerLife*lyfeLayout*Pupil(saux))+
                         sum((s,r,i)$rs(s,r),freq(s,r)*PDeath2(s,r,i)*
                         CostPerLife*lyfeLayout*Pupil2(i));
*sum((i,r,s)$ri(i,r),PDeath(i,r,s)*
*                         CostPerLife*lyfeLayout*Pupil(s))
```

```
*
*******************************************************************************
*******************************************************************************
* Bounds
*
x.lo(s)= Lxs(s)/2 + st;
x.up(s)= Lx - (Lxs(s)/2 + st);
y.lo(s)= Lys(s)/2 + st;
y.up(s)= Ly - (Lys(s)/2 + st);
Dsi.lo(s,i)= 0.0;
Dsi.up(s,i)= sqrt(Lx*Lx + Ly*Ly);
costP.lo= 0;
costP.up= inf;
areaX.lo= 0.0;
areaX.up= Lx - st;
areaY.lo= 0.0;
areaY.up= ly - st;
area.lo= 0.0;
area.up= Lx*Ly;
Dss.lo(s,saux)= 0.0;
Dss.up(s,saux)= sqrt(Lx*Lx + Ly*Ly);
* Auxiliary variables
xsiL.lo(s,i)= 0.0;
xsiL.up(s,i)= Lx;
xsiR.lo(s,i)= 0.0;
xsiR.up(s,i)= Lx;
xsiAD.lo(s,i)= 0.0;
xsiAD.up(s,i)= Lx;
ysiA.lo(s,i)= 0.0;
ysiA.up(s,i)= Ly;
ysiD.lo(s,i)= 0.0;
ysiD.up(s,i)= Ly;
ysiLR.lo(s,i)= 0.0;
ysiLR.up(s,i)= Ly;

xssL.lo(s,saux)= 0.0;
xssL.up(s,saux)= Lx;
xssR.lo(s,saux)= 0.0;
xssR.up(s,saux)= Lx;
xssAD.lo(s,saux)= 0.0;
xssAD.up(s,saux)= Lx;
yssA.lo(s,saux)= 0.0;
yssA.up(s,saux)= Ly;
yssD.lo(s,saux)= 0.0;
yssD.up(s,saux)= Ly;
yssLR.lo(s,saux)= 0.0;
yssLR.up(s,saux)= Ly;

yisAR.lo(i,s,angle)= 0.0;
yisAR.up(i,s,angle)= Ly;
xisAR.lo(i,s,angle)= 0.0;
xisAR.up(i,s,angle)= Lx;
```

```
yssAR.lo(s,r,saux,angle)= 0.0;
yssAR.up(s,r,saux,angle)= Ly;
xssAR.lo(s,r,saux,angle)= 0.0;
xssAR.up(s,r,saux,angle)= Lx;

PDeath.lo(s,r,saux)= 0.0;
PDeath.up(s,r,saux)= 1.0;
*xsiRel.lo(i,r,s,Nangle)= 0.0;
*xsiRel.up(i,r,s,Nangle)= Lx;

*ysiRel.lo(i,r,s,Nangle)=0.0;
*ysiRel.up(i,r,s,Nangle)=Ly;


*
*  Initial values
*
Dsi.l(s,i)= st;
Dss.l(s,saux)= st;
x.l(s)= 0;
y.l(s)= 0;
BsiL.l(s,i)= 0;
BisAR.l(i,s,angle)=0;
BssAR.l(s,r,saux,angle)=0;

*
*   Solver definition
*
option limcol = 0;
*  Check the solution against the targets:
parameter report(*,*,*) Solution Summary;

Model FirstModel /all/
option minlp= dicopt option nlp=minos option mip= cplex;
FirstModel.domlim= 60;
FirstModel.optca=0;
FirstModel.optcr=0.1;
FirstModel.optfile= 1;
FirstModel.scaleopt= 1;
option iterlim= 500000;
*OPTION SYSOUT=ON
*
*  Solve First Relaxed Model
*
$ontext
option rminlp= conopt;
solve FirstModel using rminlp minimizing cost;
if(FirstModel.modelstat > 2.5,
   option rminlp= minos;
   solve FirstModel using rminlp minimizing cost;
)
if ( FirstModel.modelstat > 2.5,
   option rminlp= snopt;
```

```
   solve FirstModel using rminlp minimizing cost;
)
abort$(FirstModel.modelstat > 2.5) "Relaxed model could not be solved!"
$offtext
*
*  Then the minlp
*
option minlp= dicopt option nlp=minos option mip= cplex;
*option minlp= dicopt option nlp=conopt option mip= cplex;

$onecho > dicopt.opt
epsmip 1.0e-10
maxcycles 500
continue 2
stop 1
NLPITERLIM 100000
$offecho

Solve FirstModel using minlp minimizing cost;
**********************************************************************
```

APPENDIX B

GAMS CODE FOR CHAPTER IV

This code is for 3rd strategy of Chapter IV.

```
 5 ***************************************************************************************
 6 sets
 7 s  Facilities for siting  /"Plant","Utility", "CR", "Office", "MB", "LS",
   "SS1", "SS2"/
 8 *MB= warehouse
 9 *Office= administration building
10
11 r  explosion types                                  /"VCE", "BL
   EVE"/
12
13 rs(s,r)  Installed facilities having release     /"Plant"."VCE", "Plant"."
   BLEVE" /
14
15 alias (s,saux);
16 sets
17 MSS(s,saux) Interconnectivity of facilities   /   "CR"."Office"
18                                               "CR"."MB"
19                                               "CR"."LS"
20                                               "CR"."SS1"
21                                               "CR"."SS2"
22                                               "CR"."Plant"
23                                               "CR"."Utility"
24
25                                               "MB"."Office"
26                                               "MB"."LS"
27                                               "MB"."SS1"
28                                               "MB"."SS2"
29                                               "MB"."Plant"
30                                               "MB"."Utility"
31
32                                               "Office"."LS"
33                                               "Office"."SS1"
34                                               "Office"."SS2"
35                                               "Office"."Plant"
36                                               "Office"."Utility"
37
38                                               "LS"."SS1"
39                                               "LS"."SS2"
40                                               "LS"."Plant"
41                                               "LS"."Utility"
42
43                                               "SS1"."SS2"
44                                               "SS1"."Plant"
```

```
45                                      "SS1"."Utility"
46
47                                      "SS2"."Plant"
48                                      "SS2"."Utility"
49
50                                      "Plant"."Utility"
51  /
52  ;
53
54  TABLE Interconnectivity(s,saux) Interconnectivity Cost between facilities
55
56                      "CR"    "Office"        "MB"       "LS"       "
   SS1"        "SS2"    "Plant"    "Utility"
57          "CR"             0        0.1          0.1        10
   10           10         10         10
58          "Office"          0.1        0           0.1         0
    0           0          0          0
59          "MB"             0.1       0.1          0          0.1
   0.1          0.1        0.1        0.1
60          "LS"             10         0           0.1         0
   0.1          0.1        100         0
61          "SS1"            10         0           0.1        0.1
    0           0.1        100         0
62          "SS2"            10         0           0.1        0.1
   0.1           0         100         0
63          "Plant"          10         0           0.1        100
   100          100         0         100
64          "Utility"        10         0           0.1         0
    0           0         100         0;
65
66  parameters
67  Building(s) Building Cost for each facility
68       /"Plant" 0, "Utility" 1000000, "CR"  1000000, "Office"   300000, "MB"
      200000, "LS"  150000, "SS1"  100000, "SS2"  100000/
69
70  WeightFactor(s) Weight Factor for each facility
71       /"Plant" 0, "Utility" 1, "CR"  100, "Office"   150, "MB"   25, "LS"
   20, "SS1"  10, "SS2"  10/
72
73  parA(s,r,saux) sigmoid parameter /"Plant"."VCE"."CR" 1.005524, "Plant"."BL
   EVE"."CR" 1.00031, "Plant"."VCE"."Office" 1.005524, "Plant"."BLEVE"."Offic
   e" 1.00031, "Plant"."VCE"."MB" 1.005524, "Plant"."BLEVE"."MB" 1.00031, "Pl
   ant"."VCE"."LS" 1.014, "Plant"."BLEVE"."LS" 1.0049, "Plant"."VCE"."SS1" 1.
   0025, "Plant"."BLEVE"."SS1" 1.019, "Plant"."VCE"."SS2" 1.0025, "Plant"."BL
   EVE"."SS2" 1.019, "Plant"."VCE"."Utility" 1.0025, "Plant"."BLEVE"."Utility
   " 1.019, "Plant"."VCE"."Plant" 0, "Plant"."BLEVE"."Plant" 0/
74  parB(s,r,saux) sigmoid parameter /"Plant"."VCE"."CR" -64.887, "Plant"."BLE
   VE"."CR" -8.00948, "Plant"."VCE"."Office" -64.887, "Plant"."BLEVE"."Office
   " -8.00948, "Plant"."VCE"."MB" -64.887, "Plant"."BLEVE"."MB" -8.00948, "Pl
   ant"."VCE"."LS" -23.2237, "Plant"."BLEVE"."LS" -2.558, "Plant"."VCE"."SS1"
    -74.53, "Plant"."BLEVE"."SS1" -10.05, "Plant"."VCE"."SS2" -74.53, "Plant"
   ."BLEVE"."SS2" -10.05, "Plant"."VCE"."Utility" -74.53, "Plant"."BLEVE"."Ut
   ility" -10.05, "Plant"."VCE"."Plant" 1.0025, "Plant"."BLEVE"."Plant" 1.000
```

```
   31/
75  parC(s,r,saux) sigmoid parameter /"Plant"."VCE"."CR" 513.22, "Plant"."BLEV
   E"."CR" 64.69438, "Plant"."VCE"."Office" 513.22, "Plant"."BLEVE"."Office"
   64.69438, "Plant"."VCE"."MB" 513.22, "Plant"."BLEVE"."MB" 64.69438, "Plant
   "."VCE"."LS" 208.777, "Plant"."BLEVE"."LS" 33.138, "Plant"."VCE"."SS1" 524
   .124, "Plant"."BLEVE"."SS1" 66.186, "Plant"."VCE"."SS2" 524.124, "Plant"."
   BLEVE"."SS2" 66.186, "Plant"."VCE"."Utility" 524.124, "Plant"."BLEVE"."Uti
   lity" 66.186, "Plant"."VCE"."Plant" 1.0025, "Plant"."BLEVE"."Plant" 1.0003
   1/
76
77  parameters
78  xrfd(s,r) Displacement in x to ubicate the release of f  /"Plant"."VCE"  0
   , "Plant"."BLEVE"  0/
79  yrfd(s,r) Displacement in y to ubicate the release of f  /"Plant"."VCE"  0
   , "Plant"."BLEVE"  0/
80  freq(s,r) "Frequency of the release (times/year)"   /"Plant"."VCE" 0.00000
   51, "Plant"."BLEVE"  0.00000375/
81  Lxs(s)  Length in x of siting facility s            /
82                                          "CR"       10
83                                          "Office"   20
84                                          "MB"        5
85                                          "LS"       10
86                                          "SS1"       4
87                                          "SS2"       4
88                                          "Plant"    30
89                                          "Utility"  15/
90  Lys(s)  Length in y of siting facility s            /
91                                          "CR"       10
92                                          "Office"   15
93                                          "MB"       10
94                                          "LS"       10
95                                          "SS1"       4
96                                          "SS2"       4
97                                          "Plant"    40
98                                          "Utility"  15/
99
100  Border(s)                                  /"CR"       30
101                                          "Office"    8
102                                          "MB"        8
103                                          "LS"       30
104                                          "SS1"      30
105                                          "SS2"      30
106                                          "Plant"    30
107                                          "Utility"  30/;
108  TABLE STss(s,saux)
109                        "CR"    "Office"       "MB"       "LS"       "
   SS1"       "SS2"    "Plant"    "Utility"
110         "CR"             0       5           5         30
   60          60        30        30
111         "Office"         5       0           5         60
   60          60        60        30
112         "MB"             5       5           0         60
   60          60        60        30
```

```
113         "LS"            30       60          60        0
   10         10        15        30
114         "SS1"           60       60          60        10
    0          4         5         30
115         "SS2"           60       60          60        10
    4          0         5         30
116         "Plant"         30       60          60        15
    5          5         0         30
117         "Utility"       30       30          30        30
   30         30        30         0;
118
119
120  scalar Lx   Maximum length of land in x direction (m)          /500/
121  scalar Ly   Maximum length of land in y direction (m)          /500/
122
123  scalar st   Minimum separation distance (m)                    /5/
124
125  scalar Lc   "Price per m2 of land ($/m2)"                     /5/
126  scalar lifeLayout  Life time of layout (years)                /50/
127  *scalar WeightFactor to compensate Risk                        /1/
128  * Calculated Parameters
129  *
130  *parameter maxFIx  Minimum x value to calculate the occupied area;
131  *
132  parameter Dminsx(s,saux) Minimum sitting-sitting facilities x-separation;
133  Dminsx(s,saux)= (Lxs(saux) + Lxs(s))/2.0 + STss(s,saux);
134  parameter Dminsy(s,saux) Minimum sitting-sitting facilities x-separation;
135  Dminsy(s,saux)= (Lys(saux) + Lys(s))/2.0 + STss(s,saux);
136  *
137  ***************************************************************************
   ******
138  ***
139  ***                 VARIABLES
140  ***
141  variables
142  x(s)        Position in x of siting facility
143  y(s)        Position in y of siting facility
144  Dss(s,saux)  "Distance between center-center, siting facilities"
145  PstDam(s,r,saux) Probability of Structural Damage because of VCE due to re
   lease in i affecting s
146
147  *
148  areaX       The extreme side in x direction for the final occupied area
149  areaY       The extreme side in x direction for the final occupied area
150  area       The occupied area
151  costP       Piping cost for siting-siting
152  costL       Land cost
153  costR       Cost for toxic release
154  cost       Total cost
155  *
156
157  xssL(s,saux)   Convex hull variable for siting-siting facilities
158  xssR(s,saux)   Convex hull variable for siting-siting facilities
```

```
159  xssAD(s,saux)  Convex hull
160  yssA(s,saux)   Convex hull variable for siting-siting facilities
161  yssD(s,saux)   Convex hull variable for siting-siting facilities
162  yssLR(s,saux)  Convex hull
163  BssL(s,saux)   Binary for siting-siting facilities
164  BssR(s,saux)   Binary for siting-siting facilities
165  BssAD(s,saux)  Binary for siting-siting facilities
166  BssA(s,saux)   Binary for siting-siting facilities
167  BssD(s,saux)   Binary for siting-siting facilities
168  *
169  DssxL(s,saux)  Convex hull variable for siting-siting facilities
170  DssxR(s,saux)  Convex hull variable for siting-siting facilities
171  DssxAD(s,saux) Convex hull variable for siting-siting facilities
172  DssyLR(s,saux) Convex hull variable for siting-siting facilities
173  DssyA(s,saux)  Convex hull variable for siting-siting facilities
174  DssyD(s,saux)  Convex hull variable for siting-siting facilities
175  BssL(s,saux)   Binary for siting-siting facilities
176  BssR(s,saux)   Binary for siting-siting facilities
177  BssAD(s,saux)  Binary for siting-siting facilities
178  BssA(s,saux)   Binary for siting-siting facilities
179  BssD(s,saux)   Binary for siting-siting facilities
180  *
181  Binary variable  BssL(s,saux), BssR(s,saux), BssAD(s,saux), BssA(s,saux),
182                   BssD(s,saux);
183  *Bris(i,r,s,Nangle);
184  *
185  *     Equations
186  *
187  *
188  *  Separation distances
189  *
190  Equation eqDss(s,saux)  Distances between siting-siting facilities;
191  eqDss(s,saux)$(ord(saux) gt ord(s)).. Dss(s,saux)=e=
192                                  sqrt((x(s) - x(saux))*(x(s) - x(saux)
     )
193                                +  (y(s) - y(saux))*(y(s) - y(saux)));
194  *
195  *  Non overlapping convex hull for siting-installed facilities
196  *
197  *
198  *  Non overlapping convex hull for siting-siting facilities
199  *
200  Equation eqSS1(s,saux)  Non overlapping using convex hull: disaggregation
     of x(s);
201  eqSS1(s,saux)$(ord(saux) gt ord(s)).. x(s) =e= xssL(s,saux) + xssR(s,saux)
      + xssAD(s,saux);
202  Equation eqSS1A(s,saux)  Non overlapping using convex hull: disaggregation
      of x(s);
203  eqSS1A(s,saux)$(ord(saux) gt ord(s)).. x(saux) =e= xssL(saux,s) + xssR(sau
     x,s) + xssAD(saux,s);
204  Equation eqSS2(s,saux)  Non overlapping using convex hull: disaggregation
     of y(s);
205  eqSS2(s,saux)$(ord(saux) gt ord(s)).. y(s) =e= yssA(s,saux) + yssD(s,saux)
```

```
     + yssLR(s,saux);
206  Equation eqSS2A(s,saux)  Non overlapping using convex hull: disaggregation
     of y(s);
207  eqSS2A(s,saux)$(ord(saux) gt ord(s)).. y(saux) =e= yssA(saux,s) + yssD(sau
     x,s) + yssLR(saux,s);
208  Equation eqSS3(s,saux)  Non overlaping left dijunction;
209  eqSS3(s,saux)$(ord(saux) gt ord(s)).. xssL(s,saux)=l= xssL(saux,s) - Dmins
     x(s,saux)*BssL(s,saux);
210  Equation eqSS4(s,saux)  Non overlaping right dijunction;
211  eqSS4(s,saux)$(ord(saux) gt ord(s)).. xssR(s,saux) =g= xssR(saux,s) + Dmin
     sx(s,saux)*BssR(s,saux);
212  Equation eqSS5(s,saux)  Non overlaping right dijunction ;
213  eqSS5(s,saux)$(ord(saux) gt ord(s)).. xssAD(s,saux) =g= xssAD(saux,s) - Dm
     insx(s,saux)*BssAD(s,saux);
214  Equation eqSS6(s,saux)  Non overlaping right dijunction ;
215  eqSS6(s,saux)$(ord(saux) gt ord(s)).. xssAD(s,saux) =l= xssAD(saux,s) + Dm
     insx(s,saux)*BssAD(s,saux);
216  Equation eqSS7(s,saux)  Non overlaping right dijunction ;
217  eqSS7(s,saux)$(ord(saux) gt ord(s)).. yssA(s,saux) =g= yssA(saux,s) + Dmin
     sy(s,saux)*BssA(s,saux);
218  Equation eqSS8(s,saux)  Non overlaping right dijunction ;
219  eqSS8(s,saux)$(ord(saux) gt ord(s)).. yssD(s,saux) =l= yssD(saux,s) - Dmin
     sy(s,saux)*BssD(s,saux);
220  Equation eqSS9(s,saux)  Non overlaping right dijunction ;
221  eqSS9(s,saux)$(ord(saux) gt ord(s)).. BssL(s,saux) + BssR(s,saux) + BssAD(
     s,saux) =e= 1;
222  Equation eqSS10(s,saux)  Non overlaping right dijunction ;
223  eqSS10(s,saux)$(ord(saux) gt ord(s)).. BssA(s,saux) + BssD(s,saux) =e= Bss
     AD(s,saux);
224  Equation eqSS11(s,saux)  Non overlaping right dijunction ;
225  eqSS11(s,saux)$(not sameas(saux,s)).. xssL(s,saux) =g= 0.0;
226  Equation eqSS12(s,saux)  Non overlaping right dijunction ;
227  eqSS12(s,saux)$(not sameas(saux,s)).. xssR(s,saux) =g= 0.0;
228  Equation eqSS13(s,saux)  Non overlaping right dijunction ;
229  eqSS13(s,saux)$(not sameas(saux,s)).. xssAD(s,saux) =g= 0.0;
230  Equation eqSS14(s,saux)  Non overlaping right dijunction ;
231  eqSS14(s,saux)$(not sameas(saux,s)).. yssA(s,saux) =g= 0.0;
232  Equation eqSS15(s,saux)  Non overlaping right dijunction ;
233  eqSS15(s,saux)$(not sameas(saux,s)).. yssD(s,saux) =g= 0.0;
234  Equation eqSS16(s,saux)  Non overlaping right dijunction ;
235  eqSS16(s,saux)$(not sameas(saux,s)).. yssLR(s,saux) =g= 0.0;
236  Equation eqSS17(s,saux)  Non overlaping right dijunction ;
237  eqSS17(s,saux)$(ord(saux) gt ord(s)).. xssL(s,saux) =l= (Lx - STss(s,saux)
     - Lxs(s)/2)*BssL(s,saux);
238  Equation eqSS17A(s,saux)  Non overlaping right dijunction ;
239  eqSS17A(s,saux)$(ord(saux) gt ord(s)).. xssL(saux,s) =l= (Lx - STss(s,saux
     ) - Lxs(saux)/2)*BssL(s,saux);
240  Equation eqSS18(s,saux)  Non overlaping right dijunction ;
241  eqSS18(s,saux)$(ord(saux) gt ord(s)).. xssR(s,saux) =l= (Lx - STss(s,saux)
     - Lxs(s)/2)*BssR(s,saux);
242  Equation eqSS18A(s,saux)  Non overlaping right dijunction ;
243  eqSS18A(s,saux)$(ord(saux) gt ord(s)).. xssR(saux,s) =l= (Lx - STss(s,saux
     ) - Lxs(saux)/2)*BssR(s,saux);
```

```
244  Equation eqSS19(s,saux)  Non overlaping right dijunction ;
245  eqSS19(s,saux)$(ord(saux) gt ord(s)).. xssAD(s,saux) =l= (Lx - STss(s,saux
     ) - Lxs(s)/2)*BssAD(s,saux);
246  Equation eqSS19A(s,saux)  Non overlaping right dijunction ;
247  eqSS19A(s,saux)$(ord(saux) gt ord(s)).. xssAD(saux,s) =l= (Lx - STss(s,sau
     x) - Lxs(saux)/2)*BssAD(s,saux);
248  Equation eqSS20(s,saux)  Non overlaping right dijunction ;
249  eqSS20(s,saux)$(ord(saux) gt ord(s)).. yssA(s,saux) =l= (Ly - STss(s,saux)
      - Lys(s)/2)*BssA(s,saux);
250  Equation eqSS20A(s,saux)  Non overlaping right dijunction ;
251  eqSS20A(s,saux)$(ord(saux) gt ord(s)).. yssA(saux,s) =l= (Ly - STss(s,saux
     ) - Lys(saux)/2)*BssA(s,saux);
252  Equation eqSS21(s,saux)  Non overlaping right dijunction ;
253  eqSS21(s,saux)$(ord(saux) gt ord(s)).. yssD(s,saux) =l= (Ly - STss(s,saux)
      - Lys(s)/2)*BssD(s,saux);
254  Equation eqSS21A(s,saux)  Non overlaping right dijunction ;
255  eqSS21A(s,saux)$(ord(saux) gt ord(s)).. yssD(saux,s) =l= (Ly - STss(s,saux
     ) - Lys(saux)/2)*BssD(s,saux);
256  Equation eqSS22(s,saux)  Non overlaping right dijunction ;
257  eqSS22(s,saux)$(ord(saux) gt ord(s)).. yssLR(s,saux) =l= (Ly - STss(s,saux
     ) - Lys(s)/2)*(1 - BssAD(s,saux));
258  Equation eqSS22A(s,saux)  Non overlaping right dijunction ;
259  eqSS22A(s,saux)$(ord(saux) gt ord(s)).. yssLR(saux,s) =l= (Ly - STss(s,sau
     x) - Lys(saux)/2)*(1 - BssAD(s,saux));
260
261  *
262  *
263  * Ocupied area:
264  *
265  Equation calcX(s) Calculate the maximum x component;
266  calcX(s).. areaX =g= x(s) + Lxs(s)/2;
267  Equation calcY(s) Calculate the maximum y component;
268  calcY(s).. areaY =g= y(s) + Lys(s)/2;
269  Equation AreaCalculation;
270  AreaCalculation.. area=e= areaX*areaY;
271  *
272  * Constraints on positions
273  *
274  Equation eqOnL1(s)  All siting facilities must layout inside the land;
275  eqOnL1(s)..  x(s) =g= Lxs(s);
276  Equation eqOnL2(s)  All siting facilities must layout inside the land;
277  eqOnL2(s)..  x(s) =l= Lx - Lxs(s);
278  Equation eqOnL3(s)  All siting facilities must layout inside the land;
279  eqOnL3(s)..  y(s) =g= Lys(s);
280  Equation eqOnL4(s)  All siting facilities must layout inside the land;
281  eqOnL4(s)..  y(s) =l= Ly - Lys(s);
282  *
283  * Defining the objective function
284  *
285  Equation eqTR1(s,r,saux) Calculate probability of structural damage at thi
     s distance;
286  eqTR1(s,r,saux)$rs(s,r)..  PstDam(s,r,saux) =e= parA(s,r,saux)/(1+exp(-(Ds
     s(s,saux)-parC(s,r,saux))/parB(s,r,saux)));
```

```
287  Equation eqLC  Building land cost: surface area occupied by units and pipe
     rack (eq 2);
288  eqLC.. costL =e= Lc*area;
289  Equation eqPC Piping cost for siting-siting facilities;
290  eqPC.. costP=e= 0.5*(sum(MSS(s,saux)$(ord(saux) gt ord(s)),Dss(s,saux)*Int
     erconnectivity(s,saux)));
291  Equation eqRC Calculate cost of death at this distance;
292  eqRC..  costR =e= sum((s,r,saux)$rs(s,r),freq(s,r)*PstDam(s,r,saux)*Weight
     Factor(saux)*lifeLayout*Building(saux));
293  Equation totalCost Includes all costs;
294  totalCost.. cost =e= costP + costL + costR;
295  *
296
297
298
299
300  ************************************************************************
     ******
301  ************************************************************************
     ******
302  * Bounds
303  *
304  x.lo(s)= Lxs(s)/2+Border(s);
305  x.up(s)= Lx - (Lxs(s)/2+Border(s));
306  y.lo(s)= Lys(s)/2+Border(s);
307  y.up(s)= Ly - (Lys(s)/2+Border(s));
308  costP.lo= 0;
309  costP.up= inf;
310  areaX.lo= 0.0;
311  areaX.up= Lx-st;
312  areaY.lo= 0.0;
313  areaY.up= Ly-st;
314  area.lo= 0.0;
315  area.up= Lx*Ly;
316  Dss.lo(s,saux)= 0.0;
317  Dss.up(s,saux)= sqrt(Lx*Lx + Ly*Ly);
318  * Auxiliary variables
319  xssL.lo(s,saux)= 0.0;
320  xssL.up(s,saux)= Lx;
321  xssR.lo(s,saux)= 0.0;
322  xssR.up(s,saux)= Lx;
323  xssAD.lo(s,saux)= 0.0;
324  xssAD.up(s,saux)= Lx;
325  yssA.lo(s,saux)= 0.0;
326  yssA.up(s,saux)= Ly;
327  yssD.lo(s,saux)= 0.0;
328  yssD.up(s,saux)= Ly;
329  yssLR.lo(s,saux)= 0.0;
330  yssLR.up(s,saux)= Ly;
331  *
332  *  Initial values
333  *
334  Dss.l(s,saux)= STss(s,saux);
```

```
335  x.l(s)= 10;
336  y.l(s)= 10;
337  *
338  *   Solver definition
339  *
340  option limcol = 0;
341  *  Check the solution against the targets:
342  parameter report(*,*,*) Solution Summary;
343
344  Model FirstModel /all/
345  *$ontext
346  *display'The total cost = ', costP;
347  *option nlp=minos;
348  *option nlp= knitro;
349  *option minlp= dicopt option nlp=minos option mip= cplex;
350  *option minlp= dicopt option nlp=conopt option mip= cplex;
351  *option minlp= oqnlp;
352  *option minlp= baron option nlp=minos option mip= cplex;
353  *option minlp= baron option nlp=conopt option mip= cplex;
354  option minlp= dicopt;
355  FirstModel.domlim= 60;
356  * default value is optcr= 0.1
357  FirstModel.optca=0;
358  FirstModel.optcr=0.1;
359  *FirstModel.optcr=0.0;
360  FirstModel.optfile= 1;
361  FirstModel.scaleopt= 1;
362  option iterlim= 50000000;
363  *Option Dualcheck= 1;
364  *OPTION SYSOUT=ON
365  *
366  *  Solve First Relaxed Model
367  *
     option rminlp= conopt;
     solve FirstModel using rminlp minimizing cost;
     if(FirstModel.modelstat > 2.5,
       option rminlp= minos;
       solve FirstModel using rminlp minimizing cost;
     )
     if ( FirstModel.modelstat > 2.5,
       option rminlp= snopt;
       solve FirstModel using rminlp minimizing cost;
     )
     abort$(FirstModel.modelstat > 2.5) "Relaxed model could not be solved!"
381  *
382  *  Then the minlp
383  *
384  *option minlp= baron option nlp=minos option mip= cplex;
385  *option minlp= baron option nlp=conopt option mip= cplex;
386  *option minlp= dicopt option nlp=minos option mip= cplex;
387  *option minlp= dicopt option nlp=baron option mip= cplex;
388
389
```

```
397
398  *option minlp= dicopt option nlp=conopt option mip= cplex;
399  *Solve FirstModel using minlp minimizing costP;
400  *$offtext
401
402  *option nlp=baron;
403  *option minlp= dicopt;
404  Solve FirstModel using minlp minimizing cost;
```

APPENDIX C

AMPL CODE FOR CHAPTER V

Data file is provided at the end of this appendix separately.

```
*********************************************************************************
set SCORE;
set LOCATION;
set FACILITY;

param RD     {i in LOCATION} >=  0;    # RD = Rectilinear Distance from the center;
param Land   {i in LOCATION} >=  0;
param Risk   {i in LOCATION} >=  0;
param x      {i in LOCATION} >= -50 <= 50;
param y      {i in LOCATION} >= -50 <= 50;
param M                      =  100;

param UnitPiping   {f in FACILITY} >= 0;
param BuildingCost {f in FACILITY} >= 0;
param unitland     {f in FACILITY} >= 0;

var xf      {f in FACILITY} >= -50, <= 50;
var yf      {f in FACILITY} >= -50, <= 50;
var y_14_sep1, binary;
var y_14_sep2, binary;
var y_14_sep3, binary;
var y_14_sep4, binary;
var y_15_sep1, binary;
var y_15_sep2, binary;
var y_15_sep3, binary;
var y_15_sep4, binary;
var y_16_sep1, binary;
var y_16_sep2, binary;
var y_16_sep3, binary;
var y_16_sep4, binary;
var y_17_sep1, binary;
var y_17_sep2, binary;
var y_17_sep3, binary;
var y_17_sep4, binary;

var y_24_sep1, binary;
var y_24_sep2, binary;
var y_24_sep3, binary;
var y_24_sep4, binary;
var y_25_sep1, binary;
var y_25_sep2, binary;
var y_25_sep3, binary;
var y_25_sep4, binary;
```

```
var y_26_sep1, binary;
var y_26_sep2, binary;
var y_26_sep3, binary;
var y_26_sep4, binary;
var y_27_sep1, binary;
var y_27_sep2, binary;
var y_27_sep3, binary;
var y_27_sep4, binary;

var y_34_sep1, binary;
var y_34_sep2, binary;
var y_34_sep3, binary;
var y_34_sep4, binary;
var y_35_sep1, binary;
var y_35_sep2, binary;
var y_35_sep3, binary;
var y_35_sep4, binary;
var y_36_sep1, binary;
var y_36_sep2, binary;
var y_36_sep3, binary;
var y_36_sep4, binary;
var y_37_sep1, binary;
var y_37_sep2, binary;
var y_37_sep3, binary;
var y_37_sep4, binary;

#var dijx;
#var dijy;

var b{LOCATION, FACILITY} binary;

minimize Total_cost: sum {l in LOCATION,f in FACILITY} (UnitPiping[f] * RD[l] + BuildingCost[f] *
Risk[l])*b[l,f];



s.t.

        EachFacilityPlaced{f in FACILITY}:
          sum{l in LOCATION} b[l,f] = 1;

        PreventCollision{l in LOCATION}:
          sum{f in FACILITY} b[l,f] <= 1;

subject to SeparationDistanceBigM1{f in FACILITY, i in LOCATION}:
-100*(1-b[i,f]) <= (xf[f]-x[i]);
subject to SeparationDistanceBigM2{f in FACILITY, i in LOCATION}:
(xf[f]-x[i]) <= 100*(1-b[i,f]);
subject to SeparationDistanceBigM3{f in FACILITY, i in LOCATION}:
-100*(1-b[i,f]) <= (yf[f]-y[i]);
subject to SeparationDistanceBigM4{f in FACILITY, i in LOCATION}:
(yf[f]-y[i]) <= 100*(1-b[i,f]);
```

```
subject to SepControlLargeStorage1:
        (xf[1] - xf[4]) + (yf[1] - yf[4]) >= 100*y_14_sep1 - 100*(1-y_14_sep1);

subject to SepControlLargeStorage2:
        -(xf[1] - xf[4]) + (yf[1] - yf[4]) >= 100*y_14_sep2 - 100*(1-y_14_sep2);

subject to SepControlLargeStorage3:
        (xf[1] - xf[4]) - (yf[1] - yf[4]) >= 100*y_14_sep3 - 100*(1-y_14_sep3);

subject to SepControlLargeStorage4:
        -(xf[1] - xf[4]) - (yf[1] - yf[4]) >= 100*y_14_sep4 - 100*(1-y_14_sep4);

subject to SepControlLargeStorage5:
        y_14_sep1 + y_14_sep2 + y_14_sep3 + y_14_sep4 = 1;



subject to SepControlSmall1Storage1:
        (xf[1] - xf[5]) + (yf[1] - yf[5]) >= 43*y_15_sep1 - 100*(1-y_15_sep1);

subject to SepControlSmall1Storage2:
        -(xf[1] - xf[5]) + (yf[1] - yf[5]) >= 43*y_15_sep2 - 100*(1-y_15_sep2);

subject to SepControlSmall1Storage3:
        (xf[1] - xf[5]) - (yf[1] - yf[5]) >= 43*y_15_sep3 - 100*(1-y_15_sep3);

subject to SepControlSmall1Storage4:
        -(xf[1] - xf[5]) - (yf[1] - yf[5]) >= 43*y_15_sep4 - 100*(1-y_15_sep4);

subject to SepControlSmall1Storage5:
        y_15_sep1 + y_15_sep2 + y_15_sep3 + y_15_sep4 = 1;



subject to SepControlSmall2Storage1:
        (xf[1] - xf[6]) + (yf[1] - yf[6]) >= 43*y_16_sep1 - 100*(1-y_16_sep1);

subject to SepControlSmall2Storage2:
        -(xf[1] - xf[6]) + (yf[1] - yf[6]) >= 43*y_16_sep2 - 100*(1-y_16_sep2);

subject to SepControlSmall2Storage3:
        (xf[1] - xf[6]) - (yf[1] - yf[6]) >= 43*y_16_sep3 - 100*(1-y_16_sep3);

subject to SepControlSmall2Storage4:
        -(xf[1] - xf[6]) - (yf[1] - yf[6]) >= 43*y_16_sep4 - 100*(1-y_16_sep4);

subject to SepControlSmall2Storage5:
        y_16_sep1 + y_16_sep2 + y_16_sep3 + y_16_sep4 = 1;



subject to SepControlUtility1:
```

```
        (xf[1] - xf[7]) + (yf[1] - yf[7]) >= 43*y_17_sep1 - 100*(1-y_17_sep1);

subject to SepControlUtility2:
        -(xf[1] - xf[7]) + (yf[1] - yf[7]) >= 43*y_17_sep2 - 100*(1-y_17_sep2);

subject to SepControlUtility3:
        (xf[1] - xf[7]) - (yf[1] - yf[7]) >= 43*y_17_sep3 - 100*(1-y_17_sep3);

subject to SepControlUtility4:
        -(xf[1] - xf[7]) - (yf[1] - yf[7]) >= 43*y_17_sep4 - 100*(1-y_17_sep4);

subject to SepControlUtility5:
        y_17_sep1 + y_17_sep2 + y_17_sep3 + y_17_sep4 = 1;


subject to SepOfficeLargeStorage1:
        (xf[2] - xf[4]) + (yf[2] - yf[4]) >= 100*y_24_sep1 - 100*(1-y_24_sep1);

subject to SepOfficeLargeStorage2:
        -(xf[2] - xf[4]) + (yf[2] - yf[4]) >= 100*y_24_sep2 - 100*(1-y_24_sep2);

subject to SepOfficeLargeStorage3:
        (xf[2] - xf[4]) - (yf[2] - yf[4]) >= 100*y_24_sep3 - 100*(1-y_24_sep3);

subject to SepOfficeLargeStorage4:
        -(xf[2] - xf[4]) - (yf[2] - yf[4]) >= 100*y_24_sep4 - 100*(1-y_24_sep4);

subject to SepOfficeLargeStorage5:
        y_24_sep1 + y_24_sep2 + y_24_sep3 + y_24_sep4 = 1;
subject to SepOfficeSmall1Storage1:
        (xf[2] - xf[5]) + (yf[2] - yf[5]) >= 22*y_25_sep1 - 100*(1-y_25_sep1);

subject to SepOfficeSmall1Storage2:
        -(xf[2] - xf[5]) + (yf[2] - yf[5]) >= 22*y_25_sep2 - 100*(1-y_25_sep2);

subject to SepOfficeSmall1Storage3:
        (xf[2] - xf[5]) - (yf[2] - yf[5]) >= 22*y_25_sep3 - 100*(1-y_25_sep3);

subject to SepOfficeSmall1Storage4:
        -(xf[2] - xf[5]) - (yf[2] - yf[5]) >= 22*y_25_sep4 - 100*(1-y_25_sep4);

subject to SepOfficeSmall1Storage5:
        y_25_sep1 + y_25_sep2 + y_25_sep3 + y_25_sep4 = 1;



subject to SepOfficeSmall2Storage1:
        (xf[2] - xf[6]) + (yf[2] - yf[6]) >= 22*y_26_sep1 - 100*(1-y_26_sep1);

subject to SepOfficeSmall2Storage2:
        -(xf[2] - xf[6]) + (yf[2] - yf[6]) >= 22*y_26_sep2 - 100*(1-y_26_sep2);

subject to SepOfficeSmall2Storage3:
```

```
        (xf[2] - xf[6]) - (yf[2] - yf[6]) >= 22*y_26_sep3 - 100*(1-y_26_sep3);

subject to SepOfficeSmall2Storage4:
        -(xf[2] - xf[6]) - (yf[2] - yf[6]) >= 22*y_26_sep4 - 100*(1-y_26_sep4);

subject to SepOfficeSmall2Storage5:
        y_26_sep1 + y_26_sep2 + y_26_sep3 + y_26_sep4 = 1;



subject to SepOfficeUtility1:
        (xf[2] - xf[7]) + (yf[2] - yf[7]) >= 43*y_27_sep1 - 100*(1-y_27_sep1);

subject to SepOfficeUtility2:
        -(xf[2] - xf[7]) + (yf[2] - yf[7]) >= 43*y_27_sep2 - 100*(1-y_27_sep2);

subject to SepOfficeUtility3:
        (xf[2] - xf[7]) - (yf[2] - yf[7]) >= 43*y_27_sep3 - 100*(1-y_27_sep3);

subject to SepOfficeUtility4:
        -(xf[2] - xf[7]) - (yf[2] - yf[7]) >= 43*y_27_sep4 - 100*(1-y_27_sep4);

subject to SepOfficeUtility5:
        y_27_sep1 + y_27_sep2 + y_27_sep3 + y_27_sep4 = 1;


#subject to SepMaintenanceBuildingtoLargeStorage1:
#       (xf[3] - xf[4]) + (yf[3] - yf[4]) >= 100*y_34_sep1 - 100*(1-y_34_sep1);

#subject to SepMaintenanceBuildingtoLargeStorage2:
#       -(xf[3] - xf[4]) + (yf[3] - yf[4]) >= 100*y_34_sep2 - 100*(1-y_34_sep2);

#subject to SepMaintenanceBuildingtoLargeStorage3:
#       (xf[3] - xf[4]) - (yf[3] - yf[4]) >= 100*y_34_sep3 - 100*(1-y_34_sep3);

#subject to SepMaintenanceBuildingtoLargeStorage4:
#       -(xf[3] - xf[4]) - (yf[3] - yf[4]) >= 100*y_34_sep4 - 100*(1-y_34_sep4);

#subject to SepMaintenanceBuildingtoLargeStorage5:
#       y_34_sep1 + y_34_sep2 + y_34_sep3 + y_34_sep4 = 1;

#subject to SepMaintenanceBuildingtoSmall1Storage1:
#       (xf[3] - xf[5]) + (yf[3] - yf[5]) >= 22*y_35_sep1 - 100*(1-y_35_sep1);

#subject to SepMaintenanceBuildingtoSmall1Storage2:
#       -(xf[3] - xf[5]) + (yf[3] - yf[5]) >= 22*y_35_sep2 - 100*(1-y_35_sep2);

#subject to SepMaintenanceBuildingtoSmall1Storage3:
#       (xf[3] - xf[5]) - (yf[3] - yf[5]) >= 22*y_35_sep3 - 100*(1-y_35_sep3);

#subject to SepMaintenanceBuildingtoSmall1Storage4:
#       -(xf[3] - xf[5]) - (yf[3] - yf[5]) >= 22*y_35_sep4 - 100*(1-y_35_sep4);
```

```
#subject to SepMaintenanceBuildingtoSmall1Storage5:
#	y_35_sep1 + y_35_sep2 + y_35_sep3 + y_35_sep4 = 1;

#subject to SepMaintenanceBuildingtoSmall2Storage1:
#	(xf[3] - xf[6]) + (yf[3] - yf[6]) >= 22*y_36_sep1 - 100*(1-y_36_sep1);

#subject to SepMaintenanceBuildingtoSmall2Storage2:
#	-(xf[3] - xf[6]) + (yf[3] - yf[6]) >= 22*y_36_sep2 - 100*(1-y_36_sep2);

#subject to SepMaintenanceBuildingtoSmall2Storage3:
#	(xf[3] - xf[6]) - (yf[3] - yf[6]) >= 22*y_36_sep3 - 100*(1-y_36_sep3);

#subject to SepMaintenanceBuildingtoSmall2Storage4:
#	-(xf[3] - xf[6]) - (yf[3] - yf[6]) >= 22*y_36_sep4 - 100*(1-y_36_sep4);

#subject to SepMaintenanceBuildingtoSmall2Storage5:
#	y_36_sep1 + y_36_sep2 + y_36_sep3 + y_36_sep4 = 1;

#subject to SepMaintenanceBuildingtoUtility1:
#	(xf[3] - xf[7]) + (yf[3] - yf[7]) >= 43*y_37_sep1 - 100*(1-y_37_sep1);

#subject to SepMaintenanceBuildingtoUtility2:
#	-(xf[3] - xf[7]) + (yf[3] - yf[7]) >= 43*y_37_sep2 - 100*(1-y_37_sep2);

#subject to SepMaintenanceBuildingtoUtility3:
#	(xf[3] - xf[7]) - (yf[3] - yf[7]) >= 43*y_37_sep3 - 100*(1-y_37_sep3);

#subject to SepMaintenanceBuildingtoUtility4:
#	-(xf[3] - xf[7]) - (yf[3] - yf[7]) >= 43*y_37_sep4 - 100*(1-y_37_sep4);

#subject to SepMaintenanceBuildingtoUtility5:
#	y_37_sep1 + y_37_sep2 + y_37_sep3 + y_37_sep4 = 1;



subject to DistanceStorage1:
sum {j in LOCATION} ((x[j]*b[j,4]-x[j]*b[j,5])+(y[j]*b[j,4]-y[j]*b[j,5])) <= 30;

subject to DistanceStorage2:
sum {j in LOCATION} ((x[j]*b[j,4]-x[j]*b[j,5])-(y[j]*b[j,4]-y[j]*b[j,5])) <= 30;

subject to DistanceStorage3:
sum {j in LOCATION} -((x[j]*b[j,4]-x[j]*b[j,5])+(y[j]*b[j,4]-y[j]*b[j,5])) <= 30;

subject to DistanceStorage4:
sum {j in LOCATION} -((x[j]*b[j,4]-x[j]*b[j,5])-(y[j]*b[j,4]-y[j]*b[j,5])) <= 30;

subject to DistanceStorage5:
sum {j in LOCATION} ((x[j]*b[j,4]-x[j]*b[j,6])+(y[j]*b[j,4]-y[j]*b[j,6])) <= 30;

subject to DistanceStorage6:
sum {j in LOCATION} ((x[j]*b[j,4]-x[j]*b[j,6])-(y[j]*b[j,4]-y[j]*b[j,6])) <= 30;
```

```
subject to DistanceStorage7:
sum {j in LOCATION} -((x[j]*b[j,4]-x[j]*b[j,6])+(y[j]*b[j,4]-y[j]*b[j,6])) <= 30;

subject to DistanceStorage8:
sum {j in LOCATION} -((x[j]*b[j,4]-x[j]*b[j,6])-(y[j]*b[j,4]-y[j]*b[j,6])) <= 30;

subject to DistanceStorage9:
sum {j in LOCATION} ((x[j]*b[j,5]-x[j]*b[j,6])+(y[j]*b[j,5]-y[j]*b[j,6])) <= 30;

subject to DistanceStorage10:
sum {j in LOCATION} ((x[j]*b[j,5]-x[j]*b[j,6])-(y[j]*b[j,5]-y[j]*b[j,6])) <= 30;

subject to DistanceStorage11:
sum {j in LOCATION} -((x[j]*b[j,5]-x[j]*b[j,6])+(y[j]*b[j,5]-y[j]*b[j,6])) <= 30;

subject to DistanceStorage12:
sum {j in LOCATION} -((x[j]*b[j,5]-x[j]*b[j,6])-(y[j]*b[j,5]-y[j]*b[j,6])) <= 30;



subject to OccupiedBuildings13:
sum {j in LOCATION} ((x[j]*b[j,1]-x[j]*b[j,2])+(y[j]*b[j,1]-y[j]*b[j,2])) <= 30;

subject to OccupiedBuildings14:
sum {j in LOCATION} ((x[j]*b[j,1]-x[j]*b[j,2])-(y[j]*b[j,1]-y[j]*b[j,2])) <= 30;

subject to OccupiedBuildings15:
sum {j in LOCATION} -((x[j]*b[j,1]-x[j]*b[j,2])+(y[j]*b[j,1]-y[j]*b[j,2])) <= 30;

subject to OccupiedBuildings16:
sum {j in LOCATION} -((x[j]*b[j,1]-x[j]*b[j,2])-(y[j]*b[j,1]-y[j]*b[j,2])) <= 30;



subject to OccupiedBuildings17:
sum {j in LOCATION} ((x[j]*b[j,1]-x[j]*b[j,3])+(y[j]*b[j,1]-y[j]*b[j,3])) <= 30;

subject to OccupiedBuildings18:
sum {j in LOCATION} ((x[j]*b[j,1]-x[j]*b[j,3])-(y[j]*b[j,1]-y[j]*b[j,3])) <= 30;

subject to DOccupiedBuildings19:
sum {j in LOCATION} -((x[j]*b[j,1]-x[j]*b[j,3])+(y[j]*b[j,1]-y[j]*b[j,3])) <= 30;

subject to OccupiedBuildings20:
sum {j in LOCATION} -((x[j]*b[j,1]-x[j]*b[j,3])-(y[j]*b[j,1]-y[j]*b[j,3])) <= 30;



subject to OccupiedBuildings21:
sum {j in LOCATION} ((x[j]*b[j,2]-x[j]*b[j,3])+(y[j]*b[j,2]-y[j]*b[j,3])) <= 30;
```

```
subject to OccupiedBuildings22:
sum {j in LOCATION} ((x[j]*b[j,2]-x[j]*b[j,3])-(y[j]*b[j,2]-y[j]*b[j,3])) <= 30;

subject to OccupiedBuildings23:
sum {j in LOCATION} -((x[j]*b[j,2]-x[j]*b[j,3])+(y[j]*b[j,2]-y[j]*b[j,3])) <= 30;

subject to OccupiedBuildingse24:
sum {j in LOCATION} -((x[j]*b[j,2]-x[j]*b[j,3])-(y[j]*b[j,2]-y[j]*b[j,3])) <= 30;




data 7facilities-WF100.dat;
option solver cplexamp;
option cplex_options "mipdisplay 2";
solve;
display Total_cost;
display {l in LOCATION,f in FACILITY} b[l,f];
display xf[1], yf[1];
display xf[2], yf[2];
display xf[3], yf[3];
display xf[4], yf[4];
display xf[5], yf[5];
display xf[6], yf[6];



display y_14_sep1;
display y_14_sep2;
display y_14_sep3;
display y_14_sep4;

*********************************************************************************
DATA file for the case study in Chapter V
*********************************************************************************

set SCORE := RD Land Risk x y;

set FACILITY := 1 2 3 4 5 6 7;
# 1 (Main Control Room), 2 (Office), 3 (Auxiliary building), 4 (Large Storage), 5 (Small Storage),
6(Small Storage), 7 (Utility);


set LOCATION :=
G01 G02 G03 G04 G05 G06 G07 G08 G09 G10
G11 G12 G13 G14 G15 G16 G17 G18 G19 G20
G21 G22 G23 G24 G25 G26 G27 G28 G29 G30
G31 G32 G33 G34 G35 G36 G37 G38 G39 G40
G41 G42 G43 G44 G45 G46 G47 G48 G49 G50
G51 G52 G53 G54 G55 G56 G57 G58 G59 G60
G61 G62 G63 G64 G65 G66 G67 G68 G69 G70
G71 G72 G73 G74 G75 G76 G77 G78 G79 G80
```

G81 G82 G83 G84 G85 G86 G87 G88 G89 G90
G91 G92 G93 G94 G95 G96 G97 G98 G99 G100;

param: UnitPiping BuildingCost:=
1 10 1000000
2 0.1 300000
3 2 200000
4 100 150000
5 100 100000
6 100 100000
7 50 500000;

param: x y RD Risk :=

G01 -45 45 90 0.025541038
G02 -35 45 80 0.026641582
G03 -25 45 70 0.027950535
G04 -15 45 60 0.02961946
G05 -5 45 50 0.029017812
G06 5 45 50 0.027867812
G07 15 45 60 0.02559446
G08 25 45 70 0.022775535
G09 35 45 80 0.020201582
G10 45 45 90 0.017836038
G11 -45 35 80 0.026411582
G12 -35 35 70 0.029107068
G13 -25 35 60 0.032410627
G14 -15 35 50 0.038041706
G15 -5 35 40 0.040842999
G16 5 35 40 0.039807999
G17 15 35 50 0.033096706
G18 25 35 60 0.025970627
G19 35 35 70 0.021172068
G20 45 35 80 0.017786582
G21 -45 25 70 0.027490535
G22 -35 25 60 0.032295627
G23 -25 25 50 0.043257999
G24 -15 25 40 0.055410798
G25 -5 25 30 0.058923645
G26 5 25 30 0.057888645
G27 15 25 40 0.049775798
G28 25 25 50 0.035092999
G29 35 25 60 0.023440627
G30 45 25 70 0.018060535
G31 -45 15 60 0.02892946
G32 -35 15 50 0.037811706
G33 -25 15 40 0.055525798
G34 -15 15 30 0.064612296
G35 -5 15 20 0.064263901

G36	5	15	20	0.063343901
G37	15	15	30	0.057137296
G38	25	15	40	0.045865798
G39	35	15	50	0.027921706
G40	45	15	60	0.01869446
G41	-45	5	50	0.029017812
G42	-35	5	40	0.041417999
G43	-25	5	30	0.060073645
G44	-15	5	20	0.065528901
G45	-5	5	10	100
G46	5	5	10	100
G47	15	5	20	0.057018901
G48	25	5	30	0.050183645
G49	35	5	40	0.031527999
G50	45	5	50	0.019242812
G51	-45	-5	50	0.028557812
G52	-35	-5	40	0.040957999
G53	-25	-5	30	0.059498645
G54	-15	-5	20	0.065068901
G55	-5	-5	10	100
G56	5	-5	10	100
G57	15	-5	20	0.056673901
G58	25	-5	30	0.049838645
G59	35	-5	40	0.031182999
G60	45	-5	50	0.019012812
G61	-45	-15	60	0.02708946
G62	-35	-15	50	0.035626706
G63	-25	-15	40	0.052880798
G64	-15	-15	30	0.061162296
G65	-5	-15	20	0.060468901
G66	5	-15	20	0.059778901
G67	15	-15	30	0.054952296
G68	25	-15	40	0.044830798
G69	35	-15	50	0.027231706
G70	45	-15	60	0.01846446
G71	-45	-25	70	0.025075535
G72	-35	-25	60	0.029650627
G73	-25	-25	50	0.039692999
G74	-15	-25	40	0.051385798
G75	-5	-25	30	0.055243645
G76	5	-25	30	0.054438645
G77	15	-25	40	0.047130798
G78	25	-25	50	0.033482999
G79	35	-25	60	0.022980627
G80	45	-25	70	0.017600535
G81	-45	-35	80	0.023421582
G82	-35	-35	70	0.025772068
G83	-25	-35	60	0.028730627
G84	-15	-35	50	0.034131706
G85	-5	-35	40	0.037392999
G86	5	-35	40	0.036587999
G87	15	-35	50	0.030681706
G88	25	-35	60	0.024705627

G89	35	-35	70	0.021057068
G90	45	-35	80	0.017096582
G91	-45	-45	90	0.022091038
G92	-35	-45	80	0.023076582
G93	-25	-45	70	0.024270535
G94	-15	-45	60	0.02570946
G95	-5	-45	50	0.025567812
G96	5	-45	50	0.024762812
G97	15	-45	60	0.02283446
G98	25	-45	70	0.020475535
G99	35	-45	80	0.018591582
G100	45	-45	90	0.016916038;

****

VITA

Name: Seungho Jung

Address: Artie McFerrin Department of Chemical Engineering
Texas A&M University
Jack E. Brown Engineering Building
3122 TAMU Room 200
College Station, TX 77843-3122
c/o M. Sam Mannan

Email Address: yoman23@gmail.com

Education: B.S., Chemical Engineering, Seoul National University, 2001
M.S., Chemical Engineering, Seoul National University, 2006
Ph.D., Chemical Engineering, Texas A&M University, 2010